THE RDOA-DEPENDENT PHOSPHOPROTEOME PROFILE OF *Salmonella enterica*

by

Olivia L. Roque

A thesis submitted to the Department of Microbiology and Immunology

In conformity with the requirements for

the degree of Master of Science

Queen's University

Kingston, Ontario, Canada

(October, 2009)

Your file Votre référence
ISBN: 978-0-494-65260-2
Our file Notre référence
ISBN: 978-0-494-65260-2

Abstract

RdoA, a serine/threonine kinase, is a member of the Cpx regulon, a stress response pathway, in *Salmonella enterica* serovar Typhimurium. Phenotypic characterization of *rdoA* null mutants suggested that RdoA kinase activity affects a wide range of cell functions, which could be the result of both direct and indirect phosphorylation of targets. In a search for RdoA's target(s), the phosphoproteome profile of wild-type and *rdoA* null *S. enterica* was examined through phosphoprotein enrichment followed by 2-dimensional gel electrophoresis coupled with phospho-specific fluorescent stains and western blots using phospho-specific antibodies. Three different phosphoprotein enrichment protocols, all based on metal-ion affinity chromatography, were compared for yield and phosphoprotein specificity to determine which would be the most suitable for *S. enterica.* This study showed that the Phostag Enrich Phosphoprotein kit (PerkinElmer) gave the highest yield, the majority of which were phosphoproteins. These studies also showed that western blots using phospho-specific antibodies were more sensitive than phosphoprotein-specific fluorescent stain ProQ Diamond in detecting phosphoproteins. The phosphoproteome profile of *S. typhimurium* cells grown under Cpx activating conditions included phosphoproteins involved in the heat shock response, cellular metabolism and protein synthesis. This work also identified changes in the phosphoproteome that were dependent upon the presence or absence of RdoA. Phosphoproteins that showed a significant change in phosphorylation were identified by mass spectroscopy using peptide mass fingerprinting. Proteins identified included protein foldases (DnaK and GroEL), proteins involved in metabolism (glycerol kinase, enolase and E1 subunit of the pyruvate dehydrogenase complex), and in protein synthesis (elongation factor-Tu). These proteins may be phosphorylated in an RdoA-dependent manner to allow normal cell functioning under envelope stress. Several proteins unlikely to be phosphoproteins were also RdoA-dependent. SrgA, encoded on the virulence plasmid, is a disulfide oxidoreductase specific

for the PEF fimbriae that was shown to be repressed by RdoA. This work also showed that integration host factor, previously suggested to be an RdoA target, was not affected in terms of expression or phosphorylation by RdoA. The several RdoA-dependent changes in protein expression levels and phosphorylation that were identified contribute to the elucidation of RdoA's role in the envelope stress response and provided further insight in determining RdoA target(s).

Acknowledgements

I would like to first thank my adviser, Dr. Nancy L. Martin, for her guidance and support throughout this project. I also would like to thank my committee members: Dr. Keith Poole and Dr. Ken Jarrell, for their time and contribution. I would also like to thank Dr. Katrina Gee for allowing me to use her imager for my Western blots and Dr. Wayne Swedden and Dr. William Plaxton and his lab for their help using the Typhoon for my fluorescent stains. Thank you to Mr. David MacLeod of the Protein Function Discovery Unit for working on my proteins in time for my thesis submission.

My two years in the lab would not be as exciting and fun without Janet T. Lin. I will always remember our own weekend work rules, which we just made up so that our experiments will work. Thank you for your support and endless patience during my thesis writing. It was a pleasure and a privilege working with you and I hope that we can do it again. Thanks to Melissa Shih, who has always supported me from the moment we met and who showed me how beautiful Canada is. Thank you for making me realize that I can call Canada my home.

Most importantly, I would like to thank my family whom I always looked forward to see and spend time during my free weekends. My wonderful and supporting parents: Rolando and Josefina Roque, thank you for listening to my frustrations during stressful times. Thank you for being my role models and my inspiration to work hard. To my sisters: Josephine Ann and Noelle, for helping me during certain situations because you understood that I was still a student while both of you were earning big bucks!! My most special brother: Ronan Joshua, thank you for being silly and funny. Thank you for always reminding me to have fun in everything I do. I hope that you appreciate how important education is. I hope that when you are old enough to understand what I wrote here, this will inspire you to pursue graduate studies (possibly in Microbiology or in a closely related field??) in the future. I dedicate this to all of you. I love you and I couldn't have done this without your support and prayers. Lastly, I would like to thank God. Without him, I wouldn't have finished this amazing and extremely challenging milestone in my life.

Table of Contents

List of Figures

List of Tables

List of Abbreviations

ADP	Adenosine diphosphate
AMP	Adenosine monophosphate
AMP100	100 micrograms per microliter of ampicillin
APS	Ammonium persulfate
ATP	Adenosine triphosphate
BCA	Bicinchoninic assay
bp	Base pairs
BSA	Bovine serum albumin
C	Celsius
CHAPS	3-[(3-Cholamidopropyl)dimethylammonio]-1-propanesulfonate
cm	Centimeter(s)
DNA	Deoxyribonucleic acid
DTT	Dithiothreitol
ECL	Enhanced chemiluminescence
EDTA	Ethylenediaminetetraacidic acid
EF	Elongation factor
g	Gram(s)
GTP	Guanosine triphosphate
HEPES	4-(2-hydroxyethyl)-1-piperazineethanesulfonic acid
HK	Histidine kinase
HRP	Horse radish peroxidase
IEF	Isoelectric focusing

IHF	Integration host factor
IMAC	Immobilized affinity chromatography
IPG	Immobilized pH gradient
IPTG	Isopropyl β-D-1-thiogalactopyranoside
kDa	kiloDalton
L	Liter(s)
LB	Luria-Bertani
LC	Liquid chromatography
MES	2-(N-Morpholino)ethanesulfonic acid
MBP	Maltose binding protein
µg	Microgram(s)
mg	Milligram(s)
mL	Milliliter(s)
MOAC	Metal oxide affinity chromatography
MS	Mass spectrometry
MyBP	Myelin basic protein
OD_{600}	Optical density at 600 nanometers
O/N	Overnight
PEG	Polyethylene gycol
PBS	Phosphate buffered saline
PMF	Peptide mass fingerprinting
PPK	Phosphoprotein Purification kit (Qiagen®)
RNA	Ribonucleic acid

rpm	Revolutions per minute
RR	Response regulator
RT	Room temperature
SDS	Sodium dodecyl sulfate
SDS-PAGE	Sodium dodecyl sulfate polyacrylamide gel electrophoresis
ser/thr	Serine/threonine
SMP	Skim milk powder
SPI	*Salmonella* pathogenicity island
TCA	Tricarboxylic Acid
TEMED	N,N,N',N'-tetramethylethylenediamine
TER	Transepithelial resistance
TF	Trigger factor
TTSS	Type three secretion system
V	Volts
VH	Volt/Hours
WT	Wild-type

Chapter 1

Introduction

Phosphorylation is a widely studied post-translational protein modification that can be observed in both prokaryotic and eukaryotic systems. This process is controlled by two types of enzymes, kinases and phosphatases, that enable the transfer of phosphate from a nucleotide triphosphates such as adenosine triphosphate (ATP) to a protein substrate or the removal of phosphate from a protein substrate as a conduit of information to enable different cellular functions to occur (49, 117). It was initially thought that histidine and aspartate kinases were exclusive to bacteria, while serine/threonine and tyrosine kinases were found only in eukaryotes. This has been disproved since serine/threonine and tyrosine kinases have been found in bacteria, while histidine and aspartate kinases have been observed in eukaryotes (5, 49, 94). Though these kinases have been found in two different domains of life, studies have shown and suggested that their functions are not always similar (61).

Studying protein kinases requires multiple and complementary techniques in order to characterize these proteins, which may eventually lead to the identification of their target(s). The challenge of specifying kinase substrates is great. The targets of numerous eukaryotic kinases that have been studied for many years remain unknown, putative, or assumed based on indirect evidence (94). Because of the transient nature of phosphorylation, directly determining a bacterial kinase's target is a complex task for which few specific techniques exist. The approach used in the current study is based on proteomics, specifically on a survey of the phosphoproteome of *Salmonella enterica* serovar Typhimurium (hereafter called *S. typhimurium*). These phosphoproteomic techniques are not suitable for all samples and optimization is always required to obtain repeatable results. In this study, 3 different phosphoprotein enrichment techniques were

examined to determine which would be most suitable for *S. typhimurium* phosphoproteomic studies.

The 38.5kDa kinase under study was RdoA (regulator of disulfide oxidoreductase A), a serine/threonine (ser/thr) kinase found in *S. typhimurium*, a problematic organism due to it being a food-borne human pathogen. RdoA is up-regulated upon activation of the Cpx pathway, a stress response pathway. Prior studies of RdoA, which involve phenotypic (108, 129) and structural characterization (158), and initial mutagenesis studies (78) have established key attributes of RdoA. Suntharalingam *et al.* (129) and Richards (108) showed that RdoA affects multiple functions of *S. typhimurium*. Although the target of RdoA kinase activity is currently unknown, the results from these studies suggest that RdoA's target may be a global regulator or RdoA may have multiple targets. The search for RdoA's target(s) is the primary goal of the research. One aspect of this study was to examine a potential RdoA target known as integration host factor (IHF), a global regulator (130). This study also examined the phosphoproteome profile of *S. typhimurium* in cells that were overexpressing NlpE (an outer membrane lipoprotein) in order to activate the Cpx pathway. This study followed RdoA-dependent changes in the phosphoproteome in order to clarify the role of RdoA in the cell and identify new potential RdoA target(s). Knowing the mechanisms and the characteristics of RdoA and its target(s) will allow researchers to manipulate these enzyme-target complexes in order to more effectively control bacterial functions for the future development of therapeutic tactics.

Chapter 2

Literature Review

2.1 Phosphoproteome of Bacteria

Protein phosphorylation is a highly regulated and reversible signaling process found in prokaryotes and eukaryotes, which transmits/relays information for normal cellular function (34). Recent studies examined the phosphophoproteomes of several bacterial species. Two different experimental approaches using 2-D SDS-PAGE or a gel-free method are most frequently used. The first and conventional approach is to use phosphoprotein enrichment with 2-D SDS-PAGE followed by several phosphoprotein detection methods and lastly, peptide mass fingerprinting (PMF) by mass spectrometry (MS). Between 20 and 50 phosphoproteins were identified using fluorescent staining, western blotting using anti-phospho-specific antibodies and/or [^{33}P]-labeling in these studies (8, 29, 63). A gel-free approach, which consists of phosphopeptide enrichment and high accuracy MS, were performed on proteins from several bacteria (71, 72, 105, 121). Using this approach approximately 100 phosphorylation sites, including some proteins with multiple phosphorylation sites, were identified. These studies could determine the percentage of different phosphorylation sites, with serine residues most frequently modified, followed by threonine and lastly, tyrosine (71, 72, 121), with the exception of *Lactococcus lactis* IL403 that had the higher number of phosphothreonine sites compared to the other bacterial species examined (121). While none of these techniques were able to identify phosphohistidine residues, using these two approaches, the majority of identified phosphoproteins were involved in central metabolism. Phosphoproteins were also identified from protein biosynthesis and protein folding pathways (29, 63, 71, 121). Using the conventional approach to determine the phosphoproteome of a bacterium provided a lower number of phosphoproteins compared to the gel-free approach

because of the limited range in which phosphoproteins can be resolved. Several studies examined changes in phosphorylation patterns that occur when cells are in exponential, stationary phase or when cells are stressed (29, 63, 105). This allowed identification of important phosphorylation events that are dependent on the given growth conditions, kinase or regulator.

2.2 Phosphorylation in *Salmonella*

Protein phosphorylation has been well documented to positively or negatively regulate different cellular functions directly or indirectly. This universal process, involved in different cellular functions such as energy use, virulence and quorum sensing, will be briefly discussed. The focus will be on those processes operating in *S. typhimurium*, a Gram-negative rod-shaped pathogen.

Bacteria use many different sources of energy for survival and normal cell growth. Proline oxidation is one widely conserved mechanism (93, 159). In *S. typhimurium*, phosphorylation occurs in association with proline oxidation where proline can be used as a source of carbon, nitrogen or energy via proline permease (PutP) and a multifunctional protein (PutA) (76). PutA is regulated via proline availability and phosphorylation. It acts as a repressor of the *put* operon in the absence of proline, or, in the presence of proline, catalyzes the conversion of proline to glutamate. Phosphorylation of PutA decreases its affinity for DNA and, hence, allows it to move to its membrane-associated sites where it acts as a dehydrogenase.

Phosphorylation not only plays a role in *S. typhimurium's* ability to use different resources for energy, but it also has a role in establishing an infection in association with different virulence genes. One unique characteristic of *S. typhimurium* is its ability to invade host cells (45). Successful bacterial invasion is dependent upon *hilA*, which encodes a transcriptional regulator that activates expression of several genes important for bacterial invasion. The *hilA* gene is regulated by several proteins and systems (46), for example, the BarA/SirA histidine-

aspartate kinase two-component signal transduction system. This system will be further discussed in detail in Section 2.4. Phosphorylated SirA binds to the *hilA* promoter and activates *hilA* transcription (134). Phosphorylation can also indirectly affect gene expression. For example, phosphorylated SirA is indirectly responsible for down-regulating expression of *flhDC*, a gene that codes for a regulator of flagellar genes (134). Phosphorylated SirA regulates CsrB expression, a component of the CsrA-CsrB system, found to be a master regulator of motility genes (146). Unlike the BarA/SirA system, the CsrA-CsrB system is a global regulatory system that affects gene expression post-transcriptionally (111). CsrA, a small RNA-binding protein, stabilized flagellar gene transcripts and promoted translation (146). On the other hand, CsrB is a non-coding RNA molecule that binds to CsrA to antagonize CsrA effects (68). Phosphorylated SirA binds to the *csrB* promoter, thus, activating its expression (134). CsrB binds to CsrA forming a CsrA-CsrB complex and inhibiting different CsrA-activated genes involved in motility, cell surface proteins, glycolysis and adherence (68, 111).

In addition to normal cell growth, intra-species and inter-species communication are necessary for invasion and/or competition *in vivo*. Quorum sensing is a cell-to-cell signaling mechanism that responds to cell density within the bacterial population (84, 106, 149). The cell signaling molecules are known as autoinducers, specifically AI-2 in *S. typhimurium*, which is actually a family of related molecules. In *S. typhimurium*, AI-2 levels play a role in regulating expression of the genes in the *lsr* operon that are necessary for AI-2 internalization and processing. AI-2 is released into the extracellular environment where it acts as a signal to other bacteria when internalized by them. Once in the cytoplasm of the neighboring bacterium, AI-2 is phosphorylated by the kinase LsrK, a bacterial small molecule kinase. Phosphorylated AI-2 then derepresses expression of *lsr* operon allowing expression of AI-2 transporter proteins and the enzymes that further process the AI-2 signal (154).

2.3 Bacterial Ser/Thr Kinases

Historically, histidine kinases were initially discovered and studied in bacteria, while tyrosine and ser/thr kinases were exclusively found in eukaryotic cells (5). Since the 1990s, tyrosine kinases and ser/thr kinases were identified in prokaryotes as well (5, 49, 94). Studies comparing the protein sequences of known eukaryotic kinases with predicted prokaryotic and archaeal kinases showed that although their amino acid sequences greatly differ, there were conserved motifs that suggested a common ancestral protein kinase (61). Many ser/thr protein kinases have a similar catalytic core. This catalytic core contains two subdomains, a small N-terminal subdomain and a larger C-terminal subdomain. The N-terminal subdomain, which is mainly composed of β-sheets, is associated with the binding of ATP or guanosine triphosphate (GTP) while the C-terminal subdomain, which is mainly composed of α-helices, is associated with substrate-binding (18, 74, 114). The nucleotide-binding pocket and residues that participate in the phosphotransfer are found in between these two subdomains (Figure 1) (18, 114). In general, the main role of the conserved kinase core is to bind ATP/GTP and the substrate to be phosphorylated and transfer the γ-phosphate from ATP/GTP to the acceptor hydroxyl residue of the substrate (35). Once the target substrate has been phosphorylated, it may be involved in direct or indirect transcriptional and translational regulations, post-translational modifications, and/or protein-protein interactions (5, 94). Phosphorylation can also control metabolism, protein localization, and target proteins for degradation by proteases. Ser/thr kinases are often intertwined with different signaling pathways, such as a histidine-aspartate kinase two-component signal transduction pathway, to co-ordinately regulate gene expression in response to the stimuli presented (61). A well studied example is in *Myxococcus xanthus*, a Gram-negative soil bacterium that changes its morphology from a cell aggregate to a fruiting body form depending on nutrient availability. A ser/thr kinase of *M. xanthus* works in concert with a histidine-aspartate

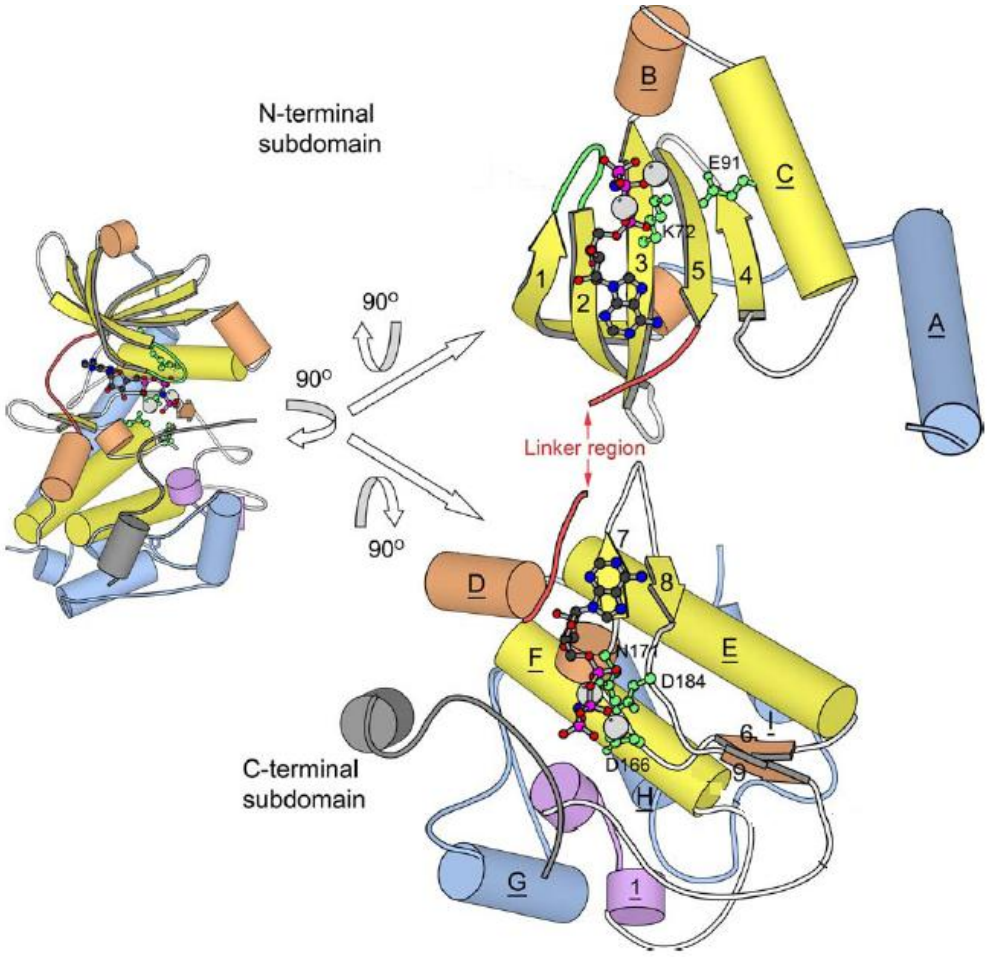

Figure 1. Universal kinase catalytic core of protein kinases. Two views of the C-terminal and N-terminal subdomains are shown. The kinase catalytic core of PknA, a cAMP dependent protein kinase, is shown as an example. Alpha-helices are numerically labeled while β-sheets are alphabetically labeled. ATP and metal ions are shown bound to the catalytic core (114).

two-component signal transduction system to coordinate a change in the cellular morphology of the bacterium (88, 125). The activity of the ser/thr kinases Pkn8 and Pkn14 regulate *mrpC* expression (88). MrpC is a key transcription factor that is regulated by two independent systems (Figure 2). The first one is the MrpA-MrpB histidine-aspartate kinase two-component signal transduction system and the second one is the Pkn8-Pkn14 ser/thr kinase cascade (70, 88). During nutrient depletion, an increase in MrpC production, controlled through the MrpA-MrpB system, results in an increase in *fruA* expression that leads to faster development of fruiting bodies (88, 89). On the other hand, the down-regulation of *M. xanthus'* fruiting body formation is controlled through the Pkn8-Pkn14 ser/thr kinase cascade. Pkn14 phosphorylates MrpC at its two threonine residues. This event down-regulates MrpC's binding activity to the *fruA* promoter region and, subsequently, maintains the bacterium in a cellular morphology (88, 89).

2.4 Histidine-Aspartate Kinase Two-Component Signal Transduction Systems

The typical two-component signal transduction system uses the transfer of phosphate groups as a means of communication between two proteins, namely a histidine kinase (HK) and a response regulator (RR) (Figure 3) (50, 127, 143). The output response of this system, that can either be activation or repression of gene expression (104), aids in survival during nutrient starvation, changes in oxygen tension (62, 91), temperature changes and to resist pH fluctuations (62, 102).

HKs are membrane-bound homodimeric proteins that contain an amino-terminal periplasmic sensing domain connected to a carboxyl-terminal kinase domain (91, 148). The periplasmic domain is variable in sequence and it recognizes the stimuli from the external environment directly or indirectly (110, 144, 148) while the conserved kinase domain is involved in the transfer of a phosphate group to the RR (91, 110, 148). These sensors are located in the

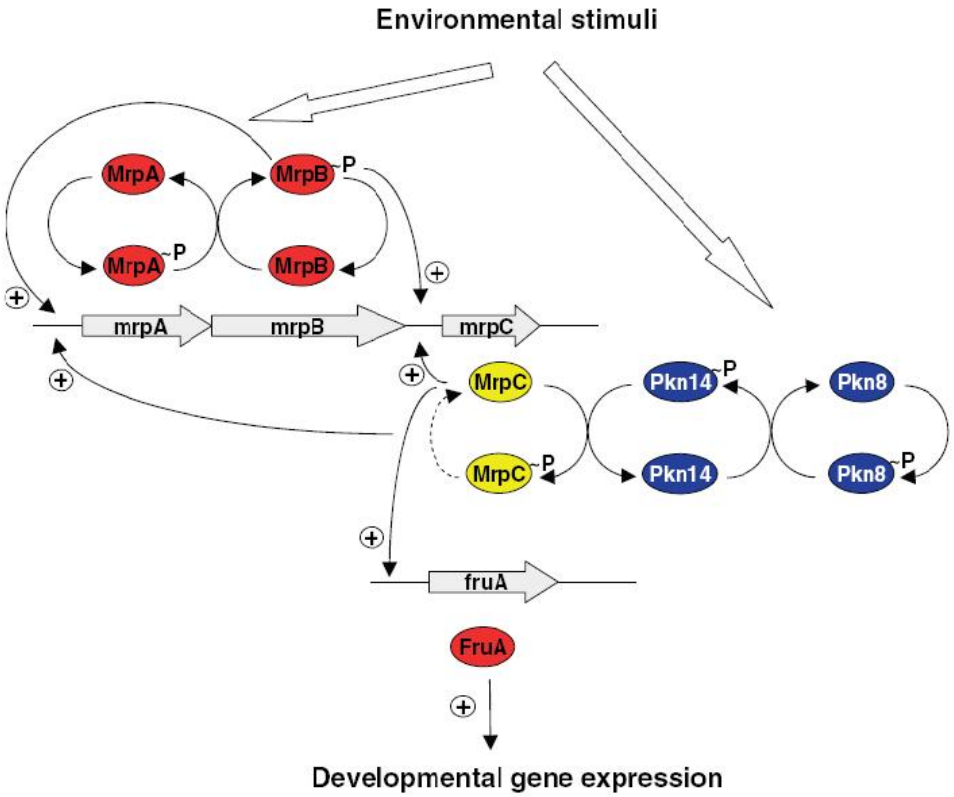

Figure 2. Pkn14-Pkn8 cascade and MrpA-MrpB system in *M. xanthus*. Environmental stimuli, such as nutrient depletion, activate the MrpA-MrpB system that causes an increase in MrpC expression. An increase in MrpC expression causes an increase in FruA expression, which is responsible for fruiting body formation. Phosphorylation of MrpC is controlled by the Pkn14-Pkn8 system. Phosphorylated MrpC cannot bind to *fruA* promoter, thus, down-regulating fruiting body formation (70).

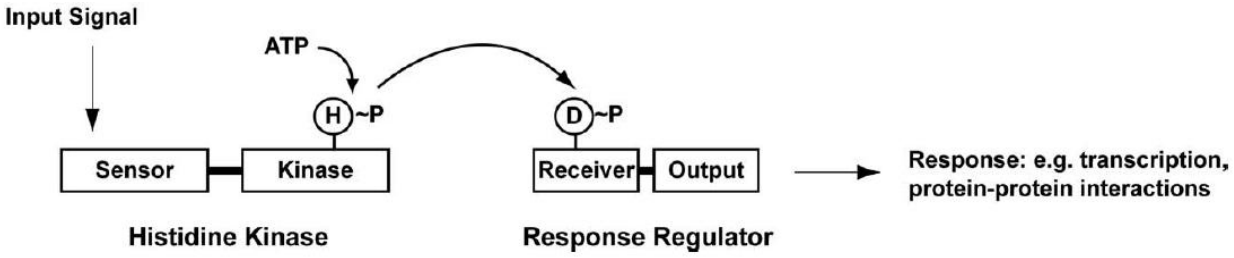

Figure 3. A typical histidine-aspartate two-component signal transduction system of bacteria. Signal is detected by the sensor domain of the HK, which then autophosphorylates at its histidine residue. RR then catalyzes the transfer of the phosphate group from the histidine residue of HK to its aspartate residue. Phosphorylated RR undergoes conformational change at its output domain, which will activate different cellular functions, such as gene transcription and protein-protein interactions (119).

inner membranes of both Gram-negative and Gram-positive bacteria (91). HKs act as a main signaling pathway between the external environment and the adaptive response (54).

RRs contain two domains namely, a conserved amino-terminal regulatory domain and a variable carboxyl-terminal effector domain (54, 91, 128, 148). The regulatory portion of the RR is also known as the receiver domain and has three major functions. First, it interacts with phosphorylated HK and facilitates the transfer of the phosphoryl group from the HK to its aspartate residue. Second, it can catalyze autodephosphorylation by hydrolysis of the phosphate via its own enzymatic activity, causing its own inactivation (54). Lastly, it can regulate its effector domain in a phosphorylation-dependent manner (91, 110, 148). The effector domain is usually a DNA-binding domain that determines the transcription of specific genes (54, 91, 110). Over all, RR's main purpose is to activate and/or repress gene expression in a controlled and regulated manner (54, 144, 148).

In *S. typhimurium*, the Cpx pathway is one example of this type of signal transduction system and is the focus of this study. This system, discussed in detail in the next section, is unique because it is made up of three components unlike most two-component systems.

2.5 The Cpx Pathway

The Cpx pathway (Figure 4) is composed of three proteins: CpxP, a periplasmic inhibitor; CpxA, the histidine kinase; and CpxR, the response regulator (22, 102). Activation of the Cpx pathway occurs in the presence of misfolded periplasmic proteins (104, 128), overproduction of the outer membrane lipoprotein NlpE (40, 128), alkaline pH (19, 86) or overexpression of a specific pilin (60). Signals such as these cause CpxP to disassociate from CpxA via a mechanism that is poorly understood (102). CpxA then autophosphorylates at a histidine residue in an ATP-dependent manner. CpxR then catalyzes the transfer of the phosphate from CpxA to an aspartate

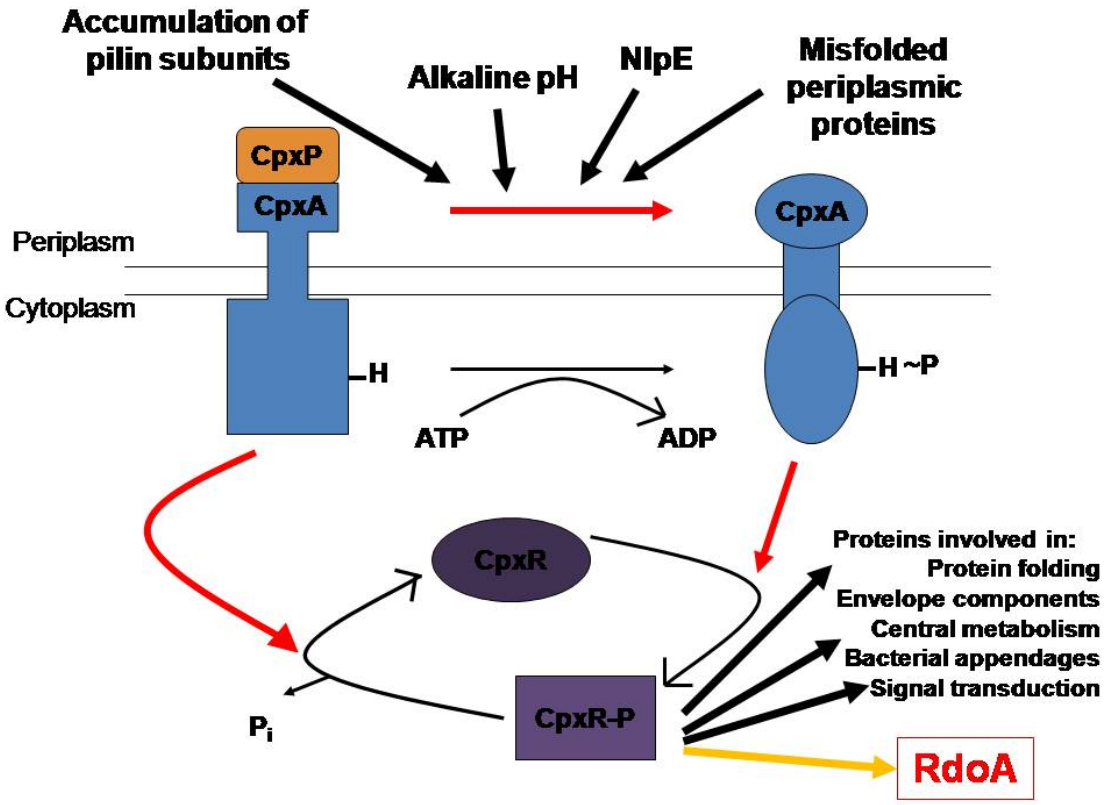

Figure 4. The Cpx pathway of *S. typhimurium.* The Cpx pathway components: CpxP (periplasmic inhibitor), CpxA (HK) and CpxR (RR) respond to signals, such as NlpE overexpression, misfolded periplasmic proteins, alkaline pH and accumulation of pilin subunits. These events cause CpxP to disassociate from CpxA. CpxA then autophosphorylates in an ATP-dependent manner at its histidine residue. CpxR then catalyzes the transfer of the phosphate from the CpxA to itself. Phosphorylated CpxR then undergoes a conformational change, enabling it to activate gene transcription involved in proper protein folding, envelope components, central metabolism, bacterial appendages and signal transduction. More importantly, phosphorylated CpxR up-regulates *rdoA* transcription. This RdoA protein is the main focus of this study. Image was taken and modified from Richards, M. 2005 (108) unpublished data.

residue of CpxR. Phosphorylation of CpxR causes its effector domain to undergo a conformational change that enhances DNA-binding to a consensus regulatory domain resulting in an alteration of gene transcription (7, 128, 148).

Studies characterizing the Cpx regulon in *Escherichia coli* showed that the Cpx pathway affects a large number of genes involved in proper protein folding, envelope components, bacterial appendages, central metabolism and signal transduction (14, 99). Both of these studies examined Cpx-regulated genes in a *cpxR* null mutant and observed that most genes were still expressed in the absence of CpxR, suggesting that most Cpx-regulated genes are not solely CpxR-dependent. The Cpx pathway acts in concert with other stress response systems, such as the σ^E and the BaeR system (14) or proteins (99) in regulating the same genes. The Cpx regulon member known as RdoA will be the focus of the remaining sections of this literature survey.

2.6 RdoA, a Bacterial Ser/Thr Kinase

The gene coding for RdoA is located immediately upstream of the coding region of the foldase called disulfide oxidoreductase A (DsbA). Comparison of the RdoA protein sequences with other predicted RdoA homologs from numerous microorganisms showed a highly conserved ATP-binding domain (158) that is also known as a Brenner's motif (H-X-D-X_4-N) (11). Studies have established that RdoA possesses ser/thr kinase activity and these focused on its structural (158), biochemical (158), and phenotypic (108, 129) characteristics. These studies are summarized below, establishing the background knowledge on RdoA, leading to the question "What is/are RdoA's target substrate(s)?"

2.6.1 Structural and Biochemical Characterization of YihE/RdoA

The structure of RdoA is inferred from structural studies of YihE, an RdoA homologue found in *E. coli*. (158). These 38.5 kDa proteins show 96% amino acid sequence similarity, including all the key residues in the catalytic domain (80, 158). The crystal structure of YihE has

a similar tertiary protein structure to choline kinase of *Caenorhabditis elegans* and an aminoglycoside phosphotransferase [APH (3')-IIIa], of *Enterococcus faecalis* – both small molecule kinases. Although YihE has a similar structure to these proteins, their percent amino acid similarity is only 17%. These structures are all similar to a canonical eukaryotic ser/thr protein kinase with a catalytic domain composed of an ATP-binding domain and a substrate-binding domain (Figure 5). The differences between YihE and its structural homologues provided clues on probable YihE substrates. The substrate-binding domain of YihE has a large substrate binding cleft that suggests its substrates are large as well, such as would be the case for protein-protein interactions. Recent studies characterizing the substrate binding domain of APH(3')IIIa (30) served to highlight the fact that this region of APH(3')IIIa and YihE share little structural homology. These differences suggest that although YihE has a similar over-all structure to choline kinase and APH (3')-IIIa, YihE is likely to phosphorylate different types of substrates, and therefore has a different function from that of the small molecule kinases (158).

RdoA was tested for its ability to autophosphorylate and phosphorylate myelin basic protein (MyBP), an universal kinase substrate. Zheng *et al.* (158) showed that purified RdoA possesses the ability to autophosphorylate and phosphorylate MyBP at its serine and threonine residues. Presumably, autophosphorylation is important for activating RdoA's substrate phosphorylation capability.

2.6.2 RdoA Regulation and its Role in Stress Response

Understanding RdoA regulation in terms of both gene expression and activation of kinase activity is important in determining how it plays a role in *S. typhimurium's* stress response. As mentioned previously, *rdoA* is up-regulated through the Cpx pathway, through a CpxR-responsive promoter region upstream of *rdoA* (129). In addition, deleting *rdoA* activates the Cpx

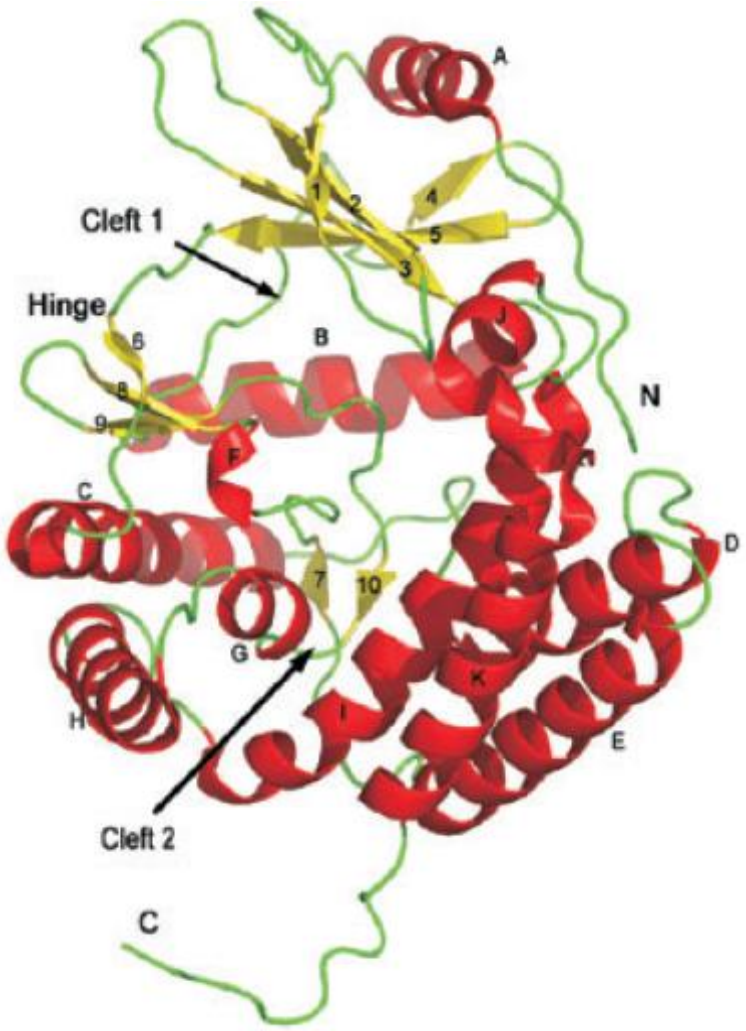

Figure 5. Crystal structure of YihE. YihE shows a similar structure to eukaryotic ser/thr kinases. N-terminal region is mostly composed of beta-sheets (yellow and numerically labeled) while alphabetically labeled C-terminal region is composed of mostly alpha-helices (red and alphabetically labeled). Conserved structural motifs are shown in yellow. Cleft 1 points to the ATP-binding domain while Cleft 2 points to the substrate binding domain (158).

pathway (38). Suntharalingam *et al.* (129) reported that activation of the Cpx pathway increased *rdoA* and *dsbA* transcript levels, unlike the increase in *rdoA-dsbA* co-transcript observed in *E. coli*. As mentioned previously, *dsbA* is the gene found downstream of the *rdoA*. They also reported that DsbA levels decreased in an *rdoA* null *S. typhimurium* and that normal DsbA levels were restored when *rdoA* was provided *in trans*.

This indicates that RdoA affects DsbA levels. In addition, they showed that deleting *dsbA* up-regulates *rdoA* transcription, concluding that the absence of DsbA up-regulates RdoA expression, through activation of the Cpx pathway (129) Lastly, they showed that *rdoA* transcript is most abundant in stationary phase, and it was later shown that protein levels were also highest at this growth phase (158). RdoA expression is therefore growth-phase dependent (129).

A study of *rdoA* null phenotypes uncovered a wide range of effects including flagellar phase variation (108, 129), long-term survival (38), curli fiber expression and involvement in colonic epithelial cell infection (108). In addition, RdoA expression increased in alkaline conditions (38) and decreased under acidic conditions (129). It is not currently known how or if all of these phenotypes relate to a Cpx-dependent response. For example, curli fibers are amyloid-like protein appendages that aid in the adhesion of *S. typhimurium* during invasion and biofilm formation (6). Zheng *et. al* (158) showed that the lack of RdoA derepressed curli fiber expression compared to wild type (WT), concluding that normally RdoA functions to down-regulate curli production (108, 158). CpxR was previously shown to repress expression of the key curlin regulator CsgD (146) Deletion of either *cpxR* or *rdoA* has less of an effect on curlin production than deleting both genes suggesting a different target exists for each (158). Although it is clear that both RdoA and CpxR are involved in expression of curli, the biological significance of either protein is not well understood.

The ability of *S. typhimurium* WT and *rdoA* null strains to invade host cells was explored by measuring transepithelial resistance (TER) of colonic epithelial cell monolayers in the

presence and absence of these bacteria. TER levels indicated the extent of bacterial invasion and destruction of the cell monolayer. TER was higher using the *rdoA* null strain compared to WT suggesting that RdoA is involved in gaining entry to intestinal epithelial cells (108). RdoA also plays a role in flagellar phase variation. *S. typhimurium* reversibly switches expression of the flagellar subunits FliC and FljB via a chromosomal DNA inversion event that results in expression of only 1 flagellin type at a time (160). The molecular mechanism of inversion is well understood, but additional posttranscriptional events are also involved (1) Recent evidence suggests that bacteria use flagella as environmental sensors and respond by switching flagellin types (157). WT *S. typhimurium* expresses predominantly FliC flagellin protein under laboratory conditions, however, an *rdoA* null mutant population expresses FljB in much higher amounts (108). Overall, this variety of phenotypes suggests that RdoA activity regulation contributes to *S. typhimurium's* ability to survive during changes in the environmental conditions.

2.7 Potential Targets of RdoA

The aforementioned studies provide initial clues on RdoA target/s. RdoA has affects several different phenotypic properties of *S. typhimurium* suggesting that this bacterial ser/thr kinase may phosphorylate a global regulator responsible for these different functions of *S. typhimurium* or that RdoA may have numerous targets. One suspected target is integration host factor (IHF), a known global regulator.

IHF is a DNA-bending protein that binds to a specific sequence in the minor groove of DNA (130, 137). It is composed of two subunits, namely IhfA (11.35kDa) and IhfB (10.65kDa), which have 25% amino acid identity and 30% amino acid similarity (162) and are encoded in separate locations on the bacterial genome. These proteins, which are most abundant in stationary phase cells (4, 25), can form both heterodimers (130) and homodimers (162). The N-termini are responsible for the dimerization of the two subunits while the β-sheet arms and, possibly, the C-

termini α-helices are responsible for binding to DNA (137) (Figure 6). Due to IHF's ability to bend DNA, it functions as a transcriptional regulator that can either repress or activate different genes important for bacterial pathogenesis, growth, and survival (32, 77, 79, 156). In *S. typhimurium*, genes affected by IHF are involved in flagellar phase variation, the type III secretion system (TTSS), SPI-1 pathogenicity island gene expression, chemotaxis, and invasion into host cells (77).

Mangan *et al.,* (77) showed both heterodimer and homodimer forms of IHF affected stationary phase survival and pathogenesis. Their study showed that absence of individual or both Ihf subunits decreased expression of a large number of genes that are important in the stationary phase and in virulence. One particular observation was that an *ihfA* null mutant expresses only FljB (77), which is similar to the phenotype exhibited by an *rdoA* null mutant (108, 129). In addition, the *ihfAB* null mutants showed decreased cell invasion ability (77) similar to an *rdoA* null mutant (108). These observations suggest that IhfA and RdoA may work in the same regulatory pathway to regulate flagellar phase variation switch.

In addition to IHF, Manu-Boateng (78) suggested that RdoA's target(s) may be a cytoplasmic protein(s) or a membrane-bound protein(s) with a cytoplasmic domain because RdoA is a cytoplasmic protein (38). Two approaches, which involved pull down assays and kinase assays using purified YihE and *rdoA* null *S. typhimurium* cell lysates, were carried out to try to trap and identify YihE/RdoA's target. Unfortunately, neither approach was successful (78).

2.8 Project Objectives and Hypothesis

Identification of RdoA's target(s) is important in understanding *S. typhimiruim's* ability to respond to different stressful conditions. This study explored the hypothesis that IHF is an RdoA target, as well as exploring more broadly the RdoA-dependent phosphoprotein population

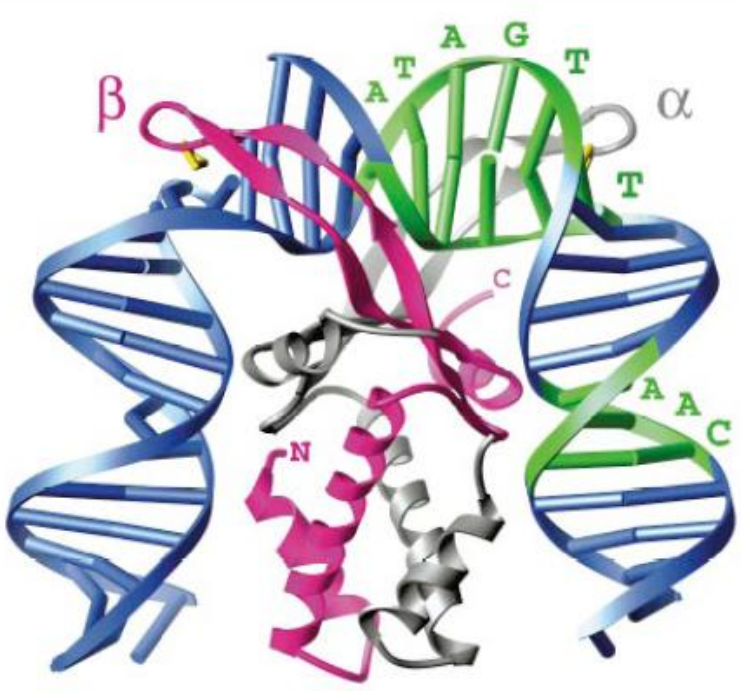

Figure 6. Structure of IHF heterodimer. IHF (IhfA: silver and IhfB: pink) bound to the minor groove of DNA (137). The IHF consensus DNA-binding sequence is shown in green, interacting with the "arm" of IhfA and the "body" of IhfB. The yellow residues are prolines at the tip of each "arm" (137).

changes using 2-dimensional sodium dodecyl sulfate polyacrylamide gel electrophoresis (2-D SDS-PAGE) with different staining methods and/or western blots. It was hypothesized that identifying changes in the phosphoproteome will elucidate the role of RdoA in the stress response system and, possibly, identify its target(s). If RdoA has multiple targets, changes in several phosphoproteins will be observed. In addition, the efficacy of 3 different phosphoprotein purification protocols were explored and determined.

Chapter 3

Materials and Methods

3.1 Bacterial Strains and Plasmids

S. typhimurium strains and plasmids used in this study are listed in Tables 1 and 2.

3.2 Preparation of Cell Lysates

Overnight cultures (O/N) of NLM2243 and NLM2215 were grown in LB broth containing AMP100 at 37°C with aeration. These *S. typhimurium* strains contain pND18 that encodes for NlpE lipoprotein, which at excess amounts activates the Cpx pathway, thereby, up-regulating expression of RdoA. Two mL of O/N culture were added to 50mL of LB containing AMP100 and grown at 37°C with aeration to late-logarithmic phase. Once the cells reached late-log phase (OD_{600} = 0.80), arabinose was added at a final concentration of 0.2% (w/v) to induce the production of NlpE. Induction was continued for 3 hours. Cultures were then centrifuged at 5,200xg for 15 minutes and the supernatants removed. Cell pellets were resuspended in 5 mL of phosphoprotein lysis solution and frozen at -70°C O/N. The next day, cell pellets were retrieved from -70°C and thawed. Cell mixtures were kept on ice and sonicated 5 times with 30 second bursts and centrifuged for 15 minutes at 10,000xg at 4°C. Supernatant was collected and total protein concentration (see below) was determined while cell debris was discarded.

For experiments concerning IHF, NLM2361 is a WT *S. typhimurium* containing pHx3-8, a plasmid that encodes both *ihf* subunits (90). A culture was grown in LB broth containing AMP100 O/N at 37°C with aeration. One mL of O/N culture was added to 50 mL LB broth containing AMP100 and grown to mid-logarithmic phase ($O.D._{600}$ = 0.60). Once the cells have reached mid-log phase, isopropyl β-D-1-thiogalactopyranoside (IPTG) was added to a final

Table 1. *S. typhimurium* strains used in the study.

Strain	Genotype	Plasmid	Source
NLM 2217	*his* strep^{R}, wild-type (SL1433)		(152)
NLM 2214	NLM 2217 *ΔrdoA*		Lab Strain Collection
NLM 2215	NLM 2214	pND18	Lab Strain Collection
NLM 2243	NLM 2217	pND18	Lab Strain Collection
NLM 2361	NLM2217	pHx3-8	This study

Table 2. Plasmids used in the study.

Plasmid	Description	Source
pBAD18	4.6kb derivative of pBR322 with a multiple cloning site downstream of the P_{BAD} promoter	(33)
pND18	pBAD18 containing the *E.coli nlpE* gene under the control of the P_{BAD} promoter Amp^R	(120)
pHx3-8	pCKR101 containing two *himA (ihfA)* and one *hip(ihfB)* gene products under the control of the P_{tac} promoter	(57)

concentration of 0.1 mM to induce the expression of IHF subunits. Induction was continued for 3 hours, after which cultures were centrifuged to obtain cell pellet(s) while the supernatant was discarded. Cells were lysed by incubating for 30 minutes at RT with agitation with 100 µL Bugbuster reagent (Novagen) and DNA was degraded by adding 1 µL of benzonase (Novagen). After incubation, this solution was centrifuged, supernatant was collected and the total protein concentration was determined (see below). The cell debris was discarded. Cell lysates with the same protein amount obtained from two different biological cultures were combined to be considered as a pooled biological sample.

3.3 Phosphoprotein Enrichment

3.3.1 Affinity Purification

3.3.1.1 Aluminum Hydroxide Metal Oxide Affinity Chromatography ($Al(OH)_3$ MOAC)

Protocol was carried out as described in Wolschin *et al.* (151) with minor revisions. Eighty mg of aluminum hydroxide were aliquoted in 2 mL microfuge tubes and washed with 1.5 mL aluminum hydroxide phosphoprotein binding buffer 2 times. One and a half mg of protein from the cell lysate was added to the washed aluminum hydroxide and incubated for 30 minutes at 4°C on a platform shaker. After incubation, the slurry was centrifuged for 1 minute at 9,900xg and the supernatant was discarded. The slurry was washed with 1.5 mL aluminum hydroxide phosphoprotein binding buffer 6 times followed by 2 washes by vortexing of 1.0mL of 10mM HEPES buffer (pH7.0). Nine hundred µL of aluminum hydroxide phosphoprotein elution buffer was added to the slurry and incubated for 20 minutes at 4°C on a platform shaker. After incubation, the slurry was centrifuged for 1 minute at 9,900xg, the supernatant removed and proteins were concentrated using methanol-chloroform precipitation or 2-D Clean-Up kit (see below) while the aluminum hydroxide was discarded. Protein yield was then determined (see below).

3.3.1.2 Phos-tag® Enrich Phosphoprotein Kit (PerkinElmer)

Phosphoprotein enrichment using Phos-tag was performed using the manufacturer's protocol with minor revisions. Two mg of total protein from the cell lysates were applied to the column and the solution was released from the column at a drip rate of 500 µL/minute. Phos-tag column contains 2 mL of resin:buffer (1:1) slurry. After washing, phosphoproteins were eluted in 3 mL of elution buffer and concentrated using methanol-chloroform precipitation. Protein yield was then determined (see below).

3.3.1.3 Phosphoprotein Purification Kit [PPK] (Qiagen®)

Phosphoprotein enrichment using PPK was performed using the manufacturer's protocol with minor revisions. Five mg of total protein from the cell lysates were applied to the column and the solution was released from the column at a drip rate of 500 µL/minute. PPK column contains highly cross-linked 6% agarose with a binding capacity of 300µg/mL. After washing, phosphoproteins were eluted in 3 mL of elution buffer and concentrated using 2-D Clean-Up kit (see below). Protein yield was then determined (see below).

3.3.2 Protein Precipitation

Protein precipitation was used to concentrate sample and decrease salts and contaminants in the samples. Protein pellets obtained from these precipitation protocols were resuspended in 25 mM MES and 0.25% (w/v) CHAPS (pH 6.0) for 1-D SDS-PAGE analyses or in 4% (w/v) CHAPS for two dimensional sodium dodecyl sulfate polyacrylamide gel electrophoresis (2-D SDS-PAGE) analyses and quantified using a protein assay (see below).

Methanol-chloroform precipitation was carried out as described in Wessel, *et al.* (147) with minor revisions. Eight hundred µL of methanol and 200 µL of chloroform were added to 300 µL protein samples. The samples were mixed, 700 µL of milliQ H_2O were added and mixed again and then centrifuged for 5 minutes at 9,900xg. After centrifugation, the solution separated

into three phases: upper phase, interface, and lower phase. Using a pipette, the upper phase was slowly removed without disturbing the interface. Five hundred µL of methanol was added and sample was mixed by vortexing. The samples were centrifuged for 15 minutes at 9,900xg at 4°C. After centrifugation, the supernatant was removed, leaving a white translucent pellet at the bottom of the microfuge tube. Pellets were dried using a speed vacuum for 2 hours and left open on the benchtop O/N to dry completely. Alternatively, protein precipitation using the 2-D Clean-Up kit (GE Healthcare Biosciences Corp.) was performed as described in the manufacturer's protocol. Sample volumes of 100µL containing less than 100µg of protein were concentrated using this approach.

3.3.3 Protein Assays

Two different protein assays were used in this study. Both assays used bovine serum albumin (BSA) to determine the standard curve.

Protein concentration was determined spectrophotometrically using the BCA Protein Assay kit (Pierce, Inc.) according to the manufacturer's instructions or using the 2-D Quant kit (GE Healthcare Biosciences Corp.) according to the manufacturer's instructions. A conversion factor was calculated to obtain the same values from both assays. It was calculated that the protein value obtained from the BCA assay was 5.5 times that of the protein value obtained from the 2-D Quant kit.

3.4 Phosphatase Treatment of Eluents

Negative controls for anti-phosphoserine, anti-phosphothreonine and anti-phosphotyrosine western blots were performed by treating eluents with lambda phosphatase (New England Biolabs) at a ratio of 1:10 (µg of eluent: units of lambda phosphatase). 10x lambda phosphatase buffer and 10x $MnCl_2$ solution were added to two sets of eluents to a concentration of 1x and mixed thoroughly. For one set of eluents, lambda phosphatase was added. Finally,

samples were incubated at 30°C O/N with gentle agitation. The next day, samples were vortexed, centrifuged and resolved in a 1-D SDS-PAGE. For 2-D SDS-PAGE, samples were concentrated using a 2-D Clean-Up kit. Finally, precipitated proteins were resuspended in 4.0% (w/v) CHAPS solution, quantified using a protein assay, and resolved in a 2-D SDS-PAGE.

3.5 Electrophoresis

3.5.1 One Dimensional Sodium Dodecyl Sulfate Polyacrylamide Gel Electrophoresis (1-D SDS-PAGE)

Protein samples were mixed with 6x SDS loading buffer at a ratio of 1:5 and heated for 5 minutes in a boiling water bath. Samples were loaded on a stacking gel and a 12% or 15% (w/v) polyacrylamide resolving gel (0.75mm). Five µL of PageRuler™ Unstained Protein Ladder (Fermentas), 6 µL of Prestained Marker Broad Range (New England Biolabs) or 0.5 µL of PeppermintStick™ Phosphoprotein Molecular Weight Standards (Molecular Probes, Inc.) were included as molecular weight standards. Gels were electrophoresed in a mini gel electrophoresis apparatus (Biorad Laboratories) at 50V for 30 minutes and then 150V for 1 hour and 30 minutes without running the dye front off. The gels were then either stained or subjected to western blotting (see below).

3.5.2 Two Dimensional Sodium Dodecyl Sulfate Polyacrylamide Gel Electrophoresis (2-D SDS-PAGE)

Protein samples were added to rehydration buffer to make a final volume of 125 µL and incubated at RT for 15 minutes with periodic mixing. Samples were loaded into the isoelectric focusing tray and 7.0 cm pH 4-7 IPG strips (Biorad Laboratories) were placed on top of it with gel side down. Mineral oil was added to cover the strips preventing dehydration, and the isoelectric tray was covered and strips underwent passive rehydration O/N. After rehydration, excess salts were washed from the rehydrated strips as described by Heppelmann, *et al.* (39). In

detail, strips were washed with 1 mL rehydration buffer containing 10 mM DTT 4 times on a platform shaker for 10 minutes. At the 4^{th} wash, 0.2% (v/v) biolytes was added to the rehydration buffer containing 10mM DTT. After the washings, strips were placed in a isoelectric focusing tray in a Biorad Protein IEF Cell and subjected to a conditioning step (rapid ramp, 500V for 15 minutes, 20°C) followed by a focusing step (rapid ramp, 8000V, 20°C). PPK and $Al(OH)_3$ MOAC samples were focused for 50,000 VH while Phostag samples were focused for 30,000 VH, for 16 µg of protein, and 50,000 VH, for 26 µg of protein. After isoelectric focusing, the strips were subjected to a volt check (rapid ramp, 8000V for 5 minutes, 20°C) to determine if the proteins have reached their isoelectric point. To determine if strips reached their isoelectric point, voltage should have reached 8,000V and current decreased from 50 µA/gel to 28 µA/gel. If voltage did not reach 8,000V and current was at 50 µA/gel, wet wicks were added at each end of the strip to absorb the salts from the sample. Strips were then focused (rapid ramp, 8000V, 20°C) for an hour and a half more. If voltage did not increase, focusing was stopped and strips were taken out of the isoelectric focusing tray, washed with 2 mL of equilibration buffer with 2% (w/v) DTT for 10 minutes at RT on a platform shaker followed by 2 mL of equilibration buffer with 2.5% (w/v) iodaacetamide for 10 minutes. Finally, strips were washed with 1x SDS running buffer. Focused and washed strips were placed on top of a 12% (w/v)polyacrylamide gel (1.0mm). A stacking gel was added and solidified to seal the strip onto the resolving gel. Six µL of Prestained Marker Broad Range (New England Biolabs) or 0.5 µL of PeppermintStick™ Phosphoprotein Molecular Weight Standards (Molecular Probes, Inc.) were added as molecular weight standards. Lastly, gels underwent SDS-PAGE.

3.6 Protein Detection

3.6.1 Silver Staining

Silver staining was followed as described in Yan *et al.* (155). In detail, electrophoresed gels were immersed in fix solution and left O/N on a platform shaker at RT. Fix solution was then discarded and gels were incubated in pre-treatment solution for 30 minutes at RT. Gels were then washed with milliQ H_2O 3 times 5 minutes. Silver solution was added and incubated for 20 minutes followed by 2 times 1 minute washes with milliQ H_2O. Gels were then immersed in developer solution and developed just until the background began to darken. Stop solution was added and incubated for 10 minutes. Final washes with milliQ H_2O were done 3 times for 5 minutes.

3.6.2 Fluorescent Staining

Two complementary fluorescent stains were used to determine phosphorylated proteins in the samples. ProQ® Diamond (Molecular Probes, Inc.) staining was performed as mentioned in the manufacturer's protocol. Stained gels were imaged using a Typhoon 8600 Variable Mode Imager (532nm/580nm bandpass). After ProQ-diamond stained gels were imaged, gels were subjected to SYPRO® Red Staining. SYPRO® Red (Molecular Probes, Inc.) staining was performed as mentioned in manufacturer's protocol. Stained gels were imaged using a Typhoon 8600 Variable Mode Imager (532nm/610nm bandpass). Once the gels were imaged, they were silver stained.

3.6.3 Western Blotting

Protein samples were separated by 1-D or 2-D SDS-PAGE and then washed with cold transfer buffer for 20 minutes. Proteins were transferred to nitrocellulose membrane for 1 hour at 100V in cold transfer buffer. After the transfer, the membrane was incubated with an appropriate blocking buffer for 1 hour at RT on a platform shaker. Membrane was then incubated with

primary antibody in an appropriate buffer solution at 4°C O/N. Primary antibodies used were anti-IHF (provided by Dr. Z. Jia), 0.25 or 0.50 µg/µL anti-phosphoserine (Stressgen), 0.25 or 0.50 µg/µL anti-phosphothreonine (Stressgen) and 0.25 µg/µL anti-phosphotyrosine (Southern Biotech) antibodies. Blocking solutions when anti-IHF was used contained 5% (w/v) skim milk powder (SMP) in 1xPBS, 2.5% (w/v) SMP in 1xPBS for primary antibody buffer and 1% (w/v) SMP in 1xPBS for secondary antibody buffer. Anti-phosphoserine and anti-phosphothreonine blocking buffer was used for all other antibodies. After O/N incubation, used primary antibody solution was collected and kept in -20°C freezer for future use. Membrane was washed with 1x PBS for 3 times 10 minutes. Secondary antibody at a dilution of 1:20,000 in an appropriate buffer, was added to the nitrocellulose membrane and incubated for 2 hours at RT on a platform shaker. Secondary antibody used for anti-IHF, anti-phosphoserine, anti-phosphothreonine antibodies was goat anti-rabbit horse radish peroxidase (HRP) while anti-phosphotyrosine antibodies was goat anti-mouse HRP. After the 2 hour incubation, solution was removed and membrane was washed with 1x PBS for 3 times for 10 minutes. Enhanced chemiluminescence (ECL) solution (GE Healthcare Biosciences Corp.) at a ratio of 1:1 was added to the membrane. Finally, membrane was exposed for 16 minutes and the imaged was captured for using a light output of 440 nm in a Alpha Innotech FluorChem HD2 Imager.

3.7 Scanning and Image Analysis

Silver-stained 2-D gels were scanned using a flatbed scanner (EPSON Perfection V700 Photo) at a resolution of 2000 dpi. All images were viewed using Adobe Photoshop Elements. Fluorescently stained gel images were converted to colored images using a gradient map tool in Abode Photoshop. SYPRO Red 2-D gel images were converted to a green/red color gradient while ProQ Diamond 2-D gel images were converted to a blue/yellow color gradient. The two converted images were manually overlaid to obtain a green/red/black gradient SYPRO Red/ProQ

Diamond 2-D gel image overlay. Overlaid image showed a green colored background while non-phosphorylated proteins became red colored spots. Black spots observed in images were determined as phosphoproteins. Intensity of the overlaid images was enhanced by the auto-contrasting tool. Scanned silver-stained 2-D gel images were manually overlaid with SYPRO Red/ProQ Diamond combined images or with western blot images by matching molecular weight markers and phosphoprotein spot patterns to determine phosphoproteins to excise for PMF (see below).

3.8 Mass Spectrometry

Selected proteins were excised from 2-D gels in a clean environment and placed in 96 well v-bottom polypropylene titre plates containing 50 µL of milliQ H_2O. The plate was covered with parafilm to avoid contamination and submitted for sample preparation and peptide mass fingerprinting mass spectrometry (MALDI-TOF) at the Queen's Proteomic Function Discovery Unit. Sample digestion was performed using the MicroMass MassPREP Robotic Protein Handling System. Excised protein samples were destained using 5mM potassium ferricyanide and 50mM sodium thiosulphate solution. Proteins were reduced and alkylated using 10mM DTT in 100mM ammonium bicarbonate for 30 minutes and 55mM iodoacetamide in 100mM ammonium bicarbonate for 20 minutes, respectively. Proteins were then washed with 100mM ammonium bicarbonate and dehydrated in 100% acetonitrile. Protein digestion was carried out using 6 ng/µL trypsin (Promega Sequencing Grade Modified Trypsin) in 25µL 50mM ammonium bicarbonate for 5 hours at 37°C. Peptides were extracted with 30µL of 1% (v/v) formic acid and 2% (v/v) acetonitrile solution followed by two extractions with 24µL of 50% (v/v) acetonitrile. The three extractions were pooled and evaporated to a 20uL volume using a speed vacuum. Digested peptides were prepared for PMF according to the dried droplet method (48) with a few modifications. Recrystallized alpha-cyano-4-hydroxy-cinnamic acid (Sigma) was prepared at a

concentration of 5mg/mL in 70% (v/v) acetonitrile, 0.1% (v/v) trifluoroacetic and 10mM diammonium citrate matrix solution. One µL of this solution was added to each sample spot on the MALDI target and allowed to dry. Digested peptides were mixed with the matrix solution at ratio of 1:1. One to 2µL of this mixture was applied to a target position and air dried. The sample was washed on the target with 1.5µL of cold ice cold 1.0% (v/v) trifluoroacetic acid for 10 seconds. Peptide standard was composed of angiotensin I (1.3kDa), [glu] fibrinopeptide (1.6kDa) and rennin (1.8kDa). Samples were analyzed using Voyager MALDI DE Pro and sample spectra were processed using Data Explorer 5.1 software (Applied Biosystems) and submitted for database searching via Mascot (Matrix Science, London, UK). The criteria used to accept identifications include the molecular weight search (MOWSE) score and whether theoretical molecular weight (+/- 20%) and pI (+/-1.0) of the matched proteins correlated with the experimental values. A minimum of 5 matched peptides within maximum tolerance for peptide mass matching of 50 ppm was used. The peptide mass fingerprinting analyses were carried out by Dr. Nancy Martin.

Chapter 4

Results

4.1 IHF is not an RdoA target

A hypothesized phosphorylation target of RdoA is IHF because these two proteins show similar phenotypes when either is deleted (77, 108). This suggested that IHF and RdoA may work in the same regulatory pathway. $Al(OH)_3$MOAC-enriched WT (NLM 2243) and *rdoA* null (NLM 2215) *S. typhimurium* phosphoproteins were analyzed to determine the presence or absence of IHF in these samples. Purified IHF (kindly provided by Dr. S. Goodman) was used as a positive experimental control. Induced and non-induced cell lysates of NLM 2361, a WT *S. typhimurium* strain containing pHX3-8 that encodes both *ihf* genes under the control of the tac promoter, were added as additional positive (with IPTG) and negative controls (without IPTG).

Silver stained gels showed no visible increase in IHF in cell lysates of NLM 2361 under inducing conditions compared to non-inducing conditions (Figure 7.A), but western blots showed that purified IHF was separated into two bands that corresponded to IhfA and IhfB (Figure 7.B). Also, immunoblots of NLM 2361 samples contained IHF under both induced and non-induced conditions. This is probably because WT IHF is normally highly abundant in stationary phase (4, 25). An increase in IHF expression was observed in inducing conditions due to overexpression of IHF via pHX3-8 (Figure 7. B). The plasmid pHX3-8 encodes two *ihfA* genes and one *ihfB* gene, but this was not reflected in these immunoblots because the IHF antiserum was more reactive to IhfB because of its higher antigenicity (Goodman, S., personal communication). Using WT and *rdoA* null $Al(OH)_3$ MOAC-enriched samples, the western blots using anti-IHF antibodies had two bands that aligned with the positive control, suggesting that these two bands are IHF (Figure 7.B).

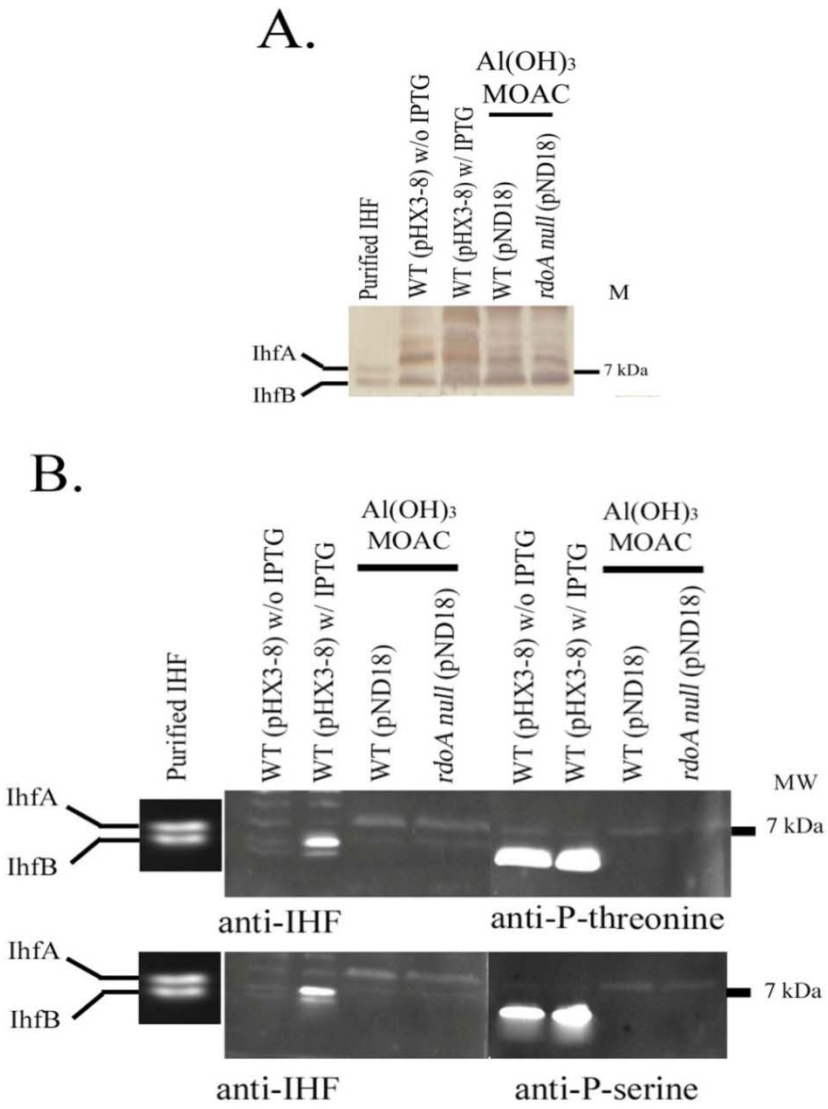

Figure 7. IHF is not an RdoA target. One-dimensional SDS-PAGE and western blot using anti-IHF, anti-phosphoserine and anti-phosphothreonine antibodies on $Al(OH)_3$ MOAC phosphoprotein-enriched samples to determine if IHF is RdoA's target. Samples were resolved in a 15% (w/v) 1-D gel and analyzed using western blot. A) Silver-stained 1-D gel; B) western blots using anti-IHF, anti-phosphoserine and anti-phosphothreonine antibodies. As a control, purified IHF (0.50 µg) and WT containing pHX3-8 were used. IHF was present in both WT and *rdoA* null *S. typhimurium* phosphoproteins. A band aligned to IhfA was observed in phosphoserine and phosphothreonine blots suggesting that this putative IHF is a phosphoprotein. Six µL of Prestained Marker Broad Range was used as a molecular weight reference.

This suggests that IHF is phosphorylated, but in an RdoA-independent manner since there is no discernable difference in the levels of IHF in the WT versus the *rdoA* null strain. Thus, IHF is not the target of RdoA. To confirm that this putative IHF is phosphorylated, the same samples were subjected to a western blot using anti-phosphoserine and anti-phosphothreonine antibodies. These blots showed that a band that comigrates with IhfA is phosphorylated at serine and threonine residues (Figure 7.B). There was a band that reacted strongly in the phosphoserine blots, found just below 7kDa (Figure 7.B), but this band did not correlate with the anti-IHF reactivity pattern suggesting that this protein was not IHF. To confirm this, western blots containing cell lysates obtained from different time points of IHF induction were analyzed using anti-IHF and anti-phosphoserine antibodies. These western blots showed an increase in IHF expression as induction time increased, however, the highly reactive band found in the anti-phosphoserine blot did not show a similar increase (Figure 8). These results suggested that the band found below the 7kDa marker in NLM2361 cell lysates is not IHF. In summary these experiments suggest that, while IhfA appears to be phosphorylated, IHF is not RdoA's target.

4.2 Comparison of Three Phosphoprotein Enrichment Techniques

Three different phosphoprotein enrichment protocols were examined in this study. Two are commercially produced kits, Qiagen's Phosphoprotein Purification Kit [PPK] and PerkinElmer's Phostag Enrich Kit [Phostag], while the third is a "home-made" kit, $Al(OH)_3$ Metal Oxide Affinity Chromatography [$Al(OH)_3$ MOAC] (151). These different enrichment kits were used to assess which is best suitable for enriching phosphoproteins from *S. typhimurium*. The proteins obtained from these kits were examined to determine similarities and differences in their ability to enrich phosphoproteins specifically. Total protein yields obtained from the 3 different phosphoprotein enrichment protocols were calculated based on several separate different biological and/or technical trials (Table 3).

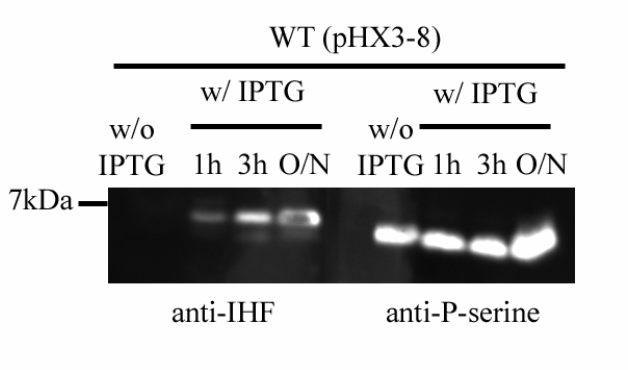

Figure 8. IhfB is not phosphorylated. One-dimensional SDS-PAGE and western blots using anti-IHF and anti-phosphoserine antibodies on induced and non-induced WT *S. typhimurium* containing pHX3-8 to confirm if an increase in IHF expression caused an increase in the aligned phosphoserine band. IHF blot showed an increasing amount of IHF as induction time was increased, however, the phosphoserine blot did not show the same pattern. Six µL of Prestained Marker Broad Range was used as a molecular weight reference.

Table 3. Total protein yield obtained from the
3 phosphoprotein enrichment methods

Technique	**Total Protein Yield***
$Al(OH)_3$ MOAC	6.59%
PPK	6.90%
Phostag**	19.28%

**Formula* = $\frac{\textit{End Protein Amount}}{\textit{Starting Protein Amount}}$ *X 100%*

*** Total protein yield was calculated using one replicate of 2 different biological samples due to the small amount of sample available.*

The Phostag protocol yielded 3 times more protein than the two other protocols while PPK and $Al(OH)_3$MOAC had the same protein yield. To determine the enrichment efficiency of each technique, flow-through samples and eluents obtained from each technique were resolved using 12% (w/v) 1-D SDS-PAGE (Figure 9). Flow-through samples showed generally similar major band patterns, while both similarities and differences in band profiles between eluents from the 3 different enrichment protocols were observed indicating that these matrices have different specificities for phosphoproteins. This difference could be due to different affinities for specific phosphorylated proteins or for non-phosphorylated proteins. Phostag appears to enrich the most abundant proteins more effectively than the two other protocols since less of the major proteins present in the eluent remained in the flow-through using Phostag (Figure 9).

Proteins eluted using these protocols were next assessed for actual phosphoprotein content. Eluents were analyzed using 1-D SDS-PAGE coupled with fluorescent staining and western blotting to determine the efficacy of each protocol to enrich for phosphoproteins versus non-phosphorylated proteins. Two μg of flow-through samples and eluents were loaded on a 12% (w/v) 1-D gel and fluorescently stained using ProQ Diamond, a phospho-specific stain, followed by SYPRO Red, a total protein stain. By comparing the intensity of the phospho-specific stain with that of the total protein stain, it was determined that all of the flow-through samples showed lower intensity phosphoprotein staining compared to their corresponding eluents (Figure 10). This indicated that all 3 methods retained significant amounts of phosphoproteins. PPK showed the highest intensity phosphoprotein staining compared to the two other protocols suggesting that PPK enriched most efficiently. A complicating factor to carrying out this work was that PerkinElmer, the company that distributes the Phostag kit, stopped distribution part way through this study. It should be noted that the experiment shown in Figure 10 was performed after multiple freeze-thaw cycles of the Phostag eluent, which may have caused degradation of some

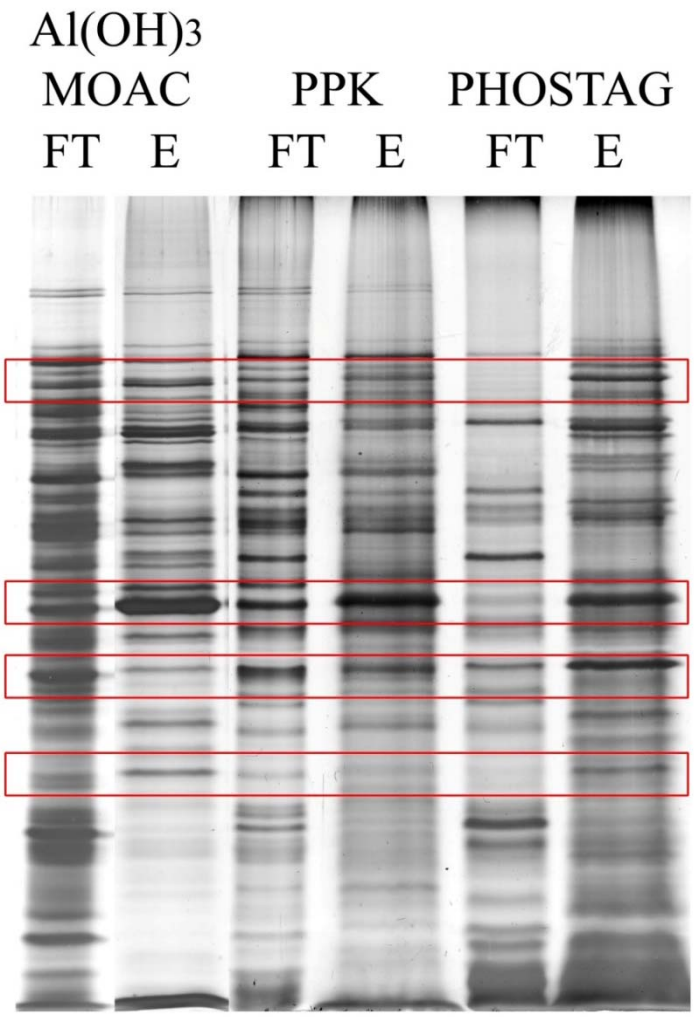

Figure 9. Enrichment efficiency of the 3 phosphoprotein enrichment methods. Two µg of flow-through (FT) and eluent (E) of the three different phosphoprotein enrichment protocols were resolved on a 12% (w/v) 1-D gel and visualized using silver staining. Red boxes highlight the most abundant proteins enriched differently by the 3 different protocols.

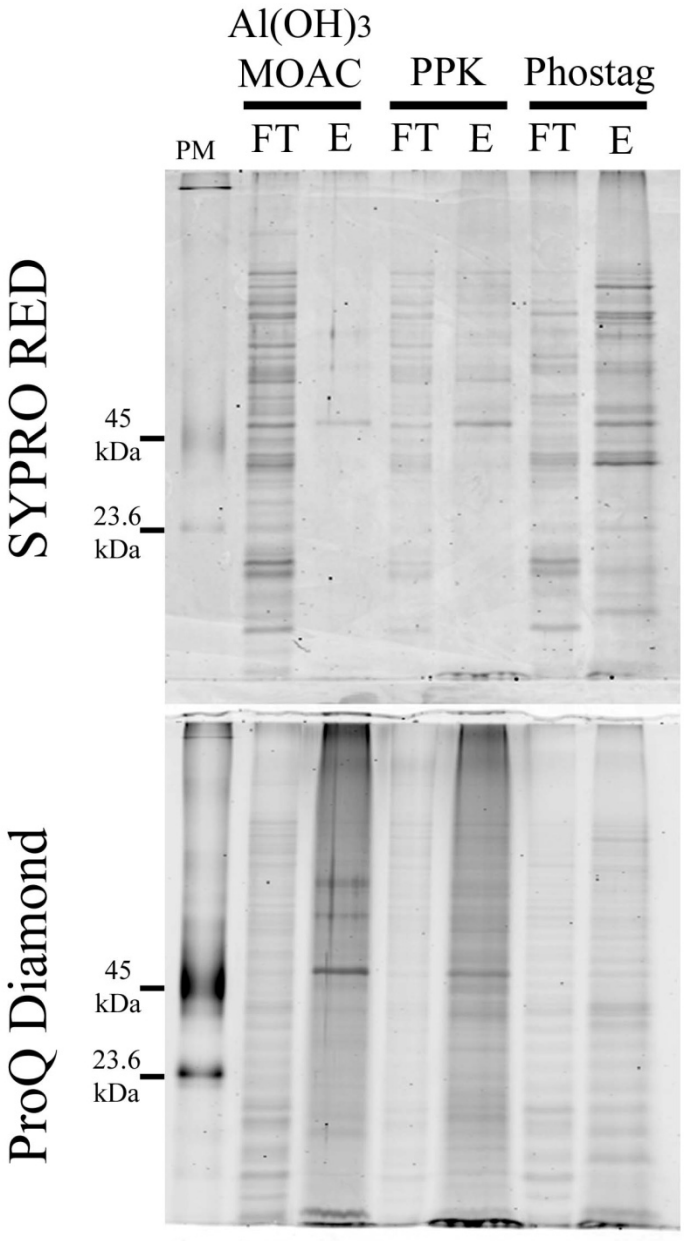

Figure 10. Fluorescent staining of flow-through and eluents from the 3 phosphoprotein methods. Flow-through (FT) and eluent(E) were resolved on a 12% (w/v) 1-D gel and analyzed using ProQ Diamond and SYPRO Red staining. Flow-through samples showed less phosphoprotein staining compared to eluents. PPK purified more phosphoproteins compared to the two other techniques, particularly in the lower molecular weight range. Peppermint Stick Molecular Weight Standards [PM] (0.025µg/µL) were added to each gel as a molecular weight standard and as a phosphoprotein control. Phosphorylated proteins in the PM were ovalbumin (45kDa) and β-casein (23.6kDa) while unphosphorylated protein (β-galactosidase at 116.25kDa) was not observed in this gel.

phosphoproteins. Results obtained from this experiment may therefore be an underestimation of Phostag's efficiency to enrich phosphoproteins. In addition to determining if the 3 protocols enrich predominantly phosphoproteins, the question of what type of phosphoproteins were being enriched was next explored.

Western blotting using anti-phosphoserine, anti-phosphothreonine and anti-phosphotyrosine antibodies was performed with PPK and $Al(OH)_3$ MOAC eluents (Figure 11). Phostag eluent was not included in this set of experiments because no sample was available. As a control to determine the phospho-specificity of the antibodies, eluents were subjected to phosphatase treatment. Phosphatase-treated PPK eluents showed lower signals compared to untreated eluents suggesting that the antibodies used were detecting phosphoproteins. A significant decrease in antibody binding was never detected in phosphatase-treated $Al(OH)_3$ MOAC eluents despite repeated attempts. The reason for this is not known, however, a similar phosphoserine and phosphothreonine profile is observed between PPK and $Al(OH)_3$ MOAC eluents suggesting that the signal detected in the $Al(OH)_3$ MOAC eluents is also due to phosphorylation. The phosphotyrosine profile showed a different band pattern compared to the phosphoserine and phosphothreonine profiles. Phosphoproteins between 45kDa-90kDa were detected by the antibodies. This observation was observed in all blots performed. In contrast, ProQ Diamond staining showed that phosphoproteins were observed outside this molecular weight range (Figure 10).

Using 1-D SDS-PAGE, proteins are separated according to their molecular mass, therefore, each band observed in a stained gel may consist of more than a single protein. A more in-depth analysis of the efficiency of the phosphoprotein enrichment techniques was therefore carried out by 2-D SDS-PAGE. Two-dimensional SDS-PAGE protein profiles were resolved and optimized with Phostag and PPK eluents. For $Al(OH)_3$ MOAC eluents, additional optimization is

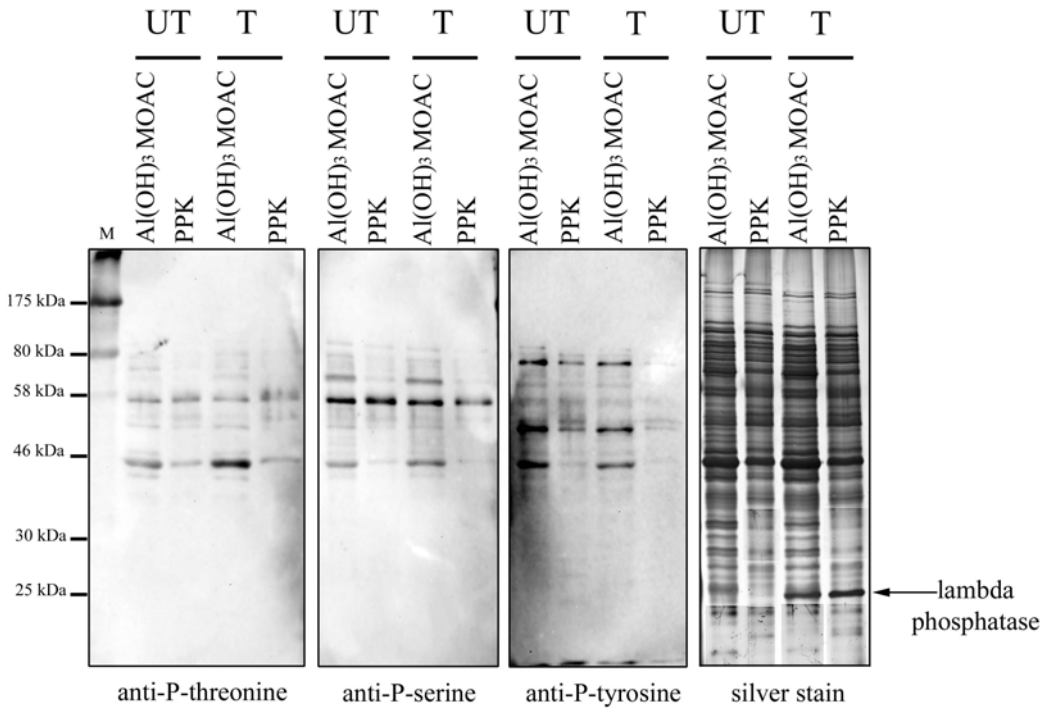

Figure 11. Western blot analyses of the eluents from the 2 phosphoprotein methods. Two μg of $Al(OH)_3$ MOAC and PPK eluents were subjected to lambda phosphatase or mock treatment. Treated (T) and untreated (UT) eluents were analyzed using 1-D SDS-PAGE and western blot analyses using anti-phosphoserine, anti-phosphothreonine and anti-phosphotyrosine antibodies. A decrease in phosphorylation is observed in phosphatase-treated PPK eluents compared to phosphatase-treated $Al(OH)_3$ MOAC eluents. The results suggest that both protocols enrich for phosphoproteins. Six μL of Prestained Marker Broad Range was used as a molecular weight reference.

still required to obtain a similar resolution to the two other techniques (Figure 12).

Protein spots were considered common to Phostag and PPK enrichment protocols, if they had the same MW, pI range and positions with respect to surrounding protein spots. Comparisons were made using pooled biological samples (28) which were run on at least 3 separate occasions. A total of 183 proteins were consistently observed in silver stained Phostag 2-D gels, while a total 165 proteins were observed in silver stained PPK 2-D gels. One hundred forty three proteins were observed to be common between the 2 techniques, indicating that the majority of the protein species were enriched by both protocols (Figure 13). The majority of the proteins identified were involved in heat shock, protein synthesis, central metabolism and the outer membrane (Figure 14 and Table 4). To determine if phosphorylation site(s) of identified proteins was consistent between *S. typhimurium* and other closely-related bacteria, sequences of known phosphorylated peptides from closely-related bacteria were compared and aligned to their corresponding sequences in *S. typhimurium*. If the sequence containing the phosphoamino acid was conserved between the 2 bacteria, it was concluded that phosphorylation on the same amino acid of the protein may occur in S. *typhimurium*. A comparison of these samples also showed differences in protein spots and patterns (Figure 15 and Table 5). Thirty seven protein spots (highlighted by blue circles) were found in only Phostag, while 23 protein spots (highlighted by red circles) were found only in PPK. Similar to changes in the banding patterns observed in 1-D SDS-PAGE, these differences may be due to different affinities of phosphoproteins for the matrices of the columns. Three protein spots that were found in Phostag enrichments only were identified as DnaK (protein spot # 180) and GroEL (protein spot 79 and 157) (Figure 15). These proteins were observed in both enrichments but at a different spot number, therefore, they were not included in Table 5 that lists proteins that were enriched by Phostag only.

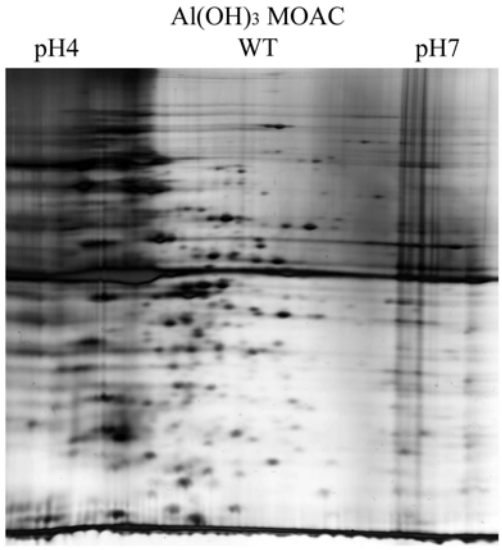

Figure 12. Two-dimensional SDS-PAGE protein resolution of $Al(OH)_3$ MOAC eluents. Sixteen µg of $Al(OH)_3$ MOAC WT *S. typhimurium* eluents were resolved using 2-D SDS-PAGE and silver stained. Additional optimization is needed to reduce streakiness and background observed at the low pH range(left).

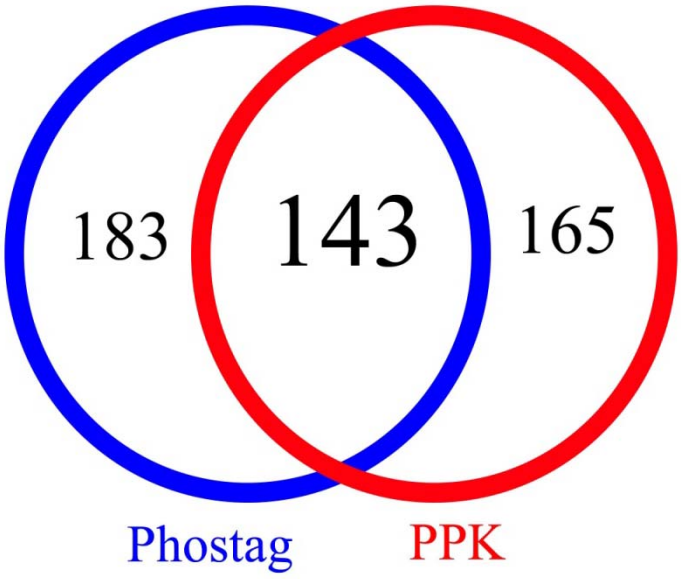

Figure 13. Common proteins found in both Phostag and PPK 2-D gels. A total of 183 reproducible protein spots were observed in Phostag 2-D gels (blue) while 165 reproducible protein spots were observed in PPK 2-D gels. Common protein spots observed between the two techniques were 143.

Figure 14. Commonly enriched proteins in Phostag and PPK 2-D gels. Sixteen µg of Phostag and PPK WT *S. typhimurium* eluents were resolved using 2-D SDS-PAGE and silver stained. Identified commonly enriched proteins were circled and numbered. The majority of the phosphoproteins identified were involved in heat shock, protein synthesis, central metabolism and the outer membrane (Table 4). The WT gels shown here are the same as in Figures 15 and 16.

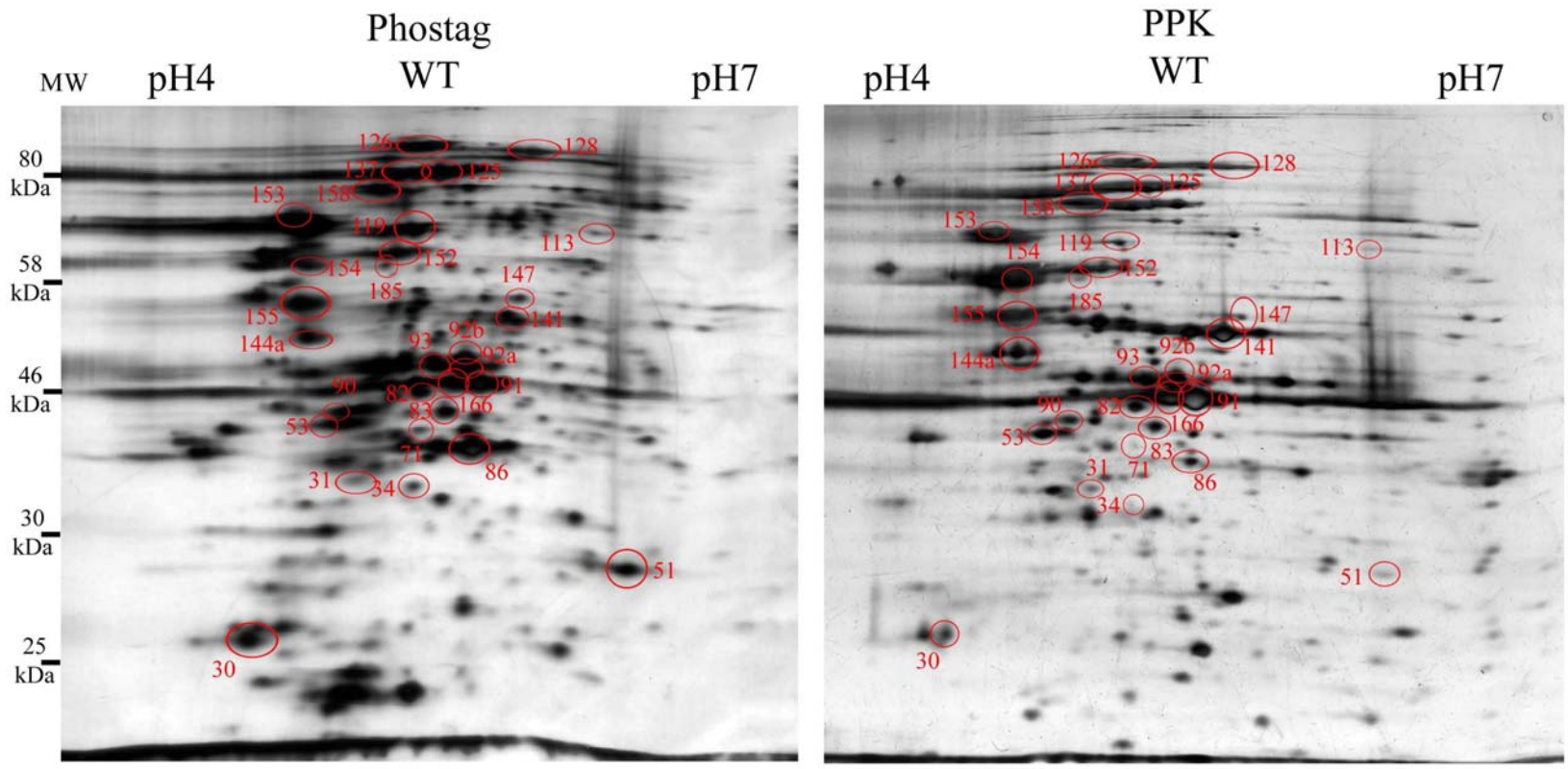
Phostag
WT
MW
pH4
pH7
80 kDa
58 kDa
46 kDa
30 kDa
25 kDa
126
128
137
6
125
153
158
119
113
154
152
147
185
155
141
144a
93
92b
92a
90
82
91
83
166
53
71
86
31
34
51
30
PPK
WT
pH4
pH7
126
128
137
125
153
158
154
119
113
152
185
147
155
141
144a
93
92b
92a
90
82
91
166
53
83
31
71
86
34
51
30

Table 4. Identity of commonly enriched proteins in Phostag and PPK 2-D gels.

Protein Function	Protein Identity	Gene Name	Phosphoprotein?	Species Studied	Spot #
Heat shock proteins or chaperones	ClpB/Hsp100	*clpB*	Y	*S. typhimurium*, enteropathogenic *E. coli* (115)	125
	DnaK/Hsp70	*dnaK*	Y	*E. coli* (82)	153
	GroEL/Cpn60	*groEL*	Y	*E. coli* (116)	154
	GrpE/Hsp 24	*grpE*	U		30
	HtpG/Hsp90	*htpG*	Y	*E. coli* (122)	119
	Trigger factor/TF (Tig)	*tig*	Y	*S. aureus* (69)	144a; 155
Protein synthesis machinery	Elongation factor/EF-Tu (TufA)	*tufA*	Y	*E. coli* (66)	31; 71; 82; 90; 91; 166
	Elongation Factor/EF-G (FusA)	*fusA*	Y	*E. coli* (109)	137; 158
	Lysine tRNA synthetase (LysRS)	*lysRS*	Y	*E. coli* (153)	152
	Protein translation initiation factor 2/ IF-2 (InfB)	*infB*	U		185
	30S ribosomal protein S1 (RpsA)	*rpsA*	Y	*E. coli* (31)	147
Outer membrane proteins	Outer membrane protein A (OmpA)	*ompA*	U		34
	Outer membrane protein 85/Omp85 (YaeT)	*yaeT*	U		not present in the figure
Central Metabolism	Aconitate hydratase 2 (AcnB)	*acnB*	Y	*E. coli* (71)	126
	Adenylosuccinate synthetase (PurA)	*purA*	U		92b
	Enolase (Eno)	*eno*	Y	*E. coli* (71)	92a; 93
	Glycerol kinase (GlpK)	*glpK*	U		141
	Malate dehydrogenase (MaeB)	*maeB*	U		113
	Pyruvate dehydrogenase E1 (AceE)	*aceE*	U		128
	Succinyl CoA synthetase beta chain (SucC)	*sucC*	Y	*E. coli* (13, 31)	83
	L-ribulose-5-phosphate 4-epimerase (AraD)	*araD*	U		51
Others	Putative alcohol dehydrogenase (YqhD)	*yghD*	U		86
	DNA-directed RNA polymerase alpha chain (RpoA)	*rpoA*	U		53

Legend: *Y = Yes*
U = Unknown

Figure 15. Proteins enriched by Phostag or PPK only. Sixteen μg of Phostag and PPK WT *S. typhimurium* eluents were resolved using 2-D SDS-PAGE and silver stained. Thirty seven protein spots (blue) were observed only in Phostag while 23 proteins (red) were observed only in PPK 2-D gels. Identified proteins excised from Phostag 2-D gels only are listed in Table 5. These protein differences were observed in multiple gels. The WT gels shown here are the same as in Figures 14 and 17.

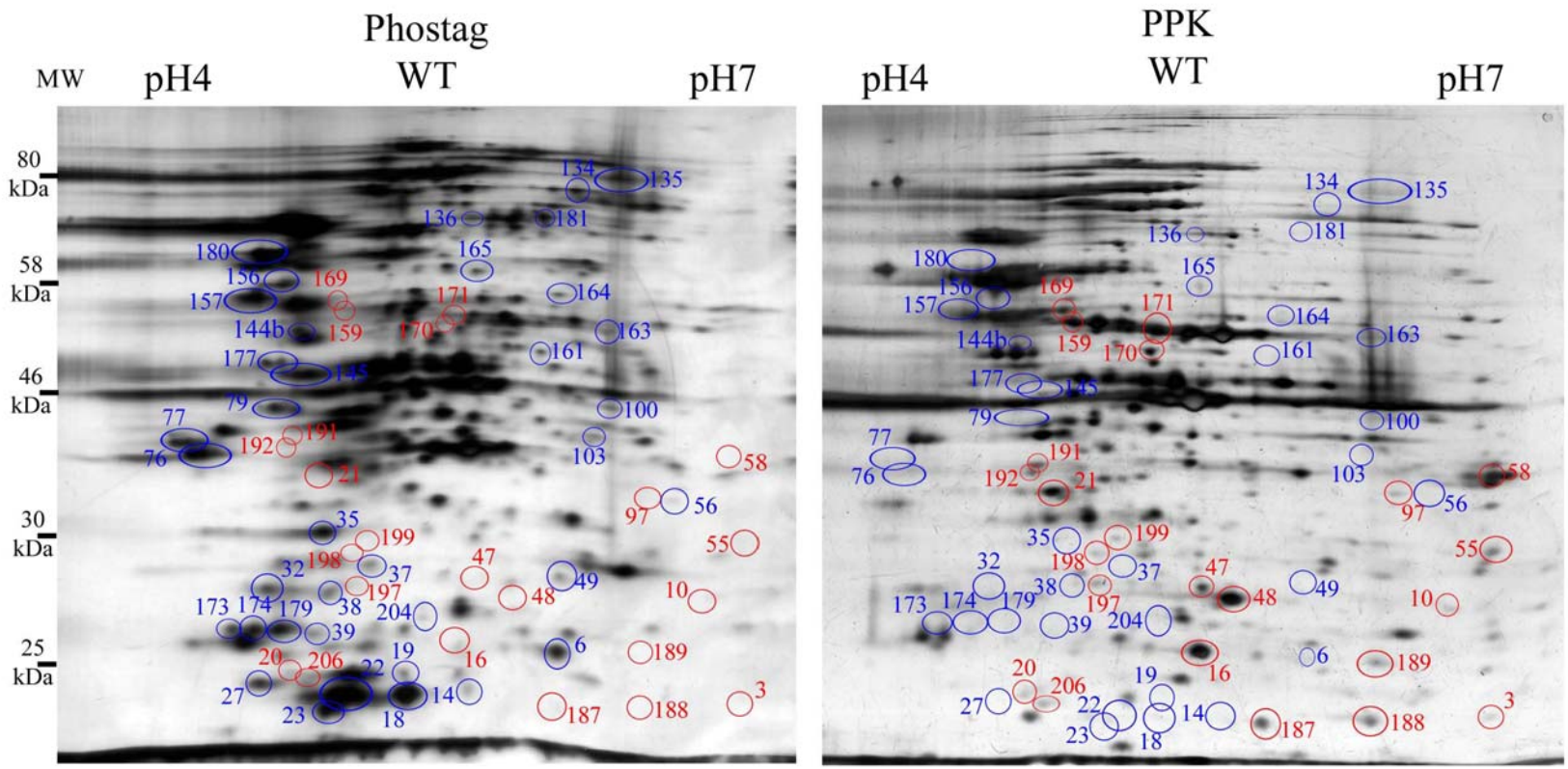
Phostag
MW
pH4
WT
pH7
80 kDa
58 kDa
46 kDa
30 kDa
25 kDa
134
135
136
181
180
165
156
169
157
171
164
144b
159
170
163
161
177
145
79
100
77
191
192
103
58
76
21
97
56
35
199
55
198
47
32
37
49
197
48
10
173
174
179
38
204
39
20
206
19
16
6
189
22
27
14
23
18
187
188
3
PPK
WT
pH4
pH7

Table 5. Identity of proteins enriched only by Phostag kit.

Protein Identity	**Gene Name**	**Phosphorylated?**	**Species Studied**	**Spot#**
Probable peroxidase	*ahpC*	U		18
Alkyl hydroperoxide reductase 22 (AhpF)	*ahpF*	U		22
Inorganic pyrophosphase (Ppa)	*Ppa*	U		23
30S ribosomal protein S1 (RpsA)	*rpsA*	Y	*E. coli* (31)	145
NlpE	*nlpE*	U		173
ATP synthetase subunit beta (AtpD)	*atpD*	U		144b

Legend: Y = Yes
U = Unknown

4.3 RdoA-dependent Changes in Protein Population

The primary focus of this study was to determine RdoA-dependent changes in phosphoprotein populations between a WT and *rdoA* null *S. typhimurium*. The strains used contain an NlpE-expressing plasmid, where expression of NlpE served to activate the Cpx pathway. RdoA expression was thereby up-regulated and RdoA-dependent protein changes between the 2 protein populations were sought. Finding the identities of the phosphoprotein changes was proposed to help elucidate the role of RdoA in *S. typhimurium's* stress response and, possibly, provide information on RdoA's target. To analyze these RdoA-dependent phosphoprotein population changes, eluents obtained from a phosphoprotein enrichment technique were analyzed by 2-D SDS-PAGE. Silver stained 2-D gels of Phostag (Figure 16) and PPK (Figure 17) eluents were analyzed manually to determine RdoA-dependent changes. Two criteria were used to determine if a protein was RdoA-dependent. First, if a protein spot was present or absent in WT versus an *rdoA* null *S. typhimurium* and vice-versa. Second, if a protein spot had increased or decreased in amount in WT versus an *rdoA* null S. *typhimurium*. A total of 45 RdoA-dependent proteins were observed in silver stained Phostag and PPK 2-D gels. Interestingly, a greater number of protein spots increased in abundance when RdoA was absent rather than present. Since RdoA is part of a stress response pathway, it is hypothesized that these proteins, which may be stress response proteins, are expressed and/or phosphorylated to make up for the absence of RdoA in cell survival. These RdoA-dependent protein spots were numerically labeled, excised and identification was attempted using PMF to determine if this hypothesis proved to be true (Table 6).

4.4 RdoA-dependent Changes in Phosphoproteins

Two different protein detection methods were performed to determine RdoA-dependent phosphoprotein population changes between WT and *rdoA* null *S. typhimurium*. The first method

Figure 16. RdoA-dependent proteins found in Phostag silver stained 2-D gels. Manual comparison of Phostag WT and *rdoA* null *S. typhimurium* silver stained 2-D gels showed 17 protein spots increased in the absence of RdoA (blue) and 5 protein spots increased in the presence of RdoA (red). RdoA-dependent proteins highlighted were observed in multiple trials. Phostag WT *S. typhimurium* 2-D gel is also shown in Figures 14 and 15.

PHOSTAG

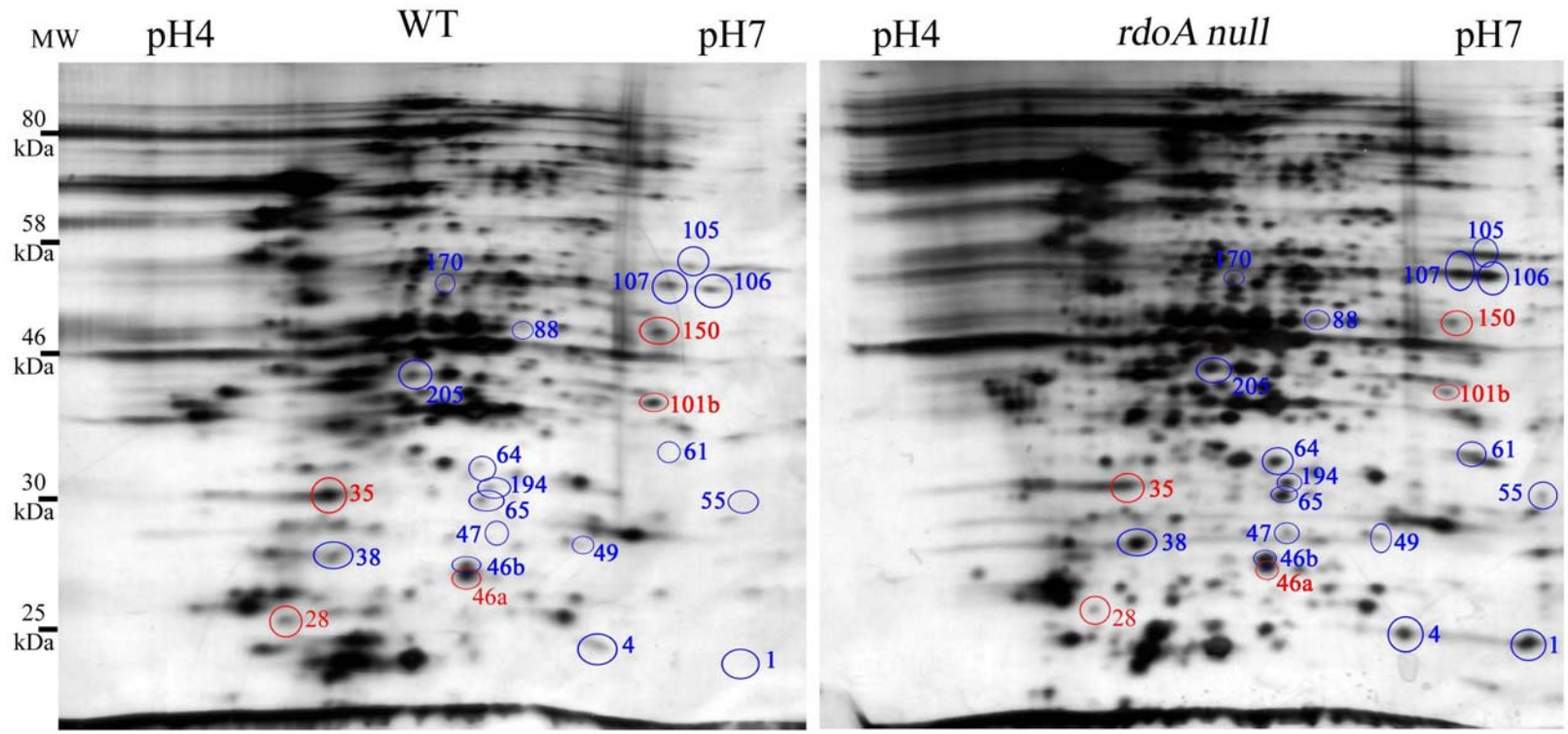
MW
pH4
WT
pH7
pH4
rdoA null
pH7
80 kDa
58 kDa
46 kDa
30 kDa
25 kDa
105
170
107
106
88
150
205
101b
61
64
194
65
55
35
47
38
49
46b
46a
28
4
1

Figure 17. RdoA-dependent proteins found in PPK silver stained 2-D gels. Manual comparison of PPK WT and *rdoA* null *S. typhimurium* silver stained 2-D gels showed 18 protein spots increased in the absence of RdoA (blue) and 7 proteins increased in the presence of RdoA (red). RdoA-dependent proteins highlighted were observed in multiple trials. PPK WT *S. typhimurium* 2-D gel is also shown in Figures 14 and 15.

PPK

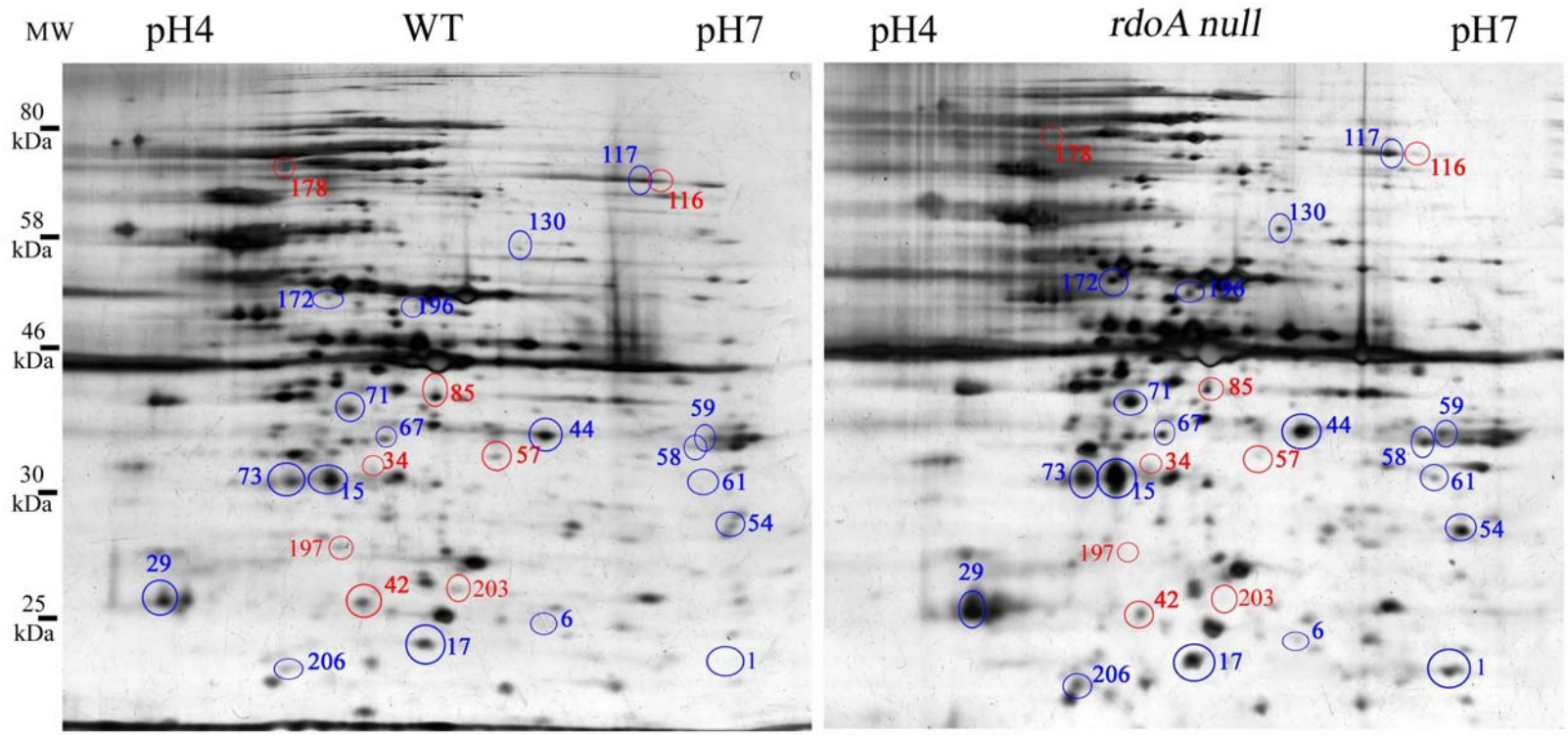
MW
pH4
WT
pH7
pH4
rdoA null
pH7
80 kDa
58 kDa
46 kDa
30 kDa
25 kDa
178
117
116
130
172
196
71
85
67
44
59
58
34
57
73
15
61
54
197
29
42
203
6
17
206
1

Table 6. Successfully identified RdoA-dependent proteins enriched by Phostag and PPK.

Spot #	**WT**	***rdoA-***	**Technique Observed**	**Protein Identity**	**Gene Name**	**Phosphoprotein?**	**Species Studied**
1	-	+	Phostag/PPK	SrgA	*srgA*	U	
34	+	-	PPK	Outer Membrane Protein (OmpA)	*ompA*	U	
71	-	+	PPK	Elongation Factor/EF-Tu (TufA)	*tufA*	Y	*E. coli* (66)

Legend: + = Present or increase in protein amounts
- = Absent or decrease in protein amounts
Y = *Yes*
U = *Unknown*

used fluorescent stains, specifically ProQ Diamond and SYPRO Red stains. As mentioned previously, ProQ Diamond staining is specific for phosphorylated proteins while SYPRO Red stain is a total protein stain. Eluents were subjected to 2-D SDS-PAGE and fluorescent staining as described in the methodology. Gels were imaged and manually overlaid to help to localize ProQ stained phosphoproteins and to assess the specificity of the ProQ stain. When compared with the silver stained gels (Figure 18.A), SYPRO Red staining was much less sensitive, however, the SYPRO Red/ProQ Diamond overlays showed that a few proteins were highly phosphorylated (Figure 18.B). Most of the protein spots did not appear to be phosphorylated using this method. The putative phosphoproteins determined by this staining procedure were excised for identification by PMF using MS (Figure 18 and Table 7).

SYPRO Red/ProQ Diamond overlay of Phostag eluents showed a total of 7 phosphoproteins (Table 7). An RdoA-dependent phosphoprotein (spot #121) was found only in the absence of RdoA. Other RdoA-independent phosphoproteins that were successfully identified using PMF are elongation factor G (spot #137) and 30S ribosomal protein subunit 1 (spot #147). The same analyses using PPK eluents showed a total of 8 phosphoproteins in multiple trials (Figure 19). Two of these 8 phosphoproteins were observed to be RdoA-dependent. Protein spot #50 was phosphorylated only in WT, while protein spot #138 was phosphorylated in the absence of RdoA.

It appeared that the lack of sensitivity of ProQ Diamond staining may have underestimated the amount of phosphorylated proteins in the enriched fractions. In order to assess these phosphoprotein-enriched samples further, western blot analyses were performed using anti-phosphoserine and anti-phosphothreonine antibodies. As controls for the specificity of the anti-phospho-specific antibodies, phosphatase treated eluents were also examined. Phosphatase-treated eluents showed very minimal detectable spots indicating dephosphorylation of phosphoproteins (data not shown). This suggests that the majority of the proteins detected by the

Figure 18. Two-dimensional SDS-PAGE and fluorescent staining of Phostag-enriched WT and *rdoA* null *S. typhimurium* eluents. Phostag-enriched WT & *rdoA* null *S. typhimurium* proteins were resolved using 2-D SDS-PAGE. Phosphoproteins were analyzed using ProQ Diamond staining, SYPRO Red staining and silver staining. A) Silver-stained 2-D gels. B) SYPRO Red/ProQ Diamond overlay of Phostag WT 2-D gels (left) and SYPRO Red/ProQ Diamond overlay of Phostag *rdoA* null 2-D gels (right). Phosphorylated proteins are shown as black spots and highlighted with black arrows. Protein spot #121 is shown to be phosphorylated in the absence of RdoA (inset on the right). Phosphoproteins that were successfully identified are elongation factor G (protein spot # 137) and 30S ribosomal protein S1 (protein spot # 147). Peppermint Stick Molecular Weight Standards [PM] (0.025µg/µL) were added to each gel as a molecular weight standard and as a phosphoprotein control. Phosphorylated proteins in the PM were ovalbumin (45kDa) and β-casein (23.6kDa) while unphosphorylated protein was β-galactosidase (116.25kDa).

A.

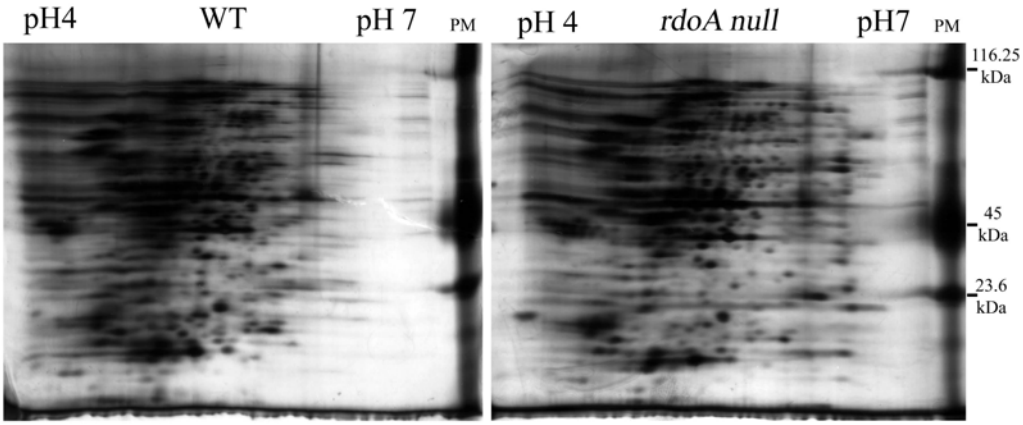
pH4
WT
pH 7
PM
pH 4
rdoA null
pH7
PM
116.25 kDa
45 kDa
23.6 kDa

B.

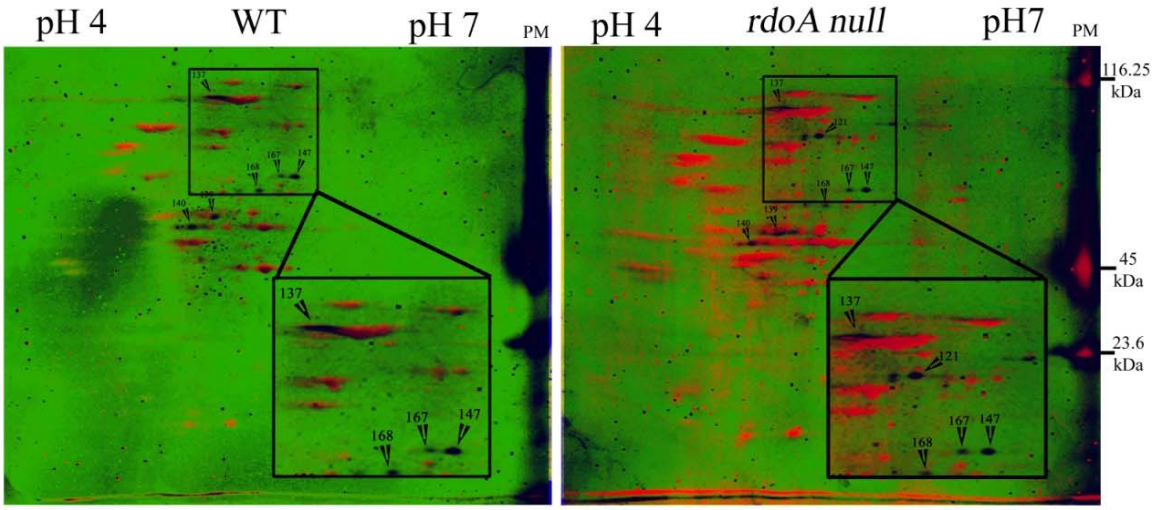
pH 4
WT
pH 7
PM
pH 4
rdoA null
pH7
PM
116.25 kDa
45 kDa
23.6 kDa
137
168
167
147
121

Table 7. Phosphoproteins observed in 2-D SDS-PAGE and fluorescent staining of Phostag samples.

Spot #	**WT**	***rdoA-***	**Protein Identity**	**Gene Name**	**Phosphoprotein?**	**Species Studied**
137	P	P	Elongation Factor G/ EF-G (FusA)	*fusA*	Y	*E. coli* (71)
147	P	P	30S ribosomal protein S1 (RpsA)	*rpsA*	Y	*E.coli* (31)

Legend: P=Phosphorylated
N=Not Phosphorylated
Y=Yes

Figure 19. Two-dimensional SDS-PAGE and fluorescent staining of PPK-enriched WT and *rdoA* null *S. typhimurium* eluents. PPK-enriched WT & *rdoA* null *S. typhimurium* proteins were resolved using 2-D SDS-PAGE. Phosphoproteins were analyzed using ProQ Diamond staining, SYPRO Red staining and silver staining. A) Silver-stained 2-D gels. B) SYPRO Red/ProQ Diamond overlay of PPK WT 2-D gels (left) and SYPRO Red/ProQ Diamond overlay of PPK *rdoA* null 2-D gels (right). Phosphorylated proteins are shown as black spots and highlighted with black arrows. Protein spot # 50 was observed to be phosphorylated in WT only, while protein spot # 138 was observed to be phosphorylated in *rdoA* null. Peppermint Stick Molecular Weight Standards [PM] (0.025 μg/μL) were added to each gel. Phosphorylated proteins in the PM were ovalbumin (45 kDa) and β-casein (23.6 kDa) while unphosphorylated protein was β-galactosidase (116.25 kDa).

A.

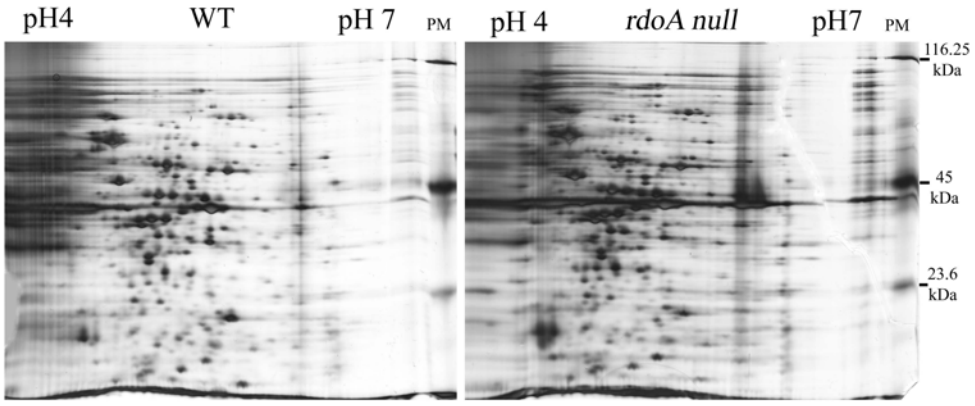
pH4
WT
pH 7
PM
pH 4
rdoA null
pH7
PM
116.25 kDa
45 kDa
23.6 kDa

B.

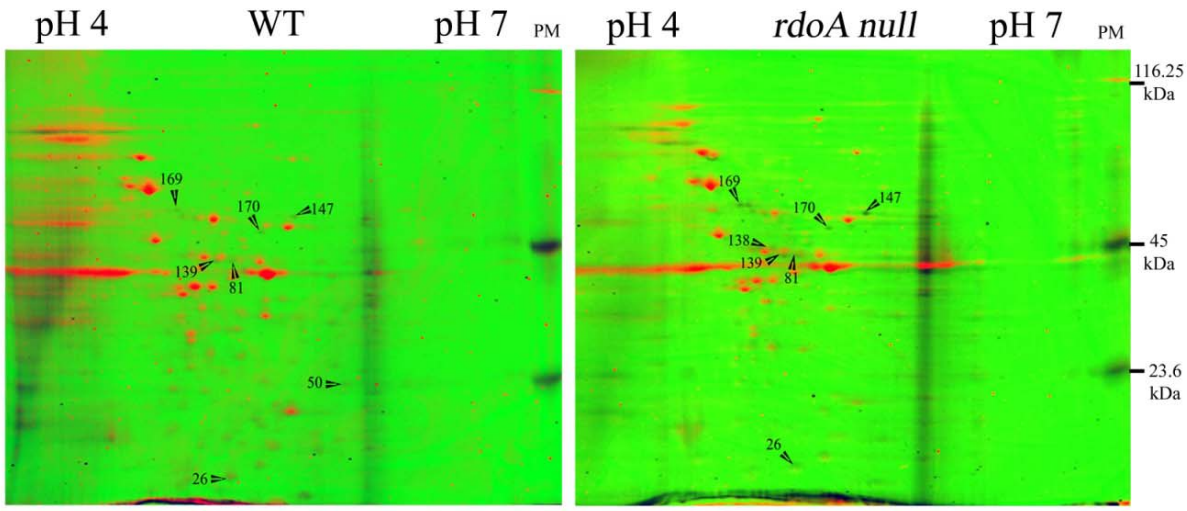
pH 4
WT
pH 7
PM
pH 4
rdoA null
pH 7
PM
169
170
147
139
81
50
26
138
116.25 kDa
45 kDa
23.6 kDa

anti-phosphoserine and anti-phosphothreonine antibodies were phosphoproteins. Western blots provided higher levels of phosphoprotein detection compared to fluorescent staining. Western blots were overlaid with the corresponding silver stained 2-D gels to determine if signals were due to proteins present in high enough levels to attempt PMF.

The phosphoproteome profile of WT versus the *rdoA* null *S. typhimurium* showed several phosphoproteins affected by RdoA. A total of 73 RdoA-dependent phosphoprotein changes were observed, consisting of 27 phosphothreonine proteins, 23 phosphoserine proteins and 23 proteins phosphorylated at both residue(s). RdoA-dependent proteins observed in Phostag and PPK silver-stained 2-D gels (Figures 16 and 17) were compared with phosphoproteins detected by western blotting. Out of 45 RdoA-dependent changes in proteins found in Phostag and PPK silver-silver stained 2-D gels, 10 of these proteins were detected using phospho-specific antibodies (Table 8).

Phosphoproteins with a significant change in the level of anti-phospho antibody reactivity (8 phosphoserine proteins, 10 phosphothreonine proteins and 6 proteins phosphorylated at both residues) were highlighted using western blotting (Figures 20-23and Tables 9-11). Identification of these RdoA-dependent phosphoproteins by PMF indicated a range of cellular functions including protein synthesis, heat shock response systems and central metabolism. Phosphorylated proteins observed in these western blots were compared to the corresponding silver stained 2-D gels (Figures 16 and 17) to determine if the signal obtained was due to changes in protein amount or due to phosphorylation. Most of the phosphoproteins observed did not change in protein amount between a WT and *rdoA* null *S. typhimurium* 2-D gel (Table 12), indicating changes in phosphorylation. Interestingly, more proteins were highly phosphorylated in the presence of RdoA in Phostag compared to PPK, while PPK showed an increase in protein phosphorylation in the absence of RdoA compared to Phostag. In addition, a higher number of phosphoserine proteins were found to be highly phosphorylated than phosphothreonine proteins. During this

Table 8. Phosphorylation patterns in RdoA-dependent proteins observed in silver stained and western blots of Phostag and PPK eluents.

Spot #	Protein Identity	Silver Stains		Technique Observed	P-Site	Western blot	
		WT	*rdoA-*			WT	*rdoA-*
15	Unidentified	-	+	PPK	Ser	-	+
35	Unidentified	+	-	Phostag	Thr	-	+
38	Unidentified	-	+	Phostag	Ser	-	+
44	Unidentified	-	+	PPK	Ser	-	+
46b	Unidentified	-	+	Phostag	Thr	-	+
59	Unidentified	-	+	PPK	Ser	-	+
67	Unidentified	-	+	PPK	Ser	-	+
116	Unidentified	+	-	PPK	Thr	+	-
117	Unidentified	-	+	PPK	Thr	-	+
178	Unidentified	+	-	PPK	Ser	+	-

Legend: *+ = Present or increase in spot intensity*
- = Absent or decrease in spot intensity
P-site = Phosphorylation Site

Figure 20. RdoA-dependent phosphothreonine protein changes of Phostag-enriched WT and *rdoA* null *S. typhimurium* eluents. Phostag-enriched WT and *rdoA* null *S. typhimurium* eluents were analyzed using 2-D SDS-PAGE and western blotting using anti-phosphothreonine antibodies. Blue arrows highlight phosphothreonine proteins that are phosphorylated in the presence of RdoA while red arrows highlight those that are phosphorylated in the absence of RdoA. Identified phosphothreonine proteins are listed in tables 9 and 11. Phosphoproteins highlighted have significantly changed in phosphorylation and were observed in multiple trials. Black spots with yellow 'X' are not protein spots but are background noise that arose during western blot imaging. Six µL of Prestained Marker Broad Range was used as a molecular weight reference.

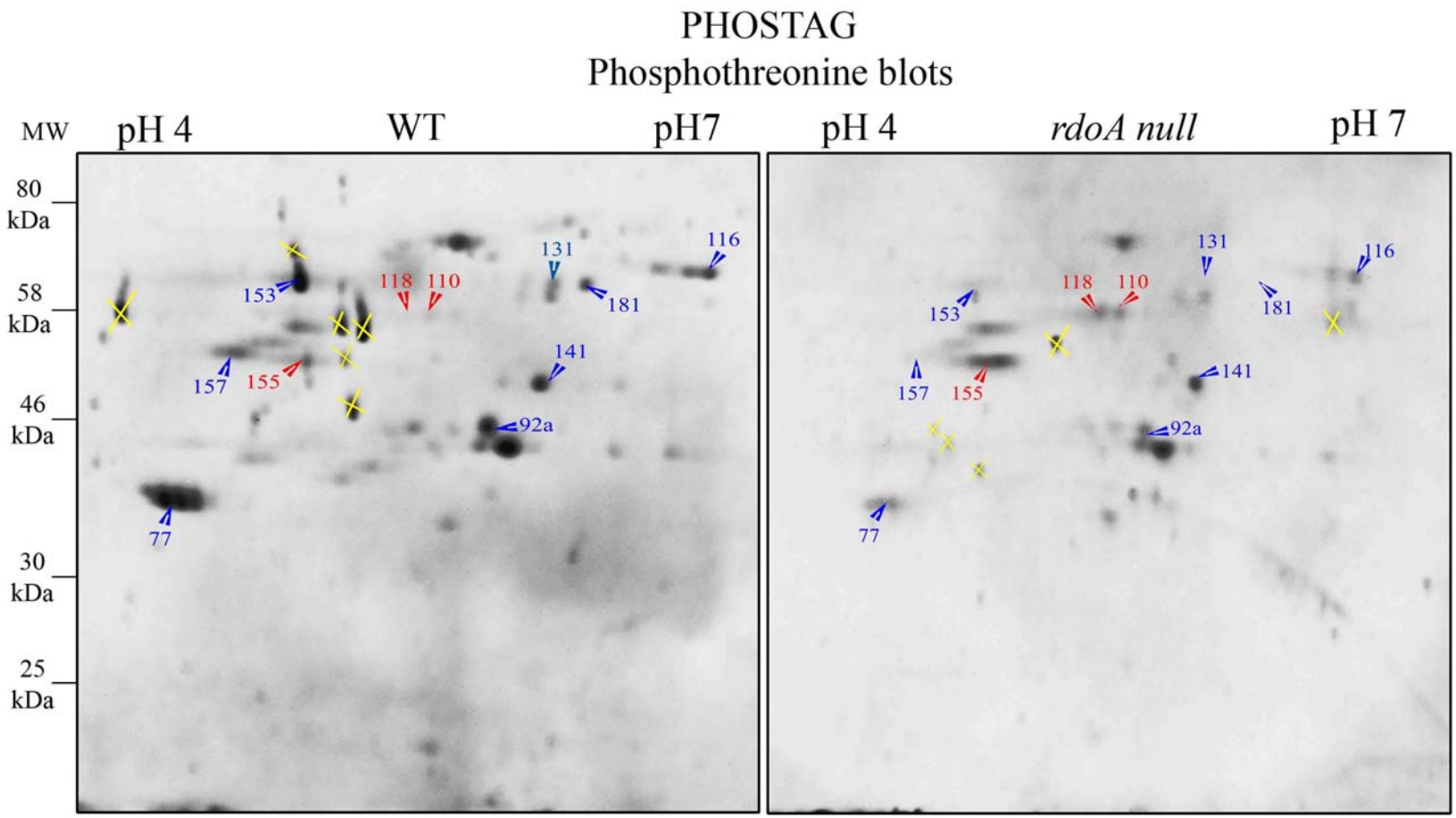
PHOSTAG
Phosphothreonine blots
MW
pH 4
WT
pH7
pH 4
rdoA null
pH 7
80 kDa
58 kDa
46 kDa
30 kDa
25 kDa
153
118
110
131
116
181
157
155
141
92a
77

Figure 21. RdoA-dependent phosphothreonine protein changes of PPK-enriched WT and *rdoA* null *S. typhimurium* eluents. PPK-enriched WT and *rdoA* null *S. typhimurium* eluents were analyzed using anti-phosphothreonine antibodies. Red arrows highlight phosphoproteins with significant changes in phosphorylation in the absence of RdoA. Identified phosphothreonine proteins are listed in tables 9 and 11. Black spots with yellow 'X' are not protein spots but are background noise that arose during western blot imaging. Six μL of Prestained Marker Broad Range was used as a molecular weight reference.

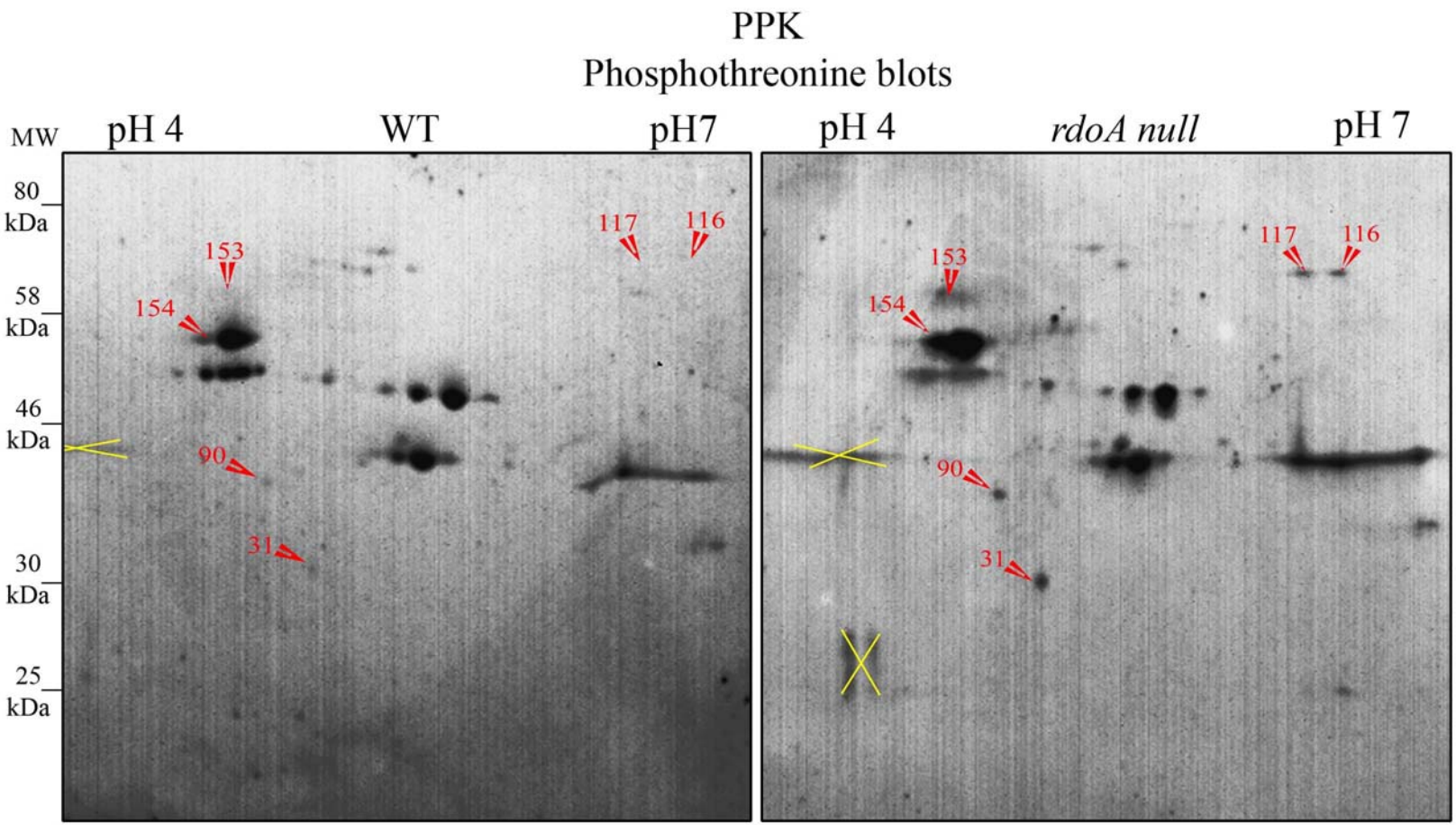
PPK
Phosphothreonine blots
MW
pH 4
WT
pH7
pH 4
rdoA null
pH 7
80 kDa
58 kDa
46 kDa
30 kDa
25 kDa
153
154
90
31
117
116
153
154
90
31
117
116

Table 9. Identified RdoA-dependent phosphothreonine proteins that significantly changed in phosphorylation observed in 2-D gels and western blots analyses of Phostag and PPK eluents.

Spot #	Phosphothreonine blot		Technique Observed	Protein Identity	Gene Name	Phosphoprotein?	Species Studied
	WT	***rdoA-***					
90	-	+	PPK	Elongation factor Tu/ EF-Tu (TufA)	*tufA*	Y	*E. coli* (66, 71)
31	-	+	PPK	Elongation factor Tu/EF-Tu (TufA)	*tufA*	Y	*E. coli* (66, 71)
153	+	-	Phostag	DnaK/Hsp70	*dnaK*	Y	*E. coli* (71, 82)
	-	+	PPK				

Legend: + = Present or increase in spot intensity
- = Absent or decrease in spot intensity
Y = Yes
U = Unknown

Figure 22. RdoA-dependent phosphoserine protein changes of Phostag-enriched WT and *rdoA* null *S. typhimurium* eluents. Phostag-enriched WT and *rdoA* null *S. typhimurium* eluents were analyzed using 2-D SDS-PAGE and western blotting using anti-phosphoserine antibodies. Blue arrows highlight phosphoserine proteins that are phosphorylated in the presence of RdoA. Phosphoproteins highlighted have significantly changed in phosphorylation and were observed in multiple trials. Identified phosphoserine proteins are listed in tables 10 and 11. Six μL of Prestained Marker Broad Range was used as a molecular weight reference.

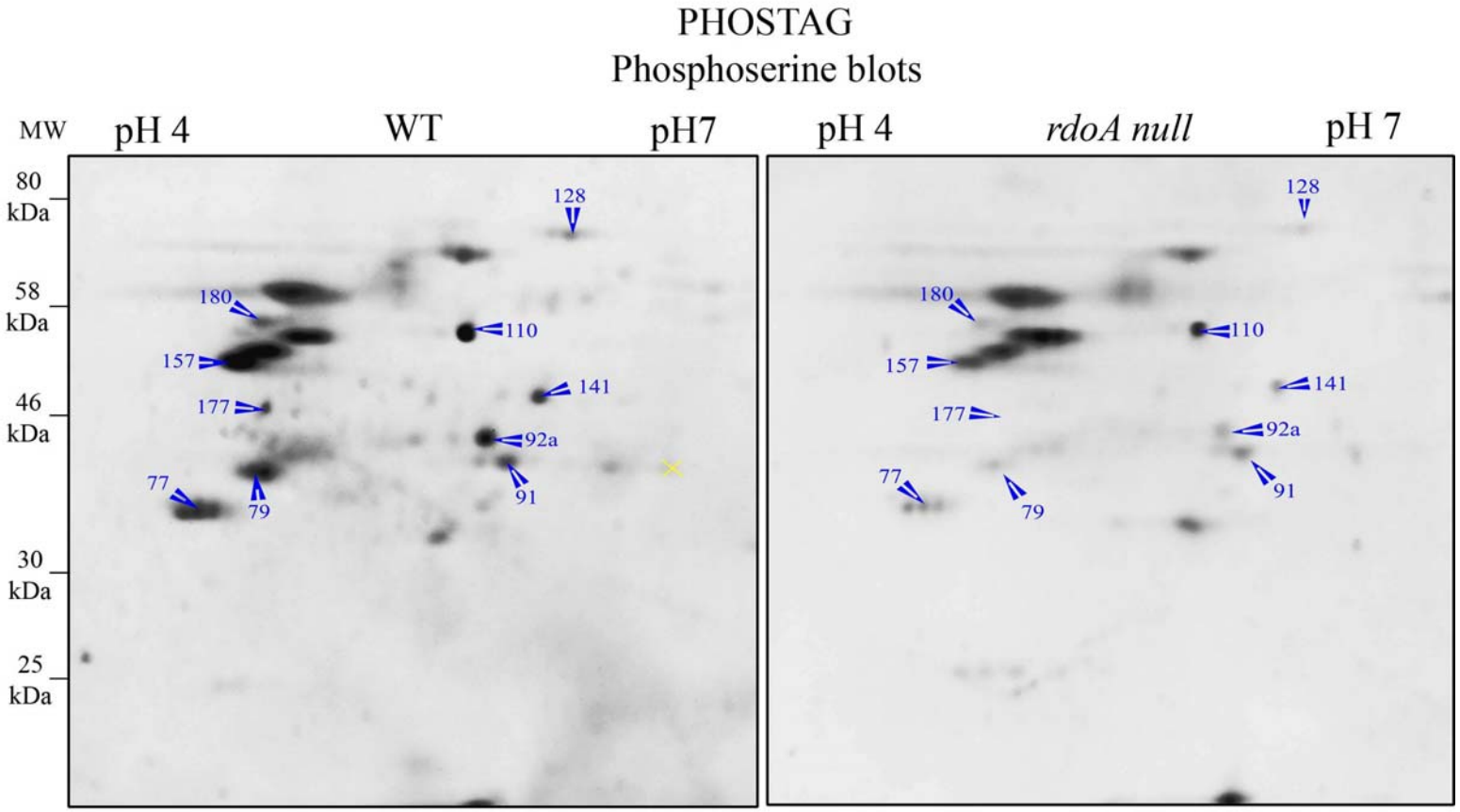
PHOSTAG
Phosphoserine blots
MW
pH 4
WT
pH7
pH 4
rdoA null
pH 7
80 kDa
58 kDa
46 kDa
30 kDa
25 kDa
128
180
110
157
141
177
92a
77
79
91

Figure 23. RdoA-dependent phosphoserine protein changes of PPK-enriched WT and *rdoA* null *S. typhimurium* eluents. PPK-enriched WT and *rdoA* null *S. typhimurium* eluents were analyzed using 2-D SDS-PAGE and western blotting using anti-phosphoserine antibodies. Blue arrows highlight phosphoserine proteins that are phosphorylated in the presence of RdoA while red arrows highlight those in the absence of RdoA. Phosphoproteins highlighted have significantly changed in phosphorylation and were observed in multiple trials. Identified phosphoserine proteins are listed on table 10 and 11. Six μL of Prestained Marker Broad Range was used as a molecular weight reference.

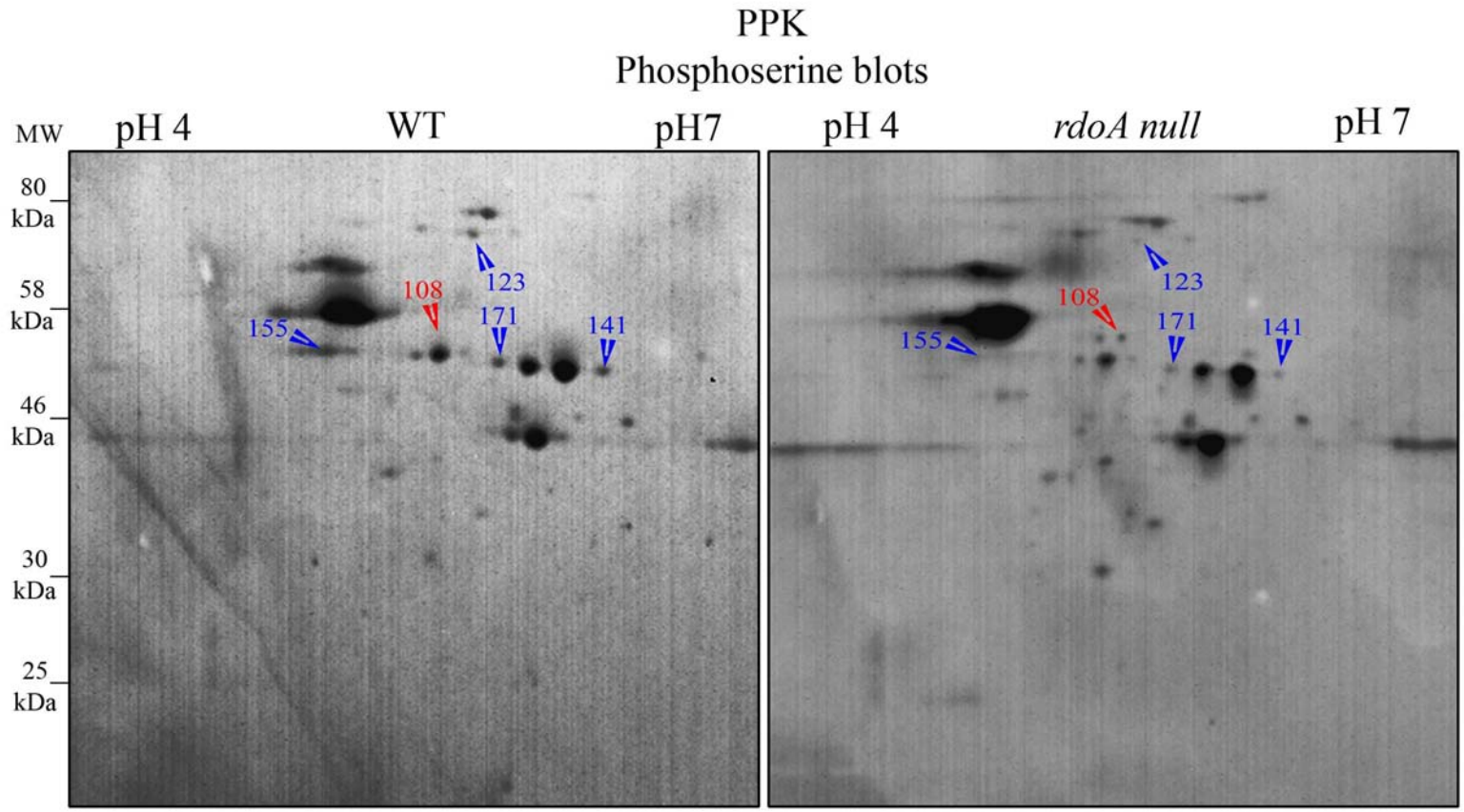
PPK
Phosphoserine blots
MW
pH 4
WT
pH7
pH 4
rdoA null
pH 7
80 kDa
58 kDa
46 kDa
30 kDa
25 kDa
155
108
123
171
141
155
108
123
171
141

Table 10.Identified RdoA-dependent phosphoserine proteins that have significantly changed in phosphorylation observed in 2-D gels and western blot analyses of Phostag and PPK eluents.

Spot #	Phosphoserine blot		Technique Observed	Protein Identity	Gene Name	Phosphoprotein?	Species Studied
	WT	***rdoA-***					
79	+	-	Phostag	GroEL/Cpn60	*groEL*	Y	*E. coli* (116)
91	+	-	Phostag	Elongation factor Tu/EF-Tu (TufA)	*tufA*	Y	*E. coli* (66, 71)
128	+	-	Phostag	Pyruvate dehydrogenase E1	*aceE*	U	
141	+	-	PPK	Glycerol kinase (GlpK)	*glpK*	U	
180	+	-	Phostag	DnaK protein	*dnaK*	Y	*E. coli* (82)

Legend: + = Present or increase in spot intensity
- = Absent or decrease in spot intensity
Y = Yes
U = Unknown

Table 11. Identified RdoA-dependent proteins phosphorylated at serine and threonine residues in 2-D SDS-PAGE and western blot analyses of Phostag and PPK eluents.

Spot #	**WT**	***rdoA-***	**Technique Observed**	**Protein Identity**	**Gene Name**	**Phosphoprotein?**	**Species Studied**
92a	+	-	Phostag	Enolase (Eno)	*eno*	Y	*E. coli* (71)
141	+	-	Phostag	Glycerol kinase (GlpK)	*glpK*	U	
157	+	-	Phostag	GroEL/Cpn60	*groEL*	Y	*E. coli* (116)

Legend: + = Present or increase in spot intensity
- =Absent or decrease in spot intensity
Y =Yes
U = Unknown

analysis, identified phosphoproteins, namely DnaK, GroEL and EF-Tu, were observed in multiple spots.

Lastly, comparing these immunoblots to the Phostag SYPRO Red/ProQ Diamond overlay 2-D gels (Figure 18), protein spot # 121 was not detected in the anti-phosphoserine or anti-phosphothreonine immunoblots (Figures 20 and 22). This suggests that this protein may be phosphorylated at its tyrosine residue(s). For the PPK SYPRO Red/ProQ Diamond overlay 2-D gels (Figure 19), RdoA-dependent phosphoprotein # 138 was observed to be phosphorylated at serine residue(s) in the absence of RdoA but did not show a significant change in phosphorylation. RdoA-dependent phosphoprotein #50 was not detected in any of the PPK western blots (Figure 21 and 23).

Table 12. Comparison of RdoA-dependent phosphoproteins observed in western blots and silver-stained 2-D gels.

Protein Identity	Gene Name	P-protein?	Species Studied	Technique Observed	P- Site	Western blot		Silver Stains		Spot #
						WT	*rdoA-*	WT	*rdoA-*	
GroEL/ Cpn60	*groEL*	Y	*E. coli* (116)	Phostag	Ser	+	-	nd	nd	79
				Phostag	Ser & Thr	+	-	nd	nd	157
Elongation factor Tu/ EF-Tu (TufA)	*tufA*	Y	*E. coli* (66, 71)	PPK	Thr	-	+	nd	nd	31
				PPK	Thr	-	+	nd	nd	90
				Phostag	Ser	+	-	nd	nd	91
Enolase (Eno)	*eno*	Y	*E. coli* (71)	Phostag	Ser & Thr	+	-	nd	nd	92a
Pyruvate dehydrogenase E1	*aceE*	Y	*E. coli* (71)	Phostag	Ser	+	-	nd	nd	128
Glycerol kinase (GlpK)	*glpK*	U		Phostag	Ser & Thr	+	-	nd	nd	141
				PPK				nd	nd	
DnaK/Hsp70	*dnaK*	Y	*E. coli* (71, 82)	Phostag	Thr	+	-	nd	nd	153
				PPK	Thr	-	+	nd	nd	
				Phostag	Ser	+	-	nd	nd	180

Legend: + = Present or increase in spot intensity
- = Absent or decrease in spot intensity
Y = Yes
U = Unknown
Nd =No difference
P-site = Phosphorylation Site
P-protein = Phosphoprotein

Chapter 5

Discussion

5.1 IHF as a target of RdoA kinase activity

Richards (108) hypothesized that IHF may be RdoA's target based on the appearance of similar *S. typhimurium* phenotypic characteristics if either of these genes were deleted. In addition, computer modeling using the crystal structures of IHF and YihE (158) suggested that IHF could be inserted into the proposed peptide binding domain of YihE, resulting in a threonine residue from IHF resting in ideal proximity to the catalytic loop for phosphorylation to occur (N. Martin, personal communication). To test this hypothesis, it was first determined if IHF was a member of the phosphoproteome population enriched by the techniques used in this study, as no one had previously demonstrated phosphorylation of IHF. The phosphoprotein-enriched *S. typhimurium* samples were analyzed by western blotting using anti-IHF antibodies (Figure 7). Both IhfA and IhfB were present in low levels, however, there was no difference in the IHF levels when samples from WT and *rdoA* strains were compared suggesting that RdoA plays no role in the control of expression of these proteins. To confirm that the IHF subunits were phosphorylated and to determine if phosphorylation levels were different between the WT and *rdoA* strains, anti-phosphoserine and anti-phosphothreonine blots were carried out. IhfA was phosphorylated at both serine and threonine residues, but IhfB phosphorylation was not detected. A strong signal using anti-phosphoserine antibodies in the whole cell lysates, was initially thought to be IhfB, but this band did not react with the IHF anti-serum (Figure 8). IhfA from *S. typhimurium* has 5 serine and 4 threonine residues (47), none of which are conserved in IhfB. This correlates with the reactivity of the anti-phospho antibodies seen with IhfA and B. IhfB

likely formed heterodimers with phosphorylated IhfA *in vivo* and was co-enriched with IhfA. Alternatively, IhfB contains tyrosine residues that could be phosphorylated. Overall, these observations suggest that IHF is not RdoA's target since phosphorylation levels did not change between the WT and *rdoA* strains. Understanding how IHF becomes phosphorylated at ser/thr residue(s) requires further study outside the scope of this thesis.

5.2 Comparison of Phosphoprotein Enrichment Techniques

Phosphoproteins are often in low abundance compared to the total proteome, making a enrichment a necessary step. Phosphoproteins are also transiently phosphorylated, therefore a global phosphoproteome profile of any bacterium will be different under varying growth conditions. An established technique, Immobilized Metal Affinity Chromatography (IMAC) enables enrichment of phosphoproteins. This technique relies on electrostatic interactions between negatively charged phosphate groups from phosphoproteins and positively charged metal ions bound to a matrix (107) to separate phosphorylated proteins from a complex solution. There are numerous types of IMAC systems using different metal ions to trap phosphoproteins (2, 26, 73, 98). Optimization of IMAC enrichments is required to obtain phosphoprotein yields reproducibly. In this study, 3 different phosphoprotein enrichment protocols were used select phosphoproteins from *S. typhimurium* cell lysates. These 3 enrichment techniques consists of two commercially produced kits, namely the Phostag Enrich Phosphoprotein kit (Phostag) and the Qiagen Phosphoprotein Purification kit (PPK), and one "home-made" kit known as $Al(OH)_3$ MOAC (151). Protein yield, cost-effectiveness and phosphoprotein enrichment efficiency were used as criteria to determine which method is suitable for *S. typhimurium* phosphoprotein enrichment.

Phostag uses an alkoxide-bridged dinuclear zinc (II) complex, technically known as 1,3-bis[bis(pyridine-2-ylmethyl)amino]propan-2-olato dizinc (II) complex, bound to highly cross-linked agarose to trap phosphoproteins. This matrix attracts negatively charged phosphorylated proteins by binding the phosphate monoester dianion to the zinc ion resulting in a phosphorylated protein-zinc complex with a total charge of +1 (52, 53, 87). Published studies have reported using Phostag to enrich phosphoproteins from a complex mixture containing phosphorylated and non-phosphorylated protein standards and from eukaryotic cell lysates (52, 53, 87). These studies concluded that Phostag is a suitable means of enriching phosphoproteins from a complex protein mixture.

The PPK metal ion embedded in its matrix is unknown due to proprietary measures. Voisin *et al.* (142) used PPK or Fe (III) IMAC to enrich phosphoproteins from *Campylobacter jejuni.* Machida *et al.* (73) compared the efficacy of PPK and Ga(III) IMAC to select for phosphoproteins from cell lysates. Results from that study showed that both protocols enriched a similar amount of phosphoprotein, however, they observed that PPK did not efficiently enrich high MW phosphoproteins compared to Ga (III) IMAC, which is consistent with our PPK 2-D gels when compared to our Phostag 2-D gels (Figure 14).

$Al(OH)_3$ MOAC was first reported by Wolschin *et al.* (150, 151) and relies on the affinity of phosphorylated proteins for the insoluble metal hydroxide $Al(OH)_3$. These authors tested $Al(OH)_3$ MOAC's phosphoprotein enrichment properties using a protein mixture, containing standard phosphorylated and non-phosphorylated proteins, *Arabidopsis thalia* leaf proteins and *Chlamydomonas reinhardtii* (a single cell algae) proteins. They found that phosphoproteins were effectively enriched from these complex protein mixtures using the appropriate buffer system. This study indicated that the $Al(OH)_3$ MOAC technique is highly selective for phosphorylated

proteins, cost effective and easily optimized to suit any given experimental conditions in contrast to commercially produced IMAC kits (150, 151).

In this thesis, the highest yield (Table 3) and best enrichment efficiency (Figure 9) of phosphoproteins were obtained using Phostag followed by PPK and $Al(OH)_3$ MOAC. ProQ Diamond staining of eluents from each of these protocols show significant enrichment of phosphoproteins, with PPK having a higher intensity overall of phosphoprotein staining followed by the 2 other methods. The ProQ Diamond staining of Phostag eluents showed a slightly lower phosphoprotein staining compared to PPK in the presented gel, however this may have been a result of repeated freezing and thawing of this particular Phostag sample. Phostag prepared samples were estimated to have at least the same or higher phosphoprotein content as PPK. This could be explored more thoroughly when the Phostag kit goes back into distribution. Interestingly, Wolschin *et al.* (151) compared the efficiency of PPK and $Al(OH)_3$ MOAC for the enrichment of phosphoproteins using a standardized protein mixture containing both phosphorylated and non-phosphorylated standards. They concluded that the efficiency of $Al(OH)_3$ MOAC and PPK were comparable. In the current study, PPK and $Al(OH)_3$ MOAC showed similar protein yields (Table 3), although, based on ProQ Diamond staining, they appeared to give different phosphoprotein yields (Figure 10), with PPK enriching a higher percentage of phosphoproteins than $Al(OH)_3$ MOAC. One possible reason why more phosphoproteins were enriched by PPK than $Al(OH)_3$ MOAC under the given conditions was because of the nature of the buffer the cell lysates were resuspended in. Cell lysates were resuspended in a column-specific buffer before running through the column. Since $Al(OH)_3$ MOAC involves small volumes, the concentration of the column-specific buffer became more dilute due to the addition of a significant volume of cell lysate. In this case, the buffer

environment may not have been optimal for phosphoproteins to bind to the metal ion. Adjusting the binding buffer stock concentration to accommodate this higher dilution factor should be assessed in future experiments.

In order to better assess the ratio of phosphorylated to nonphosphorylated proteins present using these difference enrichment protocols, western blotting was carried out using phospho-specific antibodies. As a means to assess the phospho-specificity of these antibodies, samples that had been dephosphorylated or mock treated with lambda phosphatase (101) were compared using the PPK and $Al(OH)_3$ MOAC eluents. Despite repeated attempts, only the phosphatase-treated PPK eluents showed a significant decrease in signal after phosphatase treatment with all 3 phospho-specific antibodies. Although this confirms that PPK effectively enriched phosphoproteins, it is not understood why phosphatase-treated $Al(OH)_3$ MOAC eluents did not show a decrease in signal detection with any of the phospho-specific antibodies. These samples were subjected to the same clean up protocol as the PPK samples which should remove salts and buffer components and there should not be any $Al(OH)_3$ associated with the eluted proteins (151). However, similar phospho-specific protein patterns were observed between PPK and $Al(OH)_3$, suggesting that the bands observed in $Al(OH)_3$ MOAC samples could be the same phosphoproteins as visualized in the PPK samples. Future experiments should address phosphatase-treatment on $Al(OH)_3$ MOAC eluents in order to confirm the type of phosphoproteins present.

Phosphoproteins detected in western blots were limited in size to between 45kDa and 90kDa (Figure 11) although there clearly were proteins present in these samples of both larger and smaller sizes and the ProQ Diamond staining was capable of detecting phosphoproteins in a wider range of sizes (Figures 10). Although it appears that the phosphospecific antibodies are

detecting phosphorylated proteins, the results suggest that they are only detecting a specific subset of these proteins. This could be due to localization of primary antibody at the center of the membrane during O/N incubation.

Some bacterial proteins are known to be phosphorylated at both serine and threonine residues (23, 113, 140). This coincides with the similar phosphoserine and phosphothreonine band profiles observed in western blots of PPK eluents (Figure 11). Tyrosine phosphorylation is the least prevalent type of phosphorylation reported to occur in the phosphoproteome studies in bacteria to date (71, 72, 105, 142). The epitope that the anti-phosphotyrosine antibodies detect is a limited portion of the phosphotyrosine sequence, which is the phosphate group attached to a phenyl group, therefore they could also detect phenyl phosphates. Consequently, the number of phosphotyrosine-modified proteins, as detected using anti-phosphotyrosine antibodies, could be an overestimation. Published studies have explored the phosphoproteome of *Bacillus subtilis* (72) and *E. coli* (71) and reported the percentage of phosphoserine, phosphothreonine and phosphotyrosine peptides in the phosphopeptide-enriched eluent. Both studies reported that the phosphoproteome of *B. subtilis* and *E. coli* have a high percentage of phosphorylation sites in serine followed by threonine and, finally, tyrosine (71, 72). Based on qualitative analysis, western blots using phospho-specific antibodies in the current study suggested similar amounts of phosphoserine, phosphothreonine and phosphotyrosine proteins (Figure 11). To obtain an accurate percentage of phosphorylation sites in the phosphoproteome of *S. typhimurium* similar to the studies of Macek *et al.* (71, 72), a gel-free approach which involves phosphopeptide enrichment and liquid chromatography mass spectrometry (LC-MS) to determine phosphorylation sites is recommended.

Assessment of the phosphoprotein enrichment using the 3 protocols was most informative when using 2-D SDS-PAGE. A pH range of 4-7 was used in this study because most bacterial proteins have an isoelectric point in this range. This pH range provided a good resolution of *S. typhimurium* phospho/proteins in this study. Other pH ranges should be used in the future because important phospho/proteins may have been missed. Additional optimization is still needed for $Al(OH)_3$ MOAC 2-D gels (Figure 12) to obtain a comparable resolution to Phostag and PPK 2-D gels (Figure 14) and will be pursued in future studies. $Al(OH)_3$ MOAC 2-D gels showed high background staining and excessive streakiness in the low pH range. A high background indicates that proteins were not fully resuspended in rehydration buffer or that there were interfering substances in the sample. To remove interfering substances, $Al(OH)_3$ MOAC eluents were precipitated and concentrated using the 2-D Clean Up kit. This kit should concentrate proteins in buffers containing a maximum concentration of 8M urea, the amount of urea in the $Al(OH)_3$ MOAC elution buffer, however, some interfering substances may not have been effectively removed from the protein sample. To try to address the possibility of the proteins not being fully resuspended, protein solutions were sonicated briefly in rehydration buffer, although, 2-D gels still showed the same high background staining (figure not shown). Additional optimization will be necessary using modifications of the rehydration buffer composition and of the resuspension protocol in future studies.

Two-dimensional SDS-PAGE analyses of Phostag and PPK eluents showed that many of the proteins found vary in abundance between the 2 methods. These differences are probably due to differences in affinity for the matrices and buffer conditions (73, 141). However, those proteins enriched by both were found to be predominantly phosphoproteins (Table 4), while the proteins enriched only by Phostag were mostly not previously identified as phosphoproteins (Table 5).

This suggests that unspecific binding may occur during enrichment. Although there are proteins that were eluted only by Phostag or by PPK, the majority of the phosphoproteins in the cell lysate will be eluted by either of these two techniques. Considering all factors, Phostag is recommended as a suitable phosphoprotein enrichment technique for *S. typhimurium*. This is because Phostag yields more proteins and it uses a methanol-chloroform precipitation to concentrate the eluted proteins, which is more cost effective than using the 2-D Clean Up kit.

5.3 Comparison Between Two Methods of Phosphoprotein Detection: Fluorescent Staining and Western blots

The 2 phosphoprotein detection methods used in this study are fluorescent staining and western blotting. Both methods are widely used to determine phosphorylation in proteins, however, their efficacy is quite different as shown in the results. Fluorescent staining used ProQ Diamond and SYPRO Red, while western blotting used phospho-specific antibodies, primarily anti-phosphoserine and anti-phosphothreonine antibodies. ProQ Diamond binds to the phosphate moiety of the phosphorylated protein and is stated to be phospho-specific in the nanogram range of phosphoprotein abundance (126). Also, the higher the level of phosphorylation, the more intense the ProQ Diamond signal is. However, this stain does not distinguish whether phosphorylation has occurred at serine, threonine or tyrosine residue(s). For western blots, antibodies are commercially available that detect a consensus sequence that includes the phosphate group (107). Antibodies are very sensitive, being able to detect femtomoles of sample; however, some antibody target sites can be occluded by steric hindrance due to the conformation of the protein and this may decrease or prevent signal from the antibody (8, 107). Both of these detection methods may also cause false-positives because both fluorescent stains and antibodies can bind to proteins unspecifically if there are high amounts of protein present. To address this

issue, ProQ Diamond stained gels must be followed by a total protein stain, SYPRO Red or Ruby, to take into account the total protein levels. To determine which of the proteins are phosphorylated in a complex mixture that has been separated on 1 or 2-D gels, the 2 fluorescently stained gels can be computationally overlayed and artificially coloured (29). To address the specificity of the phospho-specific antibodies, studies usually phosphatase-treat a portion of the sample and subject it to the same conditions as a non-phosphatase treated portion (100, 101).

In the 2-D gels carried out in this project, ProQ Diamond detection of phosphoproteins was less sensitive than western blotting, similar to previously published studies (107), therefore few putative phosphoproteins were detected and compared between ProQ Diamond stained gels and western blots. Western blots and the corresponding silver stained 2-D gels were overlaid to locate protein spots to excise for PMF. This method is somewhat risky since antibodies are more sensitive than silver staining. Therefore, some signals observed in western blots may be phosphoproteins that cannot be detected by silver staining and these proteins would be below the detection limit for PMF. This could result in mis-identification of proteins species associated with antibody detection. Because of this, low abundance phosphoproteins detected by western blottings but not by silver staining were not chosen for identification by PMF in this study.

5.4 Techniques Used to Assess Phosphoproteomes

These 2 phosphoprotein detection methods used in this study proved useful for providing hints about the phosphoproteins in the samples, but neither technique provided a good overview of the phosphoprotein population in a given sample. Complementary or additional methods should be performed (8, 29, 107). To date, a number of studies examining the phosphoproteomes of particular cells types have been published. Phosphoproteome studies were originally carried out using 2-D SDS-PAGE in combination with fluorescent staining and/or [^{33}P]-labeling and MS

(8, 29, 63, 142). Eymann *et al*. (29) and Levine *et al.* (63) studied the phosphoproteome of log-phase and stationary-phase *B. subtilis* cells, respectively, using these techniques. In addition, they analyzed the phosphoprotein population changes in different growth phases and in cells grown under different environmental stresses. This approach identified phosphoproteins that were constitutively or transiently phosphorylated in *B. subtilis* (29, 63). Levine *et al.* (63) used *in vivo* labeling and narrow pI range 2-D SDS-PAGE to obtain a *B. subtilis* phosphoproteome profile. This approach can determine *in vivo* phosphorylation and provide a better protein resolution than typically seen in broad pH range (63). However, due to this limited pH range, many gels need to be run so that important phosphoproteins with pI's beyond specific pH range are not missed. Both studies were able to determine the phosphorylation sites of phosphoproteins using MS. Bendt *et al.* (8) used the same approach with *Corynebacterium glutamicum* (a Gram-positive soil bacterium), but added western blotting using a phospho-specific antibody. Their study showed that western blotting is a more sensitive approach in detecting phosphoproteins compared to [^{33}P]-labeling. Bendt *et al.* (8) mentioned that western blotting is a preferable approach to determine the phosphoprotein profile in short time frames compared to [^{33}P]-labeling, since the latter method requires a long labeling time frame to get the desired intensity upon autoradiography. Macek *et al.* (71, 72) reported on the phosphoproteome profile of *B. subtilis* and *E. coli* using a gel-free phosphopeptide enrichment followed by tandem MS. They compared the phosphoproteome of these 2 bacteria and observed a similar number of phosphoproteins, percentage of phosphorylation sites, and detected phosphorylation events. This suggests that there is a conserved group of phosphoproteins and phosphorylation events between the 2 bacteria. Ravichandran *et al.* (105) used a similar approach to determine and compare the phosphoproteome of a pathogenic *Pseudomonas aeruginosa* and a non-pathogenic *P. putida*.

Their study reported that different phosphoproteins were determined in the 2 bacteria, however, these phosphoproteins probably function in similar regulatory pathways (105). A similar pattern between the percentages of phosphorylation sites was observed in this study as in the Macek *et al.* (71, 72) studies. A study using the same gel-free approach was carried out using *Lactococcus lactis*, a Gram-positive non-pathogenic bacterium (121). Interestingly, compared to previously mentioned phosphoproteome studies, *L. lactis* showed higher levels of phosphothreonines followed by phosphoserines and, lastly, phosphotyrosine proteins (71). Over all, a gel free approach, such as phosphopeptide enrichment followed by LC-MS/MS, provided a higher number of identified phosphoproteins compared to 2-D SDS-PAGE methods. More importantly, these studies show that a combination of techniques should be carried out to determine a global phosphoproteome profile of a bacterium.

5.5 Phosphoproteome Profile of *S. typhimurium*

The current study focused on trying to detect changes in the phosphoproteome in relation to the presence or absence of RdoA. This work did, however, identify phosphoproteins that were present in both WT and *rdoA* null cells as a preliminary analysis of the total phosphoproteome. These proteins could either be constitutively expressed or up-regulated in response to the stress of NlpE overproduction. To date, this study has identified several different phospho/proteins involved in the heat shock response, metabolism, protein synthesis and the outer membrane (Table 4). Some proteins that participate in metabolism and protein synthesis are also known to function as stress response proteins (see below). The cells used in this study were, in fact, stressed by expressing NlpE, a lipoprotein. NlpE accumulates in the periplasm and this is detrimental to the cell, thus, activating the expression of multiple stress response genes (103). Further studies,

comparing WT stressed and unstressed cell lysates will be necessary to determine which of the phosphoproteins were altered in a stress-dependent fashion.

Proper protein translation is achieved with the help of multiple proteins and RNA in the cell. A number of phosphoproteins were identified that are involved in protein synthesis such as elongation factors G (EF-G) and Tu (EF-Tu), lysine tRNA synthetase (LysRS), and the 30S ribosomal protein S1 (RpsA). EF-G, EF-Tu, LysRS and RpsA have been previously reported to be phosphorylated (31, 66, 71, 109, 153). RpsA makes up the largest subunit of the 30S ribosomal protein, which helps to hold the mRNA in association with the ribosome (118). In *E. coli*, RpsA was reported to contain phosphoserine residues (31). Freestone *et al.* (31) indicated that phosphorylated RpsA was observed only when RNase was added to cell lysates and that phosphorylated RpsA is difficult to purify using anti-RpsA antibodies, suggesting a phosphorylation mediated conformational change. This change may either protect anchored mRNA from RNase or repress RpsA activity. EF-Tu is involved in mediating the entry of tRNA to the ribosome while EF-G is involved in translocating tRNA from the A-site of the ribosome to the P-site (123). These two proteins depend on GTP to drive their enzyme activity. Hydrolysis of GTP causes a conformational change that causes EF-G and EF-Tu to detach from the ribosome after completing their function (92, 123). When cells are under stress, EF-Tu, EF-G and IF-2 act as molecular chaperones to assist in proper protein folding. In several *Enterobacter* species, lysine tRNA synthetase (LysRS) was found to consist of two isoforms, LysS (57.8kDa) and LysU (57.6 kDa). LysS is involved in lysine biosynthesis and constitutively expressed. LysU is expressed during severe stress such as heat shock and growth at acidic pH (112). Two-dimensional gels resolved the LysRS protein as one protein spot at an approximate MW of 59 kDa (Figure 14 and Table 4). In this study, a phosphothreonine protein matching the location of

LysRS was detected in western blots, concurring with LysRS being phosphorylated in a previous study (71). In *E. coli*, phosphorylated LysU's primary function is to synthesize diadenosine 5'5'''-P^1,P^4-tetraphosphate (Ap_4A) and 5',5'''-P^1,P^3-triphosphate (Ap_3A) (153), signals for cellular stress (59), and this occurs more efficiently than with unphosphorylated LysU (153). As mentioned previously, cells were NlpE-stressed. This may have caused LysU to become phosphorylated in order to synthesize Ap_4A and Ap_3A to act as stress signaling molecules. Future experiments could examine the levels of Ap_4A and Ap_3A in WT and *rdoA* null *S. typhimurium* to extend this observation.

Increases in protein expression require several protein chaperones or systems to ensure that proteins are properly folded to be functional. It is possible that overexpression of NlpE affected not only the Cpx stress response, but also additional protein folding pathways and this may account for the number of phosphoproteins identified in the phosphoproteome profile of *S. typhimurium* as heat shock proteins or chaperones. Known phosphoproteins ClpB, DnaK, GroEL, HtpG and TF were identified. GrpE was also identified but is not known as a phosphoprotein. None of these chaperones have been previously shown to respond directly to CpxR-mediated regulation (99).

Molecular chaperones recognize unfolded proteins via exposed hydrophobic amino acid side chains, which signals chaperones to assist in protein folding (36, 37). Most chaperones require ATP hydrolysis in order to carry out their functions. One such system is an Hsp70/Hsp40 chaperone system known as the DnaK/DnaJ system, which binds and releases proteins in an ATP-dependent manner (37). DnaK is known to be phosphorylated at both serine (71) and threonine residue(s) (82). DnaK works with the co-chaperones DnaJ and GrpE to form a multi-chaperone system (37, 64). DnaJ enhances the ATP hydrolysis activity of DnaK while bound to

the unfolded peptide. GrpE, on the other hand, removes the ADP from DnaK causing DnaJ to disassociate from DnaK and allowing new ATP molecules to bind to DnaK. This also releases the peptide, which will fold, recycle back to the DnaJ./DnaJ system or proceed to another chaperone system for proper protein folding (36, 37). This system works with a chaperone known as trigger factor (TF) for the same purpose (37, 67, 145). TF is the first chaperone that nascent peptides interact with. TF binds to the ribosome at a 1:1 ratio and interacts with a nascent chain to form a TF-nascent chain complex (37). Although no studies have reported TF as a phosphoprotein in *S. typhimurium* or *E. coli*, Lomas *et al.* (69) reported TF as a phosphophoserine/ phosphothreonine protein in *S. aureus*. Similar to Lomas *et al.* (69), TF was observed in the current study as a phosphothreonine-containing protein in western blot analyses. The DnaK/DnaJ system has been found to interact with another chaperone, known as ClpB (27, 135, 145, 161). ClpB increases in amounts when cells experience severe stress because it can solubilize protein aggregates that occur during stress. Doyle and Wickner (27) speculated on a model of these two chaperone systems working synergistically. The study proposed that ClpB is the primary protein refolding machinery while the DnaK/DnaJ system traps and carries unfolded protein to ClpB. ClpB can also work independently of the DnaK/DnaJ system to refold proteins (27) Another identified phosphoprotein known as GroEL, a heat shock protein, works with TF to enhance proper protein folding (37, 67). GroEL works with its cofactor, GroES, to from a GroEL-GroES compartment-like machinery. In an ATP-dependent manner, this complex can bind, transfer unfolded proteins to its enclosed folding compartment and trap released unfolded proteins (36, 37). Finally, a chaperone known as HtpG is known to cause conformational changes of its targets. Unlike DnaK/DnaJ and GroEL-GroES chaperone systems that bind to unfolded proteins at the earlier stages, HtpG interacts with its targets at later stages of protein folding in normal cellular

conditions (55). Thomas and Baneyx (135) also showed that HtpG works with the DnaK/DnaJ system at early stages of protein folding in stressed *E. coli* cells. These chaperones were shown to be beneficial for *S. typhimurium* to resist acid environments (9), to grow in high temperatures (82) and to successfully secrete proteins-encoded by the SPI-I for bacterial invasion of epithelial cells (132). These heat shock phosphoproteins are constitutively expressed during normal cell growth, but levels increase during stress and are, therefore, abundant in *S. typhimurium's* phosphoproteome profile.

The phosphoproteome profile of *S. typhimurium* showed different phosphoproteins involved in metabolism. These key phosphoproteins are aconitate hydratase 2 (AcnB), adenylosuccinate synthetase (PurA), enolase (Eno), glycerol kinase (GlpK), pyruvate dehydrogenase E1 (AceE), succinyl CoA synthetase beta chain (SucC), malate dehydrogenase (MaeB), and L-ribulose-5-phosphate 4-epimerase (AraD).

Complex compounds that can act as sources of energy, are not directly used by the bacterium but need to be converted to a usable form. One metabolic system, the Embden Meyerhof pathway, converts glucose to pyruvate for use by the cell to derive energy from. Enolase, identified in the phosphoproteome profile of *S. typhimurium,* is part of this process. Enolase catalyzes the interconversion of phosphoenolpyruvate and 2-phospho-D-glycerate. It is also widely studied as a component of the RNA degradosome (17), which is involved in mRNA degradation. Similar to Macek *et al.* (71), this study showed enolase was phosphorylated at serine and threonine residue(s). The role of enolase and its phosphorylation status in the RNA degradosome or in the Embden Meyerhof pathway is still being elucidated.

When pyruvate has been made through glycolysis, this organic acid is further modified to acetyl-CoA before it enters the tricarboxylic acid cycle (TCA), a pathway involving several

enzyme-catalyzed reactions to obtain oxygen, water and energy for the bacteria. This requires the pyruvate dehydrogenase multi-enzyme complex. Pyruvate dehydrogenase E1, which is one of the components of this multi-enzyme complex, is responsible for pyruvate decarboxylation to form acetyl-CoA. In eukaryotic cells, regulation of this enzyme is via phosphorylation by the ser/thr kinase pyruvate dehydrogenase kinase. It was found that phosphorylated pyruvate dehydrogenase inhibits E1 activity (21). Pyruvate dehydrogenase E1 (AceE) was reported to contain phosphoserine and phosphothreonine in residues in *S. aureus* (69), however, no studies have addressed phosphorylation of AceE as a means of regulation in bacteria. The current study suggests that AceE is phosphorylated at serine residue(s) similar to *S. aureus.* Once acetyl-CoA has been made, it enters the TCA cycle to be further modified into different molecules to obtain energy, water and carbon dioxide. Four proteins involved in this cycle, namely malate dehydrogenase (MaeB), succinyl CoA synthetase (SucC) and aconitate hydratase 2 (AcnB), were identified in the current study with *S. typhimurium*. AcnB catalyzes the reversible conversion of citrate and isocitrate. Phosphorylated AcnB was not detected in this study to date, however, Macek *et al.* (71) reported a phosphorylated form in *E. coli*. SucC makes up the β-chain of the succinyl-CoA synthetase, which catalyzes the conversion of succinyl-CoA to succinate. It is assembled with SucD, the α-chain, which autophosphorylates at histidine residue(s) (31). This study detected a phosphothreonine signal that corresponded to SucC but phosphohistidine residues were not examined.

One protein identified in the current study is GlpK, which is part of the Glp system that is involved in glycerol metabolism (41, 96). GlpK kinase phosphorylates glycerol in an ATP-dependent manner to form glycerol-3-phosphate, which undergoes several chemical modifications to become pyruvate that is then modified as acetyl-CoA in order to enter TCA

cycle (65). In this study, GlpK was observed to be phosphorylated at serine and threonine residues (Figures 20, 22, 23 and Table 12). In Gram-negative bacteria, GlpK activity is repressed allosterically (41, 96). However, GlpK found in Gram-positive bacteria is activated by phosphorylation at a histidine residue Though no studies were found identifying phosphorylated GlpK in Gram-negative bacteria, the results reported here suggest it is phosphorylated. This suggests an unknown regulatory mechanism via ser/thr phosphorylation of GlpK that is yet to be elucidated.

In this study, AraD was detected as a phosphothreonine-containing protein. AraD takes part in arabinose metabolism, which converts arabinose into a usable form to enter the pentose phosphate pathway. It is responsible for the conversion of L-ribulose-5-phosphate to D-xylulose-5-phosphate, which occurs at the third step of this type of metabolism (58). Arabinose metabolism was expected to occur in this study since arabinose was added to the cells to induce the expression of NlpE. However, it was surprising to observe that AraD may potentially be a phosphothreonine protein, which had not been previously reported.

Four other proteins, a putative alcohol dehydrogenase (YghD), DNA-directed RNA polymerase alpha chain (RpoA) and 2 outer membrane proteins, namely OmpA and Omp85, were identified in the phospho-enriched protein population profile of *S. typhimurium*. Both outer membrane proteins are involved in bacterial adhesion and membrane structure (136). These proteins have not been reported as phosphoproteins and were not detected by any phosphospecific methods in this study. YqhD levels were shown to increase during stress (42, 97) and this protein was reported to have an aldehyde reductase activity that potentially served to protect cells from oxidative stress (95). Lastly, RpoA is part of multi-protein complex RNA polymerase. Although these proteins are not known to be phosphorylated, western blotting results suggested that these

proteins may be phosphorylated at ser/thr residue(s). Additional studies should be carried out to determine if these truly are phosphorylated or if the western blots are detecting other phosphoproteins that are co-migrating with these proteins. Higher resolution 2-D gels using narrow pI ranges would help to clarify the phosphorylation status of these proteins. .

This study of the phosphoproteome of *S. typhimurium* elucidated key phosphoproteins important for normal cell growth and function. A few phosphoproteins, namely TF, EF-G, EF-Tu and enolase, were identified in more than one spot in Phostag or PPK 2-D gels (Table 4). Proteins that appear as multiple spots in 2-D gels may have undergone additional modifications or protein degradation may have occurred during sample processing (8, 122). Several identified proteins in phosphoprotein-enriched eluents are not known to be phosphoproteins, or may co-purify with phosphoproteins however, no published data is available to confirm these observations. Further experimentation must be carried out to determine if these proteins are truly phosphoproteins.

5.6 RdoA-dependent Changes in Phospho/protein Population

In this study, RdoA-dependent phosphoprotein population changes were involved in different cellular functions of *S. typhimurium*. Phostag and PPK 2-D gels and western blots showed different phosphorylation patterns, as well as differences in protein abundance. The proteins found to change in abundance in an RdoA-dependent manner as observed in silver-stained 2-D gels were compared to the western blots (Table 8). Only 10 out of 45 proteins that were found to change in the amount present in an RdoA-dependent manner were found to be phosphorylated on serine or threonine residues. The majority of the RdoA-dependent proteins that changed in protein levels were not observed in any western blots, which suggested that these proteins may be phosphorylated at histidine or tyrosine residue(s). Alternatively, these proteins

could be complexed with a phosphoprotein *in vivo*, and therefore be included during enrichment for phosphoproteins.

Phosphoproteins that showed a significant change in phosphorylation between WT and *rdoA* null *S. typhimurium* were of particular interest because the changes suggested that RdoA has an impact on their phosphorylation status or that these phosphoproteins may be potential RdoA target(s). The phosphoproteins successfully identified by PMF were DnaK, GroEL, EF-Tu, enolase, glycerol kinase, and pyruvate dehydrogenase E1. These proteins did not change significantly in protein levels between a WT and an *rdoA* null *S. typhimurium* in silver-stained 2-D gels (Table 12) but additional analyses using image analysis software would need to be carried out to confirm this. One possibility is that these phosphoproteins may be phosphorylated at several sites by multiple kinases, which may include RdoA. Therefore, enrichment of these phosphoproteins would not be predicted to significantly change whether RdoA is present or absent and it would only be through western blotting using anti-phospho-specific antibodies, can it be established that RdoA was involved in the phosphorylation of these proteins.

The results of this study suggest that RdoA affects phosphorylation of numerous proteins that are involved in different regulatory processes to combat stressful conditions. GroEL was highly phosphorylated in the presence of RdoA (Figures 20, 22 and Tables 11, 12). An increase in temperature (heat shock) causes GroEL to become phosphorylated and this causes structural modifications, which affects the interaction of GroEL with unfolded peptides (116). These structural modifications of GroEL may explain the multiple spots found in 2-D gels. Two protein spots were identified as GroEL (Table 12). GroEL spot #157, at approximately 50kDa, was observed to be phosphorylated at serine and threonine residue(s) while GroEL spot #79, at approximately 40kDa, was phosphorylated at only serine residue(s). It is possible that a portion of

GroEL containing the phosphothreonine residue(s) was cleaved, which resulted in a smaller GroEL protein that contained only phosphoserine residue(s). GroEL has been widely studied as a heat shock protein (37) and several studies have reported its importance in intracellular survival in macrophages (12, 124). Phosphorylation of GroEL is likely necessary to properly function in a hostile environment, such as macrophages. Studies on RdoA's importance in cellular invasion has been established (108), however, its role in intracellular survival has not been. Comparing the intracellular survival between WT and *rdoA* null *S. typhimurium* may be difficult to perform since *S. typhimurium's* initial entry into the cell is compromised in the absence of RdoA. As presented in the current study and known literature, RdoA may be involved in intracellular survival of *S. typhimurium* through GroEL phosphorylation. Further studies should be carried out to test this hypothesis.

Another phosphoprotein affected by RdoA was EF-Tu, which is involved in protein synthesis. EF-Tu was phosphorylated at threonine and serine residue(s), which concurs with published reports (66, 71). In this study, three protein spots were identified as EF-Tu (Table 12). As mentioned previously, EF-Tu has two functions and regulation of these functions involves phosphorylation at different amino acids. To date, no studies have shown how EF-Tu phosphorylation at serine or threonine residue(s) can regulate its function as an elongation factor or as a molecular chaperone. It was observed that EF-Tu does not undergo autophosphorylation. In addition, overexpression of EF-Tu does not increase the relative amount of phosphorylated EF-Tu, suggesting that normal cell function maintain a basal level of phosphorylated EF-Tu. Lippmann *et al.* (66) suggested that phosphorylation of EF-Tu may regulate GTP-binding. Macek *et al.* (71) reported that EF-Tu peptides encoded by *tufA* were phosphorylated. A deletion in *tufA* resulted in a decrease in growth rate and translational elongation rates compared to WT (43, 138).

Rapid growth of bacteria occurs in exponential phase, suggesting that high amounts of EF-Tu are needed and that its kinase would be abundant at this particular growth phase. RdoA expression is growth phase dependent with a maximum level found in the stationary phase (158). It is unlikely then that RdoA normally phosphorylates EF-Tu during the exponential phase. However, this current study suggests that RdoA is involved in EF-Tu phosphorylation under NlpE-stressed conditions. In *E. coli*, EF-Tu acts as a molecular chaperone during stressful conditions (15, 75). EF-Tu bound to GDP is inactive in aminoacyl-tRNA binding but was observed to be active in protein folding (15). Phosphorylation of EF-Tu may enable it to function as a chaperone, similar to other chaperones. Further experimentation is needed to determine the relationship between EF-Tu and RdoA in *S. typhimurium.*

DnaK was observed as two protein spots in Phostag 2-D gels (spots #153 and 180) (Figures 20, 22 and Tables 9 10). DnaK spot #153 has a MW of 63 kDa while spot #180 has a MW of 57kDa. It is likely that protein spot #180 represents an isoform of DnaK, which has lost 6kDa from either the N- or C-terminus. The reactivity of the antibodies suggested that there is a conserved phosphorylated serine residue(s) common to both fragments while all the phosphorylated threonine residue(s) are contained in the region of DnaK that was cleaved off. This suggests that RdoA influences the phosphorylation of serine residue(s) found in the core protein and also phosphorylation of threonine residue(s) within the cleaved peptide (Table 12). Therefore, RdoA influences phosphorylation of DnaK at multiple amino acid residues. It was previously documented that a decrease or absence of DnaK decreased or abolished the amount of FliC expressed (132, 133). Two-dimensional gel electrophoresis of secreted proteins showed that a *dnaK* null strain of *S. typhimurium* did not express FljB. DnaK was shown to regulate FliC expression by stabilizing the $FlhD_2C_2$ complex, which is the transcriptional master regulator for

flagellar genes (131). As mentioned previously, RdoA affects flagellar phase variation, preferring FliC expression over FljB expression (108, 158). It is possible that RdoA is involved in DnaK phosphorylation, thus, promoting FliC expression. Based on this pathway, the absence or low levels of any of these regulatory proteins will cause low levels of FliC expression. Further experimentation is required to define the mechanism influencing RdoA-dependent FliC/FljB expression.

Colonic epithelial invasion was shown to be repressed in a *dnaK* null (81, 132) and *rdoA* null *S. typhimurium* strains (108). *Salmonella* invasion proteins are encoded in the SPI-1 (group of horizontally acquired genes termed a pathogenicity island), suggesting that both DnaK and RdoA may be involved in SPI-1 regulation. DnaK was observed to be involved in expression of SPI-1 genes via σ^{23} (81). σ^{23} is a stress-induced alternative sigma factor that binds with RNA polymerase to form a complex that can up-regulate the transcription of several stress-induced genes. Regulation of σ^{23} and several heat shock proteins, such as DnaK and GroEL, is through a feedback loop. During stressful conditions, σ^{23} levels increase resulting in up-regulation of DnaK while σ^{23} is degraded by DnaK and other regulon members when stressful conditions have diminished (3). The absence of DnaK in *S. typhimurium* causes overexpression of σ^{23}, which up regulates Lon protease. This protease degrades HilD and, subsequently, prevents *hilA* transcription. The absence of HilA, the master regulator of SPI-1 genes, prevents expression of proteins important for cell invasion (3). Studies have also reported that DsbA, which is up-regulated by RdoA, was necessary for the proper secretion of proteins indicating its importance in the TTSS encoded at the SPI-1 locus (83). RtsA is another protein that binds to the *hilA* promoter and activates SPI-1 invasion and secretory genes. This protein was also observed to bind and influence expression from an uncharacterized *dsbA* promoter, up-regulating *dsbA* transcription

independently of Cpx pathway activation. The coordinate regulation of *hilA* and *dsbA* via RtsA showed that DsbA is required for proper SPI-1 TTSS function, thus, enabling *S. typhimurium* to effectively invade epithelial cells. Maintenance of DsbA levels, through RdoA and RtsA, may increase *S. typhimurium's* pathogenicity via SPI-1. This suggests that RdoA's effect on colonic epithelial invasion is controlled by the SPI-1 through overlapping pathways, via DsbA and/or DnaK.

It was also observed that RdoA may be involved in *S. typhimurium's* metabolism through glycerol kinase, enolase and E1 component of the pyruvate dehydrogenase complex. Enolase is phosphorylated at serine and threonine residue(s) (71). It is part of the Embden-Meyerhof pathway, which converts glucose to pyruvate to generate ATP. Enolase is responsible for the interconversion of 2-phosphoglycerate to phosphoenolpyruvate in this pathway (44). It is still unknown if phosphorylation of enolase regulates its glycolytic activity. Enolase is also part of the RNA degradosome, a multi-protein complex responsible for messenger RNA (mRNA) degradation. However, the role of enolase in this complex still needs to be elucidated. Deletion of the gene coding for enolase or any other protein that is part of the RNA degradosome resulted in inefficient mRNA decay (16). This suggests that each protein component of the RNA degradosome is important for its function. Morita *et al.* (85) reported that enolase is a necessary part of the RNA degradosome in order to degrade *pstG* mRNA (85). *pstG* codes for the major glucose transporter, whose mRNA is destabilized and degraded when the Embden Meyerhof pathway is blocked (51). Morita *et al.* (85) suggested enolase may be engage the RNA degradosome with *pstG* mRNA for destabilization to occur. Under stressful conditions, phosphorylation may result in a conformational change in enolase, resulting in an alternative form

of the RNA degradosome sufficient to degrade *pstG* mRNA. RdoA may thus play a role in the phosphorylation and conformation of enolase.

Pyruvate dehydrogenase E1 (AceE) is part of a multi-protein complex that is responsible for the conversion of pyruvate to acetyl-CoA (21). In this study, AceE was phosphorylated at serine residue(s) in presence of RdoA. No published data have indicated that this protein is phosphorylated. In Gram-negative bacteria, AceE is regulated allosterically by glycolytic enzymes and acetyl-CoA to positively activate and repress its function, respectively (21) and it is therefore unclear what role RdoA could play. Since RdoA is required for long term cell survival, which involves adaptation to nutrient depletion (158) phosphorylation of AceE may aid in dealing with nutrient stress.

Another metabolic pathway involves using glycerol as a source of energy. As mentioned previously, the function of glycerol kinase (GlpK) is to phosphorylate available glycerol, which can then be modified by several enzymes to become acetyl-CoA, thereby, entering the TCA cycle where the cells can derive energy (65). No published data have reported GlpK to be a phosphoprotein in Gram-negative bacteria, however, this study suggested that GlpK is phosphorylated at serine and threonine residue(s). In Gram-positive bacteria, GlpK is phosphorylated at an important histidine (20, 24). GlpK may be regulated in different ways, such as through allosteric regulation (41, 96) and, possibly, through RdoA-dependent phosphorylation. GlpK may be a ser/thr kinase target and work similarly as GlpK in Gram-positive bacteria.

One particularly interesting RdoA-dependent protein is SrgA (Figures 16, 17 and Table 6). A spot corresponding to this periplasmic disulfide oxidoreductase is observed only in the absence of RdoA (10). SrgA has not been reported as a phosphoprotein nor was it observed using any of the phosphoprotein detection methods performed in this study. Though SrgA may not be a

phosphoprotein, it is interesting that it is present in an *rdoA* null *S. typhimurium*. SrgA is only 37% identical to DsbA but is also a disulfide oxidoreductase with different target substrates compared to DsbA (10, 139). Bouwman *et al.* (10) reported that SrgA was able to catalyze disulfide bond formation in PefA, a plasmid encoded-fimbrial subunit, while DsbA was unable to do so. While this suggests that these two proteins are normally substrate-specific, both can catalyze disulfide bond in a number of proteins. Miki *et al.* (83) reported that both SrgA and DsbA can oxidize SpiA, an outer membrane protein that is important for SPI-2 TTSS. Double knockouts of *srgA* and *dsbA* showed a more attenuated strain compared to single knockouts, suggesting that these proteins work in collaboration in oxidizing SpiA, however, in separate regulatory pathways. They also reported that, when highly expressed, SrgA was able to revert motility and cell invasion to normal WT levels in a *dsbA* null *S. typhimurium* strain (83). Though both disulfide oxidoreductase proteins are substrate-specific at specific conditions, maintaining either SrgA or DsbA expression at sufficient levels to ensure SpiA oxidation enables a highly virulent *S. typhimurium*. In an *rdoA* null *S. typhimurium*, a decrease in DsbA levels was observed (129), but there was also an increase in SrgA levels (Figures 16, 17 and Table 6). SrgA was able to revert motility back to WT in the absence of DsbA (83), which ties in with Richards (108) observation that motility is unchanged in a WT and an *rdoA* null *S. typhimurium*. It is possible that SrgA levels increased to make up for the low levels of DsbA, due to the absence of RdoA, to effectively oxidize SpiA, maintain motility or other DsbA/SrgA-dependent proteins in need of disulfide bond formation.

Phosphorylation can affect a protein by inducing conformational changes that alter its enzymatic activity or by changing its susceptibility to degradation or both. Various examples were presented to illustrate how RdoA-mediated phosphorylation may either repress or activate

enzyme function. RdoA-dependent protein level changes may also occur through phosphorylation induced conformations that either increase or decrease its susceptibility to endogenous proteases. Examples of RdoA-dependent changes in protein stability may be evidenced in the 2-D SDS-PAGE spot patterns of DnaK, GroEL, and EF-Tu, proteins that showed significant differences in phosphorylation and were observed in multiple spots in the gels (Table 12). It is possible that phosphorylation of these proteins promotes stability or hydrolysis of peptide fragments. If these fragments contained targeted phosphoamino acids, the multiple spots would show significant phosphorylation changes. Enolase, pyruvate dehydrogenase E1 and glycerol kinase were observed as single spots, which suggests that RdoA could affect their enzyme activity. Further experimentation should be carried out to determine how RdoA affects these proteins through their activity or stability or both.

This study supports that RdoA has an effect on multiple functions of *S. typhimurium.* RdoA-dependent phospho/proteins were observed to be involved in protein folding, which is necessary for normal and stressful cellular environments. Though the current study was unable to identify RdoA's target, it was able to provide further analyses on RdoA's role in stress response and insight on possible RdoA targets.

Chapter 6

Conclusion and Future Directions

The work presented here identified several phosphoproteins that are affected by RdoA. These RdoA-dependent phosphoproteins are involved in protein folding (DnaK and GroEL), metabolism (glycerol kinase, enolase and pyruvate dehydrogenase E1) and protein synthesis (EF-Tu). SrgA, an identified RdoA-dependent protein identified was also observed. The roles of these proteins in bacterial stress responses supports RdoA's role in the stress response system in *S. typhimurium*. This study presented important new information that will be followed up to determine potential RdoA target(s).

In addition, 3 different phosphoprotein enrichment techniques were examined and the results indicated that the Phostag Enrich kit works well in phosphoprotein enrichment for *S. typhimurium* because of its high yield of phosphoproteins and its cost-effective protein precipitation step. This work also disproved Richards' (108) hypothesis that IHF may be an RdoA target.

This work brings the knowledge of RdoA function further along the steps in identifying the RdoA-dependent phosphoproteome profile of *S. typhimurium*. PMF is currently being carried out on additional phosphoprotein enriched samples to more completely characterize those proteins involved with RdoA in handling extracellular stressors. These proteins will be analyzed in a fashion similar to the approach outlined in this study. To further examine the relationship between RdoA and identified RdoA-dependent phosphoproteins, phenotypic, functional and biochemical assays will eventually be carried out. For example, phenotypic and functional assays on double knockout of *rdoA* and RdoA-dependent phosphoprotein gene(s) should be examined to

determine if both proteins work in the same kinase-dependent pathway. Identified potential targets of RdoA kinase activity will also be cloned, expressed and purified in order to carry out *in vitro* kinase assays. The work presented here presents a major step in understanding not only the RdoA-related phosphoproteome, but also sheds light on the phosphoproteome related to the Cpx stress response.

References

1. **Aldridge, P. D., J. Gnerer, K. Karlinset, K. T. Hughes, and M. S. Sachs.** 2006. Regulatory protein that inhibits both synthesis and use of the target protein controls flagellar phase variation in *Salmonella enterica*. Proc. Natl. Acad. Sci. USA **103:**11340-11345.

2. **Andersson, L., and J. Porath.** 1986. Isolation of phosphoproteins by immobilized metal (Fe^{3+}) affinity chromatography. Anal. Biochem. **154:**250-254.

3. **Arsene, F., T. Tomoyasua, and B. Bukaua.** 2000. The heat shock response of *Escherichia coli*. Int. J. Food Microbiol. **55:**3-9.

4. **Azam, T. A., A. Iwata, A. Nishimura, S. Ueda, and A. Ishihama.** 1999. Growth phase-dependent variation in protein composition of the *Escherichia coli* nucleoid. J. Bacteriol. **181:**6361-6370.

5. **Bakal, C. J., and J. E. Davies.** 2000. No longer an exclusive club: eukaryotic signaling domains in bacteria. Trends Cell Biol. **10:**32-38.

6. **Barnhart, M. M., and M. R. Chapman.** 2006. Curli biogenesis and function. Annu. Rev. Microbiol. **60:**131-147.

7. **Beier, D., and R. Gross.** 2006. Regulation of bacterial virulence by two-component systems. Curr. Opin. Microbiol. **9:**143-152.

8. **Bendt, A. K., A. Burkovski, S. Schaff, M. Bott, M. Farwick, and T. Hermann.** 2003. Towards a phosphoproteome map of *Corynebacterium glutamicum*. Proteomics **3:**1637-1646.

9. **Berk, P. A., R. de Jonge, M. H. Zwietering, and J. Kieboom.** 2005. Acid resistance variability among isolates of *Salmonella enterica* serovar Typhimurium DT104. J. Appl. Microbiol. **99:**859-866.

10. **Bouwman, C. W., M. Kohli, A. Killoran, G. A. Touchie, R. J. Kadner, and N. L. Martin.** 2003. Characterization of SrgA, a *Salmonella enterica* serovar Typhimurium virulence plasmid-encoded paralogue of the disulfide oxidoreductase DsbA, essential for biogenesis of plasmid-encoded fimbriae. J. Bacteriol. **185:**991-1000.

11. **Brenner, S.** 1987. Phosphotransferase sequence homology. Nature **329:**21.

12. **Buchmeier, N. A., and F. Heffron.** 1990. Induction of *Salmonella* stress proteins upon infection of macrophages. Science **248:**730-732.

13. **Buck, D., M. E. Spencer, and J. R. Guest.** 1985. Primary structure of the succinyl-CoA synthetase of *Escherichia coli*. Biochemistry **24:**6245-6252.

14. **Bury-Mone, S., Y. Nomane, N. Reymond, R. Barbet, E. Jacquet, S. Imbeaud, A. Jacq, and P. Bouloc.** 2009. Global analysis of extracytoplasmic stress signaling in *Escherichia coli*. PLoS Genet. **5:**1-17.

15. **Caldas, T. D., E. Yaagoubi, and G. Richarme.** 1998. Chaperone properties of bacterial elongation factor EF-Tu. J. Biol. Chem. **273:**11478-11482.

16. **Carpousis, A. J.** 2007. The RNA degradosome of *Escherichia coli*: An mRNA-degrading machine assembled on RNase E. Annu. Rev. Microbiol. **61:**71-87.

17. **Chandran, V., and B. F. Luisi.** 2006. Recognition of enolase in the *Escherichia coli* RNA degradosome. J. Mol. Biol. **356:**8-15.

18. **Cheek, S., H. Zhang, and N. V. Grishin.** 2002. Sequence and structure classification of kinases. J. Mol. Biol. **320:**855-881.

19. **Danese, P. N., and T. J. Silhavy.** 1998. CpxP, a stress-combative member of the Cpx regulon. J. Bacteriol. **180:**831-839.

20. **Darbon, E., K. Ito, H. Huang, T. Yoshimoto, S. Poncet, and J. Deutscher.** 1999. Glycerol transport and phosphoenolpyruvate-dependent enzyme I- and HPr-catalyzed phosphorylation of glycerol kinase in *Thermus flavus*. Microbiol. **145:**3205-3212.

21. **de Kok, A., A. F. Hangeveld, A. Martin, and A. H. Westphal.** 1998. The pyruvate dehydrogenase multi-enzyme from Gram-negative bacteria. Biochim Biophys Acta. **1385:**353-366.

22. **De Wulf, P., B. J. Akerley, and E. C. C. Lin.** 2000. Presence of Cpx system in bacteria. Microbiol. **146:**247-248.

23. **Debarbouille, M., S. Dramsi, O. Dussurget, M. Nahori, E. Vaganay, G. Jouvion, A. Cozzone, T. Msadek, and B. Duclos.** 2009. Characterization of a serine/threonine kinase involved in virulence of *Staphylococcus aureus*. J. Bacteriol. **191:**4070-4081.

24. **Deutscher, J., B. Bauer, and H. Sauerwald.** 1993. Regulation of glycerol metabolism in *Enterococcus faecalis* by phosphoenolpyruvate-dependent phosphorylation of glycerol kinase catalyzed by enzyme I and HPr of the phosphotransferase system. J. Bacteriol. **175:**3730-3733.

25. **Ditto, M. D., D. Roberts, and R. Weisberg.** 1994. Growth phase variation of integration host factor level in *Escherichia coli*. J. Bacteriol. **176:**3738-3748.

26. **Dobrowolska, G., and G. Muszynska.** 1991. Model studies on iron (III) ion affinity chromatography: Interaction of immobilized metal ions with nucleotides. J. Chrom. **541:**333-339.

27. **Doyle, S. M., and S. Wickner.** 2009. Hsp104 and ClpB: protein disaggregating machines. Trends Biochem. Sci. **34:**40-48.

28. **Eravci, M., S. Fuxius, O. Broedel, S. Weist, S. Eravci, U. Mansmann, H. Schlucher, J. Tiemann, and A. Baumgartner.** 2007. Improved comparative proteome analysis based on two-dimensional gel electrophoresis. Proteomics **7:**513-523.

29. **Eymann, C., D. Becher, J. Bernhardt, K. Gronau, A. Klutzny, and M. Hecker.** 2007. Dynamics of protein phosphorylation on ser/thr/tyr in *Bacillus subtilis*. Proteomics **7:**3509-3526.

30. **Fong, D. H., and A. M. Berghuis.** 2002. Substrate promiscuity of an aminoglycoside antibiotic resistance enzyme via target mimicry. EMBO J. **21:**2323-2331.

31. **Freestone, P., S. Grant, I. Toth, and V. Norris.** 1995. Identification of phosphoproteins in *Escherichia coli*. Mol. Microbiol. **15:**573-580.

32. **Goosen, N., and P. van de Putte.** 1995. The regulation of transcription initiation by integration host factor. Mol. Microbiol. **16:**1-7.

33. **Guzman, L. M., D. Belin, M. J. Carson, and J. Beckwith.** 1995. Tight regulation, modulation, and high-level expression by vectors containing the arabinose P_{BAD} promoter. J. Bacteriol. **177:**4121-4130.

34. **Han, G., and C. Zhang.** 2001. On the origin of ser/thr kinases in a prokaryote. FEMS Microbiol. Lett. **200:**79-84.

35. **Hanks, S. K., and T. Hunter.** 1995. The eukaryotic protein kinase superfamily: kinase (catalytic) domains structure and classification. FASEB J. **9:**576-596.

36. **Hartl, F. U.** 1996. Molecular chaperones in cellular protein folding. Nature **381:**571-580.

37. **Hartl, F. U., and M. Hayer-Hartl.** 2002. Molecular chaperones in the cytosol: from nascent chain to folded protein. Science **295:**1852-1858.

38. **He, C.** 2005. Characterization of a novel protein kinase, *rdoA*, from *Salmonella enterica* serovar Typhimurium. Queen's University, Kingston, Ontario, Canada.

39. **Heppelmann, C. J., L. M. Benson, and H. Robert Bergen III.** 2007. A simple method to remove contaminating salt from IPG strips prior to IEF. Electrophoresis **28:**3988-3991.

40. **Hirano, Y., M. M. Hossain, K. Takeda, H. Tokuda, and K. Miki.** 2007. Structural studies of the Cpx pathway activator NlpE on the outer membrane of *Escherichia coli*. Structure **15:**963-976.

41. **Holtman, C. K., A. C. Pawlyk, N. D. Meadow, and D. W. Pettigrew.** 2001. Reverse genetics of *Escherichia coli* glycerol kinase allosteric regulation and glucose control of glycerol utilization in vivo. J. Bacteriol. **183:**3336-3344.

42. **Hua, Q., C. Yang, T. Oshima, H. Mori, and K. Shimizu.** 2004. Analysis of gene expression in *Escherichia coli* in response to changes of growth-limiting nutrient in chemostat cultures. Appl. Environ. Microbiol. **70:**1749-1757.

43. **Hughes, D.** 1990. Both genes for EF-Tu in *Salmonella typhimurium* are individually dispensable for growth. J. Mol. Biol. **215:**41-51.

44. **Irani, M., and P. K. Maitra.** 1974. Isolation and characterization of *Escherichia coli* mutants defective in enzymes of glycolysis. Biochem. Biophys. Res. Commun. **56:**127-133.

45. **Jones, B. D.** 1996. Salmonellosis: host immune response and bacterial virulence determinants. Annu. Rev. Immunol. **14:**533-561.

46. **Jones, B. D.** 2005. *Salmonella* invasion genes regulation: a story of environmental awareness. J. Microbiol. **43:**110-117.

47. **Juan Li., Z., D. Hillyard, and P. Higgins.** 1989. Nucleotide sequence of the *Salmonella typhimurium him*A gene. Nucleic Acids Res. **17:**8880.

48. **Karas, M., D. Bachman, U. Bahr, and F. Hillenkamp.** Matrix-assisted ultraviolet laser desorption of non-volatile compounds. Int. J. Mass Spectrom. Ion Processes **78:**53-68.

49. **Kennelly, P. J., and M. Potts.** 1996. Fancy meeting you here! A fresh look at "prokaryotic" protein phosphorylation. J. Bacteriol. **178:**4759-4764.

50. **Khorchid, A., and M. Ikura.** 2006. Bacterial histidine kinase as signal sensor and transducer. IJBCB **38:**307-312.

51. **Kimata, K., Y. Tanaka, T. Inada, and H. Aiba.** 2001. Expression of the glucose transporter gene, *pstG*, is regulated at the mRNA degradation step in response to glycolytic flux in *Escherichia coli*. EMBO J. **20:**3587-3595.

52. **Kinoshita, E., E. Kinoshita-Kikuta, K. Takiyama, and T. Koike.** 2006. Phosphate-binding tag, a new tool to visualize phosphorylated proteins. Mol. Cell. Proteomics **5.4:**749-757.

53. **Kinoshita, E., A. Yamada, H. Takeda, E. Kinoshita-Kikuta, and T. Koike.** 2005. Novel immobilized zinc(II) affinity chromatography for phosphopeptides and phosphorylated proteins. J. Sep. Sci. **28:**155-162.

54. **Kojetin, D. J., D. M. Sullivan, R. J. Thompson, and J. Cavanagh.** 2007. Classification of response regulators based on their surface properties. Methods Enzymol. **422:**141-169.

55. **Krukenberg, K. A., F. Forster, L. M. Rice, A. Sali, and D. A. Agard.** 2008. A novel conformation of *E. coli* Hsp90 in solution: insights into the conformational dynamics of Hsp90. Structure **16:**755-756.

56. **Laemmli, U. K.** 1970. Cleavage of structural proteins during the assembly of the head of bacteriophage T4. Nature **227:**680-685.

57. **Lee, E. C., M. P. MacWilliams, R. I. Gumport, and J. F. Gardner.** 1991. Genetic analysis of *Escherichia coli* integration host factor interactions with its bacteriophage lambda H' recognition site. J. Bacteriol. **173:**609-617.

58. **Lee, J., J. Nishitani, and G. Wilcox.** 1984. Genetic characterization of *Salmonella typhimurium* LT2 *ara* mutations. J. Bacteriol. **158:**344-346.

59. **Lee, P. C., B. R. Bochner, and B. N. Ames.** 1983. AppppA, heat-shock stress, and cell oxidation. Proc. Natl. Acad. Sci. USA **80:**7496-7500.

60. **Lee, Y. M., P. A. DiGiuseppe, T. J. Silhavy, and S. J. Hultgren.** 2004. P pilus assembly motif necessary for activation of the CpxRA pathway by PapE in *Escherichia coli*. J. Bacteriol. **186:**4326-4337.

61. **Leonard, C. J., L. Aravind, and E. V. Koonin.** 1998. Novel families of putative protein kinases in bacteria and archaea: evolution of the "eukaryotic" protein kinase superfamily. Genome Res. **8:**1038-1047.

62. **Levesque, C. M., R. W. Mair, J. A. Perry, P. C. Y. Lau, Y. H. Li, and D. G. Cvitkovitch.** 2007. Systematic inactivation and phenotypic characterization of two-component systems in expression of *Streptococcus mutans* virulence properties. Lett. Appl. Microbiol. **45:**398-404.

63. **Levine, A., F. Vannier, C. Absalon, L. Kuhn, P. Jackson, E. Scrivener, V. Labas, J. Vinh, P. Courtney, J. Garin, and S. J. Seror.** 2006. Analysis of the dynamic *Bacillus subtilis* ser/thr/tyr phosphoproteome implicated in a wide variety of cellular processes. Proteomics **6:**2157-2173.

64. **Liberek, K., J. Marszalek, D. Ang, C. Georgopoulos, and M. Zylicz.** 1991. *Escherichia coli* DnaJ and GrpE heat shock proteins jointly stimulate ATPase activity of DnaK. Proc. Natl. Acad. Sci. USA **88:**2874-2878.

65. **Lin, E. C.** 1976. Glycerol dissimilation and its regulation in bacteria. Annu. Rev. Microbiol. **30:**535-578.

66. **Lippmann, C., C. Lindschau, E. Vijgenboom, W. Schroder, L. Bosch, and V. A. Erdmann.** 1993. Prokaryotic elongation factor Tu is phosphorylated *in vivo*. J. Biol. Chem. **268:**601-607.

67. **Liu, C., S. Perrett, and J. Zhou.** 2005. Dimeric trigger factor stably binds folding-competent intermediates and cooperates with the DnaK-DnaJ-GrpE chaperone system to allow folding. J. Biol. Chem. **280:**3315-13320.

68. **Liu, M. Y., G. Gui, B. Wei, J. F. Preston III, L. Oakford, U. Yuksel, D. P. Giedroc, and T. Romeo.** 1997. The RNA molecule CsrB binds to the global regulator protein CsrA and antagonizes its activity in *Escherichia coli*. J. Biol. Chem. **272:**17502-17510.

69. **Lomas-Lopez, R., P. Paracuellos, M. Riberty, A. Cozzone, and B. Duclos.** 2007. Several enzymes of the central metabolism are phosphorylated in *Staphylococcus aureus*. FEMS Microbiol. Lett. **272:**35-42.

70. **Lux, R., and W. Shi.** 2005. A novel bacteria signaling system with a combination of a ser/thr kinase cascade and a his/asp two-component system. Mol. Microbiol. **58:**345-438.

71. **Macek, B., F. Gnad, B. Soufi, C. Kumar, J. V. Olsen, I. Mijakovic, and M. Mann.** 2008. Phosphoproteome analysis of *E. coli* reveals evolutionary conservation of bacterial ser/thr/tyr phosphorylation. Mol. Cell. Proteomics **7:**299-307.

72. **Macek, B., I. Mijakovic, J. V. Olsen, F. Gnad, C. Kumar, P. R. Jensen, and M. Mann.** 2007. The serine/threonine/tyrosine phosphoproteome of the model bacterium *Bacillus subtilis*. Mol. Cell. Proteomics **6:**697-707.

73. **Machida, M., H. Kosako, K. Shirakabe, M. Kobayashi, M. Ushiyama, J. Inagawa, J. Hirano, T. Nakano, Y. Bando, E. Nishida, and S. Hattori.** 2007. Purification of phosphoproteins by immobilized metal affinity chromatography and its application to phosphoproteome analysis. FEBS J. **274:**1576-1587.

74. **Madec, E., A. Stensballe, S. Kjellstrom, L. Cladiere, M. Obuchowski, O. N. Jensen, and S. J. Seror.** 2003. Mass spectrometry and site-directed mutagenesis identify several autophosphorylated residues required for the activity of PrkC, a ser/thr kinase from *Bacillus subtilis*. J. Mol. Biol. **330:**459-472.

75. **Malki, A., T. Caldas, A. Parmeggiani, M. Kohiyama, and G. Richarme.** 2002. Specificity of elongation factor EF-TU for hydrophobic peptides. Biochem. Biophys. Res. Commun. **296:**749-754.

76. **Maloy, S.** 1987. The proline utilization operon *In* Neidhardt et al. (ed.), In *Escherichia coli* and *Salmonella typhimurium*. American Society for Microbiology, Washington, D.C.

77. **Mangan, M. W., S. Lucchini, V. Danino, T. O. Croinin, J. C. D. Hinton, and C. J. Dorman.** 2006. The integration host factor (IHF) integrates stationary-phase and virulence gene expression in *Salmonella enterica* serovar Typhimurium. Mol. Microbiol. **59:**1831-1847.

78. **Manu-Boateng, A.** 2007. Analysis of bacterial serine/threonine kinase. Queen's University, Kingston, Ontario, Canada.

79. **Marshall, D. G., B. J. Sheehan, and C. J. Dorman.** 1999. A role for the leucine-responsive regulatory protein and integration host factor in the regulation of the *Salmonella* plasmid virulence (spv) locus in *Salmonella typhimurium*. Mol. Microbiol. **34:**134-135.

80. **Martin, N. L.** 2007. Sequence plus structure plus experimental inquiry: combining the clues to elucidate bacterial kinase function. Future Microbiol. **2:**223-226.

81. **Matsui, H., A. Takaya, and T. Yamamoto.** 2008. Sigma 23- mediated negative regulation of *Salmonella* pathogenicity island 1 expression. J. Bacteriol. **190:**6636-6645.

82. **McCarty, J., and G. Walker.** 1991. DnaK as a thermometer: threonine-199 is site of autophosphorylation and is critical for ATPase activity. Proc. Natl. Acad. Sci. USA **88:**9513-9517.

83. **Miki, T., N. Okada, and H. Danbara.** 2004. Two periplasmic disulfide oxidoreductase, DsbA and SrgA, target outer membrane protein SpiA, a component of the *Salmonella* pathogenicity island 2 type III secretion system. J. Biol. Chem. **279:**34631-3462.

84. **Miller, M. B., and B. L. Bassler.** 2001. Quorum sensing in bacteria. Ann. Rev. Microbiol. **55:**165-199.

85. **Morita, T., H. Kawamoto, T. Mizota, T. Inada, and H. Aiba.** 2004. Enolase in the RNA degradosome plays a crucial role in the rapid decay of glucose transporter mRNA in the response to phosphosugar stress in *Escherichia coli*. Mol. Microbiol. **54:**1063-075.

86. **Nakamaya, S. I., and H. Watanabe.** 1995. Involvement of CpxA, a sensor of a two-component regulatory system, in the pH-dependent regulation of expression of *Shigella sonnei virF* gene. J. Bacteriol. **177:**5062-5069.

87. **Nakanishi, T., E. Ando, M. Furuta, E. Kinoshita, E. Kinoshita-Kikuta, T. Koike, S. Tsunasawa, and O. Nishimura.** 2007. Identification on membrane and characterization of phosphoproteins using an alkoxide-bridged dinuclear metal complex as a phosphate-binding tag molecule. J. Biomol. Tech. **18:**278-286.

88. **Nariya, H., and S. Inouye.** 2005. Identification of a protein ser/thr kinase cascade that regulates essential transcriptional activators in *Myxococcus xanthus* development. Mol. Microbiol. **58:**367-379.

89. **Nariya, H., and S. Inouye.** 2006. A protein ser/thr kinase cascade negatively regulates the DNA-binding activity of MrpC, a smaller form of which may be necessary for the *Myxococcus xanthus* development. Mol. Microbiol. **60:**1205-1217.

90. **Nash, H. A., C. A. Roberston, E. Flamm, R. A. Weisberg, and H. I. Miller.** 1987. Overproduction of *Escherichia coli* integration host factor, a protein with nonidentical subunits. J. Bacteriol. **169:**4124-4127.

91. **Nickerson, C. A., and M. J. Schurr (ed.).** 2006. Molecular paradigms of infectious disease- a bacterial perspective. Springer Science and Business Media.

92. **Nilson, J., and P. Nissen.** 2005. Elongation factors on the ribosome. Curr. Opin. Struct. Biol. **15:**349-354.

93. **Ostrovsky, P. C., and S. Maloy.** 1995. Protein phosphorylation on serine, threonine, and tyrosine residues modulates membrane-protein interactions and transcriptional regulation in *Salmonella typhimurium*. Genes Dev. **9:**2034-2041.

94. **Pawson, T., and J. D. Scott.** 2005. Protein phosphorylation in signaling- 50 years and counting. Trends Biochem. Sci. **30:**286-290.

95. **Perez, J. M., F. A. Arenas, G. A. Pradenas, J. M. Sandoval, and C. C. Vasquez.** 2008. *Escherichia coli* YqhD exhibits aldehyde reductase activity and protects from harmful effect of lipid peroxidation-derived aldehydes. J. Biol. Chem. **283:**7346-7353.

96. **Pettigrew, D. W., W. Z. Liu, C. Hilmes, N. D. Meadow, and S. Roseman.** 1996. A single amino acid change in *Escherichia coli* glycerol kinase abolishes glucose control of glycerol utilization in vivo. J. Bacteriol. **178:**2846-2852.

97. **Phadtare, S., and M. Inouye.** 2004. Genome-wide transcriptional analysis of the cold shock response in wild-type and cold-sensitive, quadruple-*csp*-deletion strains of *Escherichia coli*. J. Bacteriol. **186:**7007-7014.

98. **Posewitz, M. C., and P. Tempst.** 1999. Immobilized gallium (III) affinity chromatography of phosphopeptides. Anal. Chem. **71:**2883-2892.

99. **Price, N. L., and T. L. Raivio.** 2009. Characterization of the Cpx regulon in the *Escherichia coli* Strain MC4100. J. Bacteriol. **191:**1798-1815.

100. **Raggiaschi, R., S. Gotta, and G. C. Terstappen.** 2005. Phosphoproteome analysis. Biosci. Rep. **25:**33-44.

101. **Raggiaschi, R., C. Lorenzetto, E. Diodato, A. Caricasole, S. Gotta, and G. C. Terstappen.** 2006. Detection of phosphorylation patterns in rat cortical neurons by combining phosphatase-treatments and DIGE technology. Proteomics **6:**748-756.

102. **Raivio, T. L.** 2005. Envelope stress responses and Gram-negative bacterial pathogenesis. Mol. Biol. **56:**1119-1128.

103. **Raivio, T. L., M. W. Laird, J. C. Joly, and T. J. Silhavy.** 2000. Tethering of CpxP to the inner membrane prevents spheroplast induction of the Cpx envelope stress response. Mol. Microbiol. **37:**1186-1197.

104. **Raivio, T. L., and T. J. Silhavy.** 2001. Periplasmic stress and ECF sigma factor. Ann. Rev. Microbiol. **55:**591-624.

105. **Ravichandran, A., N. Sugiyama, M. Tomita, S. Swarup, and Y. Ishihama.** 2009. Ser/thr/tyr phosphoproteome analysis of pathogenic and non-pathogenic *Pseudomonas* species. Proteomics **9:**2764-2775.

106. **Reading, N. C., and V. Sperandio.** 2006. Quorum sensing: the many languages of bacteria. FEMS Microbiol. Lett. **254:**1-11.

107. **Reinders, J., and A. Sickmann.** 2005. State-of-the-art in phosphoproteomics. Proteomics **5:**4052-4061.

108. **Richards, M.** 2006. The effect of RdoA and the Cpx pathway on flagellar phase variation in *S. typhimurium*. Queen's University, Kingston, Ontario, Canada.

109. **Robertson, E. S., L. A. Aggison, and A. W. Nicholson.** 1994. Phosphorylation of elongation factor G and ribosomal protein S6 in bacteriophage T7-infected *Escherichia coli*. Mol. Microbiol. **11:**1045-1057.

110. **Robinson, V. L., D. R. Buckler, and A. M. Stock.** 2000. A tale of two components: a novel kinase and a regulatory switch. Nat. Struct. Biol. **7:**626-633.

111. **Romeo, T.** 1998. Global regulation by the small RNA-binding protein CsrA and the non-coding RNA molecule CsrB. Mol. Microbiol. **29:**1321-1330.

112. **Saluta, M. V., and I. N. Hirshfield.** 1995. The occurence of duplicate lysyl-tRNA synthetase gene homologs in *Escherichia coli* and other procaryotes. J. Bacteriol. **177:**1872-1878.

113. **Sawai, R., A. Suzuki, Y. Takano, P. Lee, and S. Horinouchi.** 2004. Phosphorylation of AfsR by multiple serine/threonine kinases in *Streptomyces coelicolor* A3(2). Gene **334:**53-61.

114. **Scheeff, E. D., and P. E. Bourne.** 2005. Structural evolution of the protein kinase-like superfamily. PLoS Comput. Biol. **1:**359-381.

115. **Schlieker, C., H. Zentgraft, P. Dersch, and A. Mogk.** 2005. ClpV, a unique Hsp100/Clp member of pathogenic proteobacteria. Biol. Chem. **386:**115-1127.

116. **Sheyman, M., and A. Goldberg.** 1992. Heat shock in *Escherichia coli* alters the protein-binding properties of the chaperonin groEL by inducing its phosphorylation. Nature **357:**167-169.

117. **Shi, L., M. Potts, and P. J. Kennelly.** 1998. The serine, threonine, and/or tyrosine-specific protein kinases and protein phosphatases of prokaryotic organisms: a family portrait. FEMS Microbiol. Rev. **22:**229-253.

118. **Simonetti, A., S. Marzi, L. Jenner, A. Mayasnikov, P. Romby, G. Yusupova, B. P. Klaholz, and M. Yusupov.** 2009. A structural view of translation initiation in bacteria. Cell. Mol. Life Sci. **66:**423-436.

119. **Skerker, J. M., M. S. Prasol, B. S. Perchuk, E. G. Biondi, and M. T. Laub.** 2005. Two-component signal transduction pathways regulating growth and cell cycle progression in a bacterium: a system-level analysis. PLoS Biol. **3:**1170-1788.

120. **Snyder, W. B., L. J. B. Davis, P. N. Danese, C. L. Cosma, and T. J. Silhavy.** 1995. Overproduction of NlpE, a new outer membrane lipoprotein, suppresses the toxicity of periplasmic LacZ by activation of the Cpx signal transduction pathway. J. Bacteriol. **177:**4216-4223.

121. **Soufi, B., F. Gnad, P. R. Jensen, D. Patrenovic, M. Mann, I. Mijakovic, and B. Macek.** 2008. The ser/thr/tyr phosphoproteome of *Lactococcus lactis* IL 1403 reveals multiply phosphorylated proteins. Proteomics **8:**3486-3493.

122. **Spence, J., and C. Georgopoulos.** 1989. Purification and properties of the *Escherichia coli* heat shock protein, HtpG. J. Biol. Chem. **264:**4398-4403.

123. **Spirin, A. S.** 2004. The ribosome as an RNA-based molecular machine. RNA Biology **1:**3-9.

124. **Spory, A., A. Bosserhoff, C. von Rhein, W. Goebel, and A. Ludwig.** 2002. Differential regulation of multiple proteins of *Escherichia coli* and *Salmonella enterica* serovar Typhimurium by the transcriptional regulator SlyA. J. Bacteriol. **184:**3549-3559.

125. **Stein, E. A., K. Cho, P. Higgs, and D. R. Zusman.** 2006. Two ser/thr protein kinases essential for efficient aggregation and spore morphogenesis in *Myxococcus xanthus*. Mol. Microbiol. **60:**1414-1431.

126. **Steinberg, T. H., B. J. Agnew, K. R. Gee, W. Leung, T. Goodman, B. Schulenberg, J. Hendrickson, J. M. Beechem, R. P. Haugland, and W. F. Patton.** 2003. Global quantitative phosphoprotein analysis using Multiplexed Proteomics technology. Proteomics **3:**1128-1144.

127. **Stephenson, K., and J. A. Hoch.** 2002. Virulence- and antibiotic resistance-associated two-component signal transduction systems of Gram-positive pathogenic bacteria: targets of antimicrobial therapy. Pharmacol. Ther. **93:**293-305.

128. **Stock, A. M., V. L. Robinson, and P. N. Goudreau.** 2000. Two-component signal transduction. Ann. Rev. Biochem. **69:**183-215.

129. **Suntharalingam, P., H. Spencer, C. V. Gallant, and N. L. Martin.** 2003. *Salmonella enterica* serovar Typhimurium *rdoA* is growth phase regulated and is involved in relaying Cpx-inducing signals. J. Bacteriol. **185:**432-443.

130. **Swinger, K. K., and P. A. Rice.** 2004. IHF and HU: flexible architects of bent DNA. Curr. Opin. Struct. Biol. **14:**28-35.

131. **Takaya, A., M. Matsui, T. Tomoyasu, M. Kaya, and Yamamoto, T.** 2006. The DnaK chaperone machinery converts the native $FlhD_2C_2$ hetero-tetramer into a functional transcriptional regulator of flagellar regulon expression in *Salmonella*. Mol. Microbiol. **59:**1327-1340.

132. **Takaya, A., T. Tomoyasu, H. Matsui, and T. Yamamoto.** 2004. The DnaK/DnaJ chaperon machinery of *Salmonella enterica* serovar Typhimurium is essential for invasion of epithelial cells and survival within macrophages, leading to systemic infection. Infect. Immun. **72:**1364-1373.

133. **Tang, Y., J. R. Guest, P. J. Artymiuk, R. C. Read, and J. Green.** 2004. Post-transcriptional regulation of bacterial motility by aconitase proteins. Mol. Microbiol. **51:**1817-1826.

134. **Teplitski, M., R. I. Goodier, and B. M. M. Ahmer.** 2003. Pathways leading from BarA/SirA to motility and virulence gene expression in *Salmonella*. J. Bacteriol. **185:**7257-7265.

135. **Thomas, J. G., and F. Baneyx.** 2000. ClpB and HtpG facilitates de novo protein folding in stressed *Escherichia coli* cells. Mol. Microbiol. **36:**1360-1370.

136. **Tokuda, H.** 2009. Biogenesis of outer membranes in Gram-negative bacteria. Biosci. Biotechnol. Biochem. **73:**465-473.

137. **Travers, A.** 1997. DNA- protein interactions: IHF-the master bender. Curr. Biol. **7:**R252-R254.

138. **Tubulekas, I., and D. Hughes.** 1993. Growth and translational elongation rate are sensitive to the concentration of EF-Tu. Mol. Microbiol. **8:**761-770.

139. **Turcot, I., T. V. Ponnampalam, C. W. Bouwman, and N. L. Martin.** 2001. Isolation and characterization of a chromosomally encoded disulphide oxidoreductase from *Salmonella enterica* serovar Typhimurium. Can. J. Microbiol. **47:**711-721.

140. **Vikströma, E., L. Buib, P. Konradssonb, and K. Magnussona.** 2009. The junctional integrity of epithelial cells is modulated by *Pseudomonas aeruginosa* quorum sensing molecule through phosphorylation-dependent mechanisms. Exp. Cell Res. **315:**313-326.

141. **Vincent, C., B. Duclos, C. Grangeasse, E. Vaganay, M. Riberyt, A. J. Cozzone, and P. Doublet.** 2000. Relationship between exopolysaccharide production and protein-tyrosine phosphorylation in Gram-negative bacteria. J. Mol. Biol. **304:**311-321.

142. **Voisin, S., D. C. Watson, L. Tessier, W. Ding, S. Foote, S. Bhatia, J. F. Kelly, and N. M. Young.** 2007. The cytoplasmic phosphoproteome of the Gram-negative bacterium *Campylobacter jejuni*: Evidence for modification by unidentified protein kinases. Proteomics **7:**4338-4348.

143. **Wagner, R.** 2000. Transcription Regulation in Prokaryotes. Oxford University Press, New York.

144. **Wanner, B. L.** 1992. Is cross regulation by phosphorylation of two-component response regulator proteins important in bacteria? J. Bacteriol. **174:**2053-2058.

145. **Watanabe, Y., K. Motohaski, H. Taguchi, and M. Yoshida.** 2000. Heat-inactivated proteins managed by DnaKJ-GrpE-ClpB chaperones are released as a chaperonin-recognizable non-native form. J. Biol. Chem. **275:**12388-12392.

146. **Wei, B. L., A. Brun-Zinkernagel, J. W. Simecka, B. M. Prue, P. Babitzke, and T. Romeo.** 2001. Positive regulation of motility and *flhDC* expression by the RNA-binding protein CsrA of *Escherichia coli*. Mol. Microbiol. **40:**245-256.

147. **Wessel, D., and U. I. Flugge.** 1984. A method for the quantitative recovery of protein in dilute solution in the presence of detergents and lipids. Anal. Biochem. **138:**141-143.

148. **West, A. H., and A. M. Stock.** 2001. Histidine kinases and response regulators in two-component signaling systems. Trends Biochem. Sci. **26:**369-376.

149. **Willey, J. M., L. M. Sherwood, and C. J. Woolverton.** 2008. Prescott, Harley, and Klein's Microbiology. McGraw Hill Higher Education, New York.

150. **Wolschin, F., and W. Weckwerth.** 2005. Combining metal oxide affinity chromatography (MOAC) and selective mass spectrometry for robust identification of *in vivo* protein phosphorylation sites. Plant Methods **1:**1-10.

151. **Wolschin, F., S. Wienkoop, and W. Weckwerth.** 2005. Enrichment of phosphorylated proteins and peptides from complex mixtures using metal oxide/hydroxide affinity chromatography (MOAC). Proteomics **5:**4389-4397.

152. **Wray, C., and W. J. Sojka.** 1978. Experimental *Salmonella typhimurium* infection in calves. Res. Vet. Sci. **25:**139-143.

153. **Wright, M., N. Boonyalai, J. A. Tanner, A. D. Hindley, and A. D. Miller.** The duality of LysU, a catalyst for both Ap4A and Ap3A formation. FEBS J. **273:**3534-3544.

154. **Xavier, K. B., S. T. Miller, W. Lu, J. H. Kim, J. Rabinowitz, I. Pelcer, M. F. Semmelhack, and B. L. Bassler.** 2007. Phosphorylation and processing of the quorum-sensing molecule autoinducer-2 in enteric bacteria. ACS Chem. Biol. **2:**128-36.

155. **Yan, J. X., R. Wait, T. Berkelman, R. A. Harry, J. A. Westbrook, C. H. Wheeler, and M. J. Dunn.** 2000. A modified silver staining protocol for visualization of proteins compatible with matrix-assisted laser desorption/ionization and electrospray ionization-mass spectrometry. Electrophoresis **21:**3666-3672.

156. **Yona-Nadler, C., T. Umanski, S. Aizawa, D. R. Friedberg and I. Rosenshine.** 2003. Integration host factor (IHF) mediates repression of flagella in enteropathogenic and enterohaemorrhagic *Escherichia coli*. Microbiol. **149:**877-884.

157. **Zhang, H., X. Sheng, S. Xu, Y. Gao, H. Du, J. Li, H. Xu, and X. Huang.** 2009. Global transcriptional response of *Salmonella enterica* serovar Typhi to anti-z66 antiserum. FEMS Microbiol. Lett. **298:**51-55.

158. **Zheng, J., C. He, V. Kumar Singh, N. L. Martin, and Z. Jia.** 2007. Crystal structure of a novel prokaryotic Ser/Thr kinase and its implication in the Cpx stress response pathway. Mol. Microbiol. **63:**1360-1371.

159. **Zhou, Y., W. Zhu, P. S. Bellur, D. Rewindkel, and D. Becker.** 2008. Direct linking of metabolism and gene expression in the proline utilization A protein from *Escherichia coli*. Amino Acids **35:**711-718.

160. **Zieg, J., M. Silverman, M. Hilmen, and M. Simon.** 1977. Recombinational switch for gene expression. Science **196:**170-172.

161. **Zolkiewski, M.** 1999. ClpB cooperates with DnaK, DnaJ, and GrpE in suppressing protein aggregation: a novel multi-chaperone system from *Escherichia coli*. J. Biol. Chem. **274:**28083-28086.

162. **Zulianello, L., de la Gorgue de Rosny, E., P. van Ulsen, P. ven de Putte, and N. Goosen.** 1994. The HimA and HimD subunits of integration host factor can specifically bind to DNA as homodimers. EMBO J. **13:**1534-1540.

Appendix A

Solutions and Media

The following media were used for growing bacterial cells:

Pre-mixed Luria-Bertani (LB) medium (Fisher-Scientific) was prepared as follows and sterilized by autoclave:

- For broth media: 20 g/L of LB
- For agar media: 20 g/L of LB and 15 g of agar

For media containing a final concentration of 100 μg/mL ampicillin (AMP100), antibiotic was added after agar media was cooled to 55°C and broth media cooled to room temperature (RT).

The following solutions were used for preparing bacterial cell lysates. All solutions used milliQ H_2O as solvent:

Phosphoprotein binding buffer (pH 6.0) contained the following and filter-sterilized:

- 25 mM MES
- 1 M sodium chloride (NaCl)

0.25% (w/v) CHAPS Phosphoprotein lysis mixture contained the following:

- 0.25% (w/v) CHAPS
- Phosphoprotein binding buffer without CHAPS
- 200 μL of protease inhibitor cocktail (Sigma)
- 200 μL of phosphatase inhibitor cocktail (Sigma)
- 20 μL benzonase (Qiagen)

The following solutions were used for aluminum hydroxide metal ion affinity chromatography ($Al(OH)_3$ MOAC) (151).

Aluminum hydroxide phosphoprotein binding buffer (pH 6.1) contained the following (151):

- 30 mM MES
- 20 mM imidazole ($C_3H_4N_2$)
- 0.2 M aspartic acid ($HO_2CCH(NH_2)CH_2CO_2H$)
- 0.2 M sodium glutamate ($C_5H_8NNaO_4$)
- 0.25% (w/v) CHAPS
- 8 M urea

Aluminum hydroxide phosphoprotein elution buffer (pH 9.0) contained the following (151):

- 100 mM potassium diphosphate ($K_4O_7P_2$)
- 8 M urea

The following solutions used for electrophoresis experiments:

6X SDS loading buffer (pH 6.8) contained the following:

- 0.35 M tris HCl
- 30% (v/v) glycerol
- 10% (w/v) SDS
- 0.6 M DTT
- 0.012% (w/v) bromophenol blue

Stacking gel (pH 6.8) contained the following (56):

- 3% (w/v) of 30:0.8% (w/v) acrylamide:bis-acrylamide
- 0.5 M tris HCl
- 0.01% (w/v) SDS
- 0.025% (w/v) APS
- 0.025% (v/v) TEMED

Resolving gel (pH 8.8) contained the following (56):

- 12%(w/v) or 15%(w/v) 30:0.8% (w/v) acrylamide:bis-acrylamide
- 0.0375 M tris HCl
- 0.01% (w/v) SDS
- 0.025% (w/v) APS
- 0.025% (v/v) TEMED

1X SDS running buffer (pH 8.3) contained the following:

- 25 mM tris HCl
- 192 mM glycine
- 0.1% (w/v) SDS

Rehydration buffer contained the following:

- 8 M urea
- 2 M thiourea
- 4% (w/v) CHAPS
- 1% (w/v) ASB-14
- 50 mM DTT
- 0.2% (v/v) biolytes

DTT and biolytes were added right before use.

Equilibration buffer (pH8.8) contained the following:

- 6 M urea
- 0.375 M tris HCl
- 0.2% (w/v) SDS
- 20% (v/v) glycerol
- Bromophenol blue for color

The following solutions were used for Western immunoblots:

Western transfer buffer contained the following:

- 25 mM tricine
- 192 mM glycine
- 20% (v/v) methanol

Phosphate-buffered saline (PBS) [pH7.4] contained the following:

- 140 mM sodium chloride (NaCl)
- 2.7 mM potassium chloride (KCl)
- 10 mM sodium phosphate (Na_2HPO_4)
- 1.8 mM potassium dihydrogen phosphate (KH_2PO_4)

Anti–phosphoserine and anti–phosphothreonine blocking buffer contained the following:

- 2X PBS
- 1% (w/v) BSA (Frac V)
- 1% (w/v) PEG 4000
- 0.2% (v/v) Tween 20

The following solutions were used for silver staining (155). All solutions used milliQ H_2O:

Fix solution contained the following:

- 20% (v/v) acetic acid
- 50% (v/v) methanol

Pre-treatment solution contained the following:

- 30% (v/v) methanol
- 0.2% (w/v) sodium thiosulfate ($Na_2S_2O_3 \cdot 5H_2O$)
- 829 mM sodium acetate (CH_3COONa)

Silver stain solution contained the following:

- 0.25% (w/v) silver nitrate ($AgNO_3$)

Developer solution contained the following:

- 235 mM sodium carbonate (Na_2CO_3)
- 14.8% (v/v) formaldehyde

Stop solution contained the following:

- 50 mM free acid EDTA
- 125 mM sodium hydroxide (NaOH)

The following solutions were used for fluorescent staining. All solutions used milliQ H_2O:

Fix solution contained the following:

- 50% (v/v) methanol
- 10% (v/v) acetic acid

Destain solution (pH 4.0) contained the following:

- 20% (v/v) acetonitrile
- 50 mM sodium acetate (CH_3COONa)